

Georgia State University

ScholarWorks @ Georgia State University

---

Geosciences Theses

Department of Geosciences

---

12-14-2016

## An Evaluation of Late Holocene Sea Level Rise and Anthropogenic Impacts; Jones Narrows Marsh, Chatham County, Georgia

Jessie Hughes

Follow this and additional works at: [https://scholarworks.gsu.edu/geosciences\\_theses](https://scholarworks.gsu.edu/geosciences_theses)

---

### Recommended Citation

Hughes, Jessie, "An Evaluation of Late Holocene Sea Level Rise and Anthropogenic Impacts; Jones Narrows Marsh, Chatham County, Georgia." Thesis, Georgia State University, 2016.

doi: <https://doi.org/10.57709/9008597>

This Thesis is brought to you for free and open access by the Department of Geosciences at ScholarWorks @ Georgia State University. It has been accepted for inclusion in Geosciences Theses by an authorized administrator of ScholarWorks @ Georgia State University. For more information, please contact [scholarworks@gsu.edu](mailto:scholarworks@gsu.edu).

AN EVALUATION OF LATE HOLOCENE SEA LEVEL RISE AND ANTHROPOGENIC  
IMPACTS; JONES NARROWS MARSH, CHATHAM COUNTY, GEORGIA

by

JESSIE HUGHES

Under the Direction of Brian Meyer, PhD

ABSTRACT

A detailed record of the Late Holocene sea level rise and landscape evolution that has taken place on the Georgia coast is contained within the sedimentary stratigraphy of its salt marsh depositional basins. Global relative sea level (RSL) has risen during the Late Holocene, and the rate of rise has accelerated during the Anthropocene. Jones Narrows marsh stratigraphy and radiocarbon analysis indicate increasing rates of RSL rise for the late Holocene on the Northern Atlantic Coast of Georgia, while FPXRF analysis of the marsh sediments facilitates a chemostratigraphic study of Jones Narrows salt marsh deposition and landscape evolution. Sedimentation and hydrology at the site have been heavily influenced by recent local anthropogenic impacts, which are examined through stratigraphic and spatial methods.

INDEX WORDS: Sea Level Rise, Sedimentary Geology, Quaternary Geology, Salt Marsh  
Dynamics

AN EVALUATION OF LATE HOLOCENE SEA LEVEL RISE AND ANTHROPOGENIC  
IMPACTS; JONES NARROWS MARSH, CHATHAM COUNTY, GEORGIA

by

JESSIE HUGHES

A Thesis Submitted in Partial Fulfillment of the Requirements for the Degree of

Master of Science

in the College of Arts and Sciences

Georgia State University

2016

Copyright by  
Jessie Robert Hughes  
2016



AN EVALUATION OF LATE HOLOCENE SEA LEVEL RISE AND ANTHROPOGENIC  
IMPACTS; JONES NARROWS MARSH, CHATHAM COUNTY, GEORGIA

by

JESSIE HUGHES

Committee Chair: Brian Meyer

Committee: Daniel Deocampo

Katie Price

Electronic Version Approved:

Office of Graduate Studies

College of Arts and Sciences

Georgia State University

December 2016

**DEDICATION**

This manuscript is dedicated to my father, Robert Arnold Hughes.

## ACKNOWLEDGEMENTS

This research would not have been possible without guidance and support from the people at the Wormsloe Institute for Environmental History (WIEH), namely Mrs. Sarah Ross, or without support from the Wormsloe Foundation. Everyone at the Wormsloe State Historic Site made the research there a pleasure. Without the maps provided by Dr. Tommy Jordan at the University of Georgia Center for Geospatial Research (UGA CGR), the spatial analysis would have been a much more difficult undertaking. I would like to thank my committee chair and advisor, Dr. Brian Meyer, for his excellent direction and guidance throughout my time as a graduate student. My committee members, Dr. Daniel Deocampo and Dr. Katie Price, I thank for their individual assistance, time, and input. The field work that produced this study would not have been possible without the hard work of Dr. Kelly Vance, John Bankhead, and Steven Dobson. Finally, I would like to thank my wife, Bess, for her patience and insight.

## TABLE OF CONTENTS

<b>ACKNOWLEDGEMENTS .....</b>	<b>v</b>
<b>LIST OF TABLES .....</b>	<b>ix</b>
<b>LIST OF FIGURES .....</b>	<b>x</b>
<b>1 INTRODUCTION .....</b>	<b>1</b>
<b>1.1 Background .....</b>	<b>4</b>
<b>1.2 Research Questions.....</b>	<b>10</b>
<b>2 STUDY AREA.....</b>	<b>12</b>
<b>2.1 Geologic Setting.....</b>	<b>12</b>
<b>2.2 Salt Marshes of the Georgia Bight .....</b>	<b>14</b>
<i>2.2.1 Marsh Subenvironments and Sedimentation.....</i>	<i>16</i>
<b>2.3 History of Wormsloe and Jones Narrows Salt Marsh.....</b>	<b>19</b>
<b>2.4 Anthropogenic Impacts .....</b>	<b>20</b>
<b>3 RESEARCH METHODS.....</b>	<b>24</b>
<b>3.1 Vibracoring Methods.....</b>	<b>24</b>
<i>3.1.1 Methodology.....</i>	<i>24</i>
<i>3.1.2 Data Processing.....</i>	<i>26</i>
<b>3.2 XRF Methods .....</b>	<b>31</b>
<i>3.2.1 Methodology.....</i>	<i>31</i>
<i>3.2.2 Data Collection.....</i>	<i>32</i>

3.2.3	<i>Data Processing and Analysis</i> .....	32
3.3	<b>Evaluation of Late Holocene Sedimentation Rate and Sea Level Rise .....</b>	<b>34</b>
3.3.1	<i>Background</i> .....	34
3.3.2	<i>Methodology</i> .....	35
3.4	<b>Spatial Analysis</b> .....	<b>37</b>
3.4.1	<i>Methodology</i> .....	37
3.4.2	<i>Data Sources</i> .....	38
4	<b>RESULTS</b> .....	<b>40</b>
4.1	<b>Vibracoring Results</b> .....	<b>40</b>
4.1.1	<i>Jones Narrows Marsh Transect 1</i> .....	41
4.1.2	<i>Jones Narrows Marsh Transect 2</i> .....	45
4.1.3	<i>WM050315-04</i> .....	45
4.2	<b>XRF Results</b> .....	<b>47</b>
4.2.1	<i>Chemostratigraphic Results</i> .....	47
4.2.2	<i>Correlation Analysis</i> .....	48
4.2.3	<i>Cluster Analysis</i> .....	51
4.3	<b>Evaluation of Late Holocene Sedimentation Rate and Sea Level Rise .....</b>	<b>52</b>
4.3.1	<i>Radiocarbon Data</i> .....	52
4.3.2	<i>Calibrated Radiocarbon Data</i> .....	53
4.3.3	<i>Late Holocene Sedimentation Rate and Sea Level Rise</i> .....	53

<b>4.4</b>	<b>Spatial Analysis .....</b>	<b>56</b>
<b>4.4.1</b>	<b><i>Dredge Sand Area and Volume.....</i></b>	<b>62</b>
<b>5</b>	<b>DISCUSSION .....</b>	<b>64</b>
<b>5.1</b>	<b>Jones Narrows Stratigraphy .....</b>	<b>64</b>
<b>5.2</b>	<b>Chemostratigraphy .....</b>	<b>64</b>
<b>5.2.1</b>	<b><i>Cluster Analysis .....</i></b>	<b>66</b>
<b>5.3</b>	<b>Evaluation of Late Holocene Sea Level Rise .....</b>	<b>71</b>
<b>5.4</b>	<b>Anthropogenic Impacts .....</b>	<b>77</b>
<b>6</b>	<b>CONCLUSIONS .....</b>	<b>79</b>
<b>6.1</b>	<b>Recommendations for Further Study .....</b>	<b>80</b>
	<b>REFERENCES.....</b>	<b>82</b>
	<b>APPENDICES .....</b>	<b>89</b>
	<b>Appendix A – Vibracore Log Forms .....</b>	<b>89</b>
	<b>Appendix B – XRF Results.....</b>	<b>104</b>

**LIST OF TABLES**

Table 1: Marsh sample errors (after Engelhart and Horton, 2012).....	37
Table 2: Vibracore locations and depths.....	40
Table 3: Matrices of intercorrelation. a) complete data set; b) muddy intervals; c) sandy intervals; d) shell rich intervals.....	50
Table 4: Radiocarbon samples .....	53

## LIST OF FIGURES

Figure 1: Index Map - Study area location on the Georgia Bight.....	3
Figure 2: Study Area: Jones Narrows and surrounding area, 2012 TC satellite imagery; inset 1999 CIR imagery (imagery courtesy of UGA CGR) .....	12
Figure 3: Successive shorelines of the Georgia Bight: a) Successive shorelines and marshes; b) Pleistocene and Holocene Shorelines; c) Cross-section of Pleistocene and Holocene formations on the Georgia Coastal Plain (modified from Meyer (2013); Hoyt (1969); Hoyt and Hails (1967)) .....	15
Figure 4: Salt marsh subenvironments (after Edwards and Frey, 1977).....	16
Figure 5: Jones Narrows marsh and major subenvironments (facing east from The Isle of Hope) .....	17
Figure 6: Wormsloe entrance road.....	20
Figure 7: Impacted marsh area - 1951 aerial photograph; inset 1999 CIR imagery (imagery courtesy of UGA CGS).....	22
Figure 8: Impacted marsh area - 2012 TC satellite imagery; inset 1999 CIR imagery (imagery courtesy of UGA CGR) .....	23
Figure 9: Vibracore extraction and analysis – a) Innov-X Systems $\alpha$ -4000 XRF; b)Vibracore extraction on Jones Narrows; c) vibracore photo stand (Meyer, 2013); d) vibracore photo example .....	26
Figure 10: Vibracore log form - WM050215-01 pg. 1 .....	29
Figure 11: Vibracore log form - WM050215-01 pg. 2 .....	30
Figure 12: Jones Narrows transects and vibracore locations. 2012 TC satellite imagery; inset 1999 CIR imagery (imagery courtesy of UGA CGR) .....	41



Figure 13: Jones Narrows Transect 1 cross-sections (corrected for compaction) .....	44
Figure 14: Jones Narrows Transect 2 cross-section (corrected for compaction).....	46
Figure 15: Jones Narrows RSL trends .....	55
Figure 16: Study area - 1908 map; inset 1999 CIR imagery (courtesy UGA CGR) .....	58
Figure 17: Study area - 1968 aerial imagery; inset 1999 CIR imagery (courtesy UGA CGR)...	59
Figure 18: Study area mid Diamond Causeway construction - 1971 aerial imagery; inset 1999 CIR imagery (courtesy UGA CGR).....	60
Figure 19: Reconnection channels- 1988 aerial imagery; inset 1999 CIR imagery. (imagery courtesy of UGA CGR) .....	61
Figure 20: Extensions to The Isle of Hope and Long Island; a) 1951 aerial imagery; b) 2012 TC imagery; inset 1999 CIR imagery (imagery courtesy UGA CGR).....	63
Figure 21: Chemostratigraphic Log - WM050215-03 (corrected for compaction) .....	69
Figure 22: Chemostratigraphic Log - WM050215-04 ( corrected for compaction) .....	70
Figure 23: Jones Narrows RSL reconstruction and Ft. Pulaski Tide Data (NOAA) .....	72
Figure 24: Southeastern US Atlantic Coast RSL curves .....	74

## 1 INTRODUCTION

Holocene sea levels have been a powerful factor in the maintenance of coastal populations and may have even had a notable effect on the genesis of civilization (Engelhart and Horton, 2012). However, some sea level research predicts that roughly half of the world's coastal wetlands will submerge within the 21st century CE due to sea level rise (SLR) acceleration (Kirwan et al., 2010). Salt marshes are critical indicators of relative sea level (RSL), in addition to their ecological value, historical importance as human food sources, and coastal storm buffering effects, and they are threatened by the very thing which they allow us to measure; rising RSL.

Salt marsh conditions are dictated by internal and external controls, the internal controls being salt tolerant halophytic vegetation and autocompaction, while the external controls are RSL, tidal regimes, and sediment supply systems (Allen, 2000). Through lithostratigraphic, chemostratigraphic, and geospatial studies, the nature of the subject marsh and its sediments can be investigated, shedding light on the RSL history of the study area and quantifying the recent human impacts upon the marsh. In order to understand the nature of the modern transgression, it is necessary to reconstruct past RSL from marsh deposits. To build these reconstructions in a reliable manner, the understanding of human impacts must be improved upon. These factors create the impetus to evaluate the RSL history of and anthropogenic effects upon the salt marsh deposits at Jones Narrows, which lies within a Holocene RSL data gap zone (Hawkes et al., 2016) along the Atlantic coast of Georgia and has been heavily impacted by human activity during the Anthropocene (1800CE – Present) (Crutzen and Stoermer, 2000) (Fig. 1). Adjacent to the Isle of Hope and Wormsloe State Historic Site, Jones Narrows sits between two relict barrier islands and is part of the extensive system of intertidal salt marshes on the Georgia Coast. Due to

the history of human interaction with Jones Narrows, which includes the construction of several causeways and major artificial channels nearby, it provides an opportunity to study not only the natural history of the marsh, but also the decadal effects of direct anthropogenic impacts.

Outside of their intrinsic ecological importance, salt marshes are valuable to humanity in their capacity to act as unique habitats for a variety of endemic species, in their role as tidal and wave energy buffers between the open ocean and terrestrial areas, and in their ability to function as carbon sinks (Townend et al., 2011). In order to gain some sense of how these fragile environments will respond to the potential environmental changes of the coming century, it is imperative that the scientific community investigates modern salt marsh conditions and past dynamics, both natural and anthropogenic. Holocene relative sea level reconstructions are crucial to the understanding of rheology models of the Earth and provide necessary data for estimating rates of ongoing glacio-isostatic adjustment (GIA), while also helping to correct estimates of Greenland and Antarctic ice loss for the effect of GIA (Engelhart and Horton, 2012). Without the assessment of RSL change due to GIA and other land level change, the isolation of climate change induced eustatic sea level trends is difficult (Kemp et al., 2014).

The quality of Holocene relative sea level data for the United States Atlantic Coast is a major limiting factor for refining GIA models, and this is a key region for Holocene data due to its nature as an independent constraint on GIA (Engelhart and Horton, 2012). The gap in RSL data sets along the coasts of Georgia and Florida have prevented RSL reconstructions and the estimate of subsidence rates in the region, data without which coastal planning and Earth-ice models will suffer (Kemp et al., 2014).



Figure 1: Index Map - Study area location on the Georgia Bight

Additionally, late Holocene RSL reconstructions provide data for comparison with past climate variability, giving evidence that historic rates of sea level rise have been greater than the background trend over the previous centuries or more (Kemp et al., 2014). Southeastern U.S. salt marshes have endured rates of sea level rise higher than those we see today, having survived a period 7 mm/yr rise in the mid-Holocene, however, models predict that the modern SLR rate (between 2-3 mm/yr) will increase to 5 mm/yr - 50 mm/yr, surpassing any rates that have occurred in the Holocene, thus far (Kirwan and Megonigal, 2013).

To further the progress of necessary late Holocene RSL research on the Georgia Coast, this study will examine the sedimentary sequence and marsh conditions at Jones Narrows Marsh and address the following questions: 1) *What is the local late Holocene trend of RSL change at Jones Narrows?;* 2) *Can the anthropogenic impacts to Jones Narrows marsh be discerned and quantified through vibracore data analysis, radiocarbon analysis, and spatial analysis methods?;* 3) *Can distinct and meaningful geochemical suites of sediment that correlate to depositional subenvironments and/or anthropogenic impacts be identified through the analysis of X-ray fluorescence data derived from the vibracore sediment data?*

## **1.1 Background**

A complex web of controls influences the nature of salt marshes, including relative sea level, tidal and sediment supply regimes, halophytic vegetation, sedimentary autocompaction, and, from the mid-Holocene forward, anthropogenic forces (Allen, 2000). The interactions of these controls affect the ability of salt marshes to survive RSL changes through accretion and/or lateral movement. Accommodation space can be created through the combined effects of rising

RSL and autocompaction, and this space can be filled via growth and sedimentation on marsh surfaces (Allen, 2000).

Halophytic marsh vegetation plays a major role in sedimentation processes on marsh surfaces. Marsh vegetation contributes organic particles to the marsh and resists flow by creating friction, thereby reducing water velocity and inducing accretion of sediment introduced by tides and waves (Allen, 2000). Vegetative growth greatly enhances marsh accretion, although the specifics of the vegetation species control the behavior of the marsh (D'Alpaos et al., 2007). On the Georgia Bight and in many other coastal regions, the tall salt marsh cordgrass *Spartina alterniflora* is one of the most important halophytes. In spite of the role that *Spartina* grasses play in the accretion of sediment within salt marshes, the development of *Spartina* saltmarshes is closely related to the supply of fine grained sediments in the regional setting (Yong-Ming et al., 2008).

*Spartina alterniflora* is not the only halophyte that proliferates within salt marsh environments, and with the variety of vegetation types comes a variety of interactions with sediment; along with *S. alterniflora*, other similar common halophytes are *Phragmites australis*, *Juncus sp.*, and *Aster tripolium*, all of which possess a variety of abilities for catching sediment and promoting deposition (Temmerman et al., 2004). Generally, halophyte spatial growth density increases flow resistance and deposition (Townend et al., 2011). Not only do the different halophyte species affect the nature of sedimentation, but they also influence creek bank stability in a variety of ways (Chen et al., 2012). The wave energy baffling effect of marsh grasses causes fine sediment to fall out of suspension and gives salt marshes their characteristic morphology (Fig. 2); as the grasses enhance settling rates at the banks of tidal creeks, the suspended sediment available rapidly decreases with distance away from the creek banks (Townend et al., 2011).

The aftermath of the BP Deepwater Horizon oil spill illustrates the dependence of marsh stability upon vegetation health; the plant death that took place consequently caused massive increases in rates of marsh-edge erosion and the erosion of historically stable channels (Kirwan and Megonigal, 2013). Reduced halophyte health and subsequent marsh erosion have also been induced by natural disasters, and these events have illustrated how various halophyte species react differently to high energy forces; higher salinity marshes are dominated by species with deeper root profiles, and, during Hurricanes Katrina and Rita, these marshes endured less damage than those lower salinity marshes dominated by halophyte species with shallower roots (Kirwan and Megonigal, 2013).

Worldwide, the three most important sources sediment supply for salt marshes are river catchments, retreating coastal cliffs, and proximal seafloor formations, yet, sediment supply regimes remain poorly understood in terms of the mineral texture and mineral content supplied, which, in turn, control channel equilibrium marsh growth (Allen, 2000). Low marsh accretion is strongly influenced by changes in sediment supply, while accretion in high marsh zones is more heavily influenced by sea level change and other hydrologic factors (Haslett et al., 2003). While fine grained sediment supply is especially important for the accretion on the marsh surface, sand sized grain accretion is also important for the building of salt marshes (V. de Groot et al., 2011). Although sand contribution to overall marsh sediment is minor (<10%), it is vital to the initial stages of marsh formation, and the sources of marsh sand can be highly variable; they include intertidal flats, marsh creeks, and aeolian sands from beach plains, dunes, and washover deposits (V. de Groot et al., 2011). Other studies (Fagherazzi et al., 2012; Ma et al., 2014) have contended that storm events, not suspended sediment, are responsible for long-term accretion rates on salt marshes.

Halophyte vegetation and sediment supply have great influence over salt marsh conditions, however, tidal regimes and RSL have ultimate control over marsh accretion and erosion. RSL variation can control whether a marsh is dominated by organogenic or mineralogenic particles (Allen, 2000) and whether or not marsh accretion can reach equilibrium (Bartholdy et al., 2010). Generally, changes in RSL are due to the simultaneous effects of GIA, ocean mass, and ocean volume, with RSL variability along the U.S. Atlantic margin having been dominated by land subsidence and geoid fall, both driven primarily by the retreat of the Laurentide Ice Sheet and the collapse of its proglacial forebulge (Kemp et al., 2014). Plate tectonic motion-induced dynamic topography and sediment compaction also have effects on RSL trends, the quantification of which, along with GIA induced change, is vital in order to isolate climate related sea level trends (Kemp et al., 2014).

Many researchers suggest that tidal salt marshes will not be able to keep pace with predictions of local RSL rise (Hughes et al., 2009). Marsh equilibrium may be achieved under rising sea levels, however, SLR rates in excess of the equilibrium rate can drown marshes (Bartholdy et al., 2010). Conversely, without sea level rise or under rates of rise below equilibrium rates, marshes grow to the upper extent of their tidal ranges, over time, and decay due to exposure (Bartholdy et al., 2010).

So, while salt marshes have proliferated during the modern marine transgression, with RSL rise often causing rapid vegetative growth, observations of recently submerged marshes indicate that there are certainly limits upon the abilities of marshes to withstand high rates of SLR, in spite of the positive feedback between marsh sedimentation, vegetation, and rising seas (Kirwan et al., 2010). Submergence is a key component of marsh existence within the intertidal zone, as the amount of time that a marsh is submerged (hydroperiod) increases the amount of



sedimentation upon the marsh; however, excessive submergence stresses marsh vegetation, eventually reducing bioproductivity within the marsh (Townend et al., 2011). Hydroperiod is mostly controlled by the tidal range at a given marsh location, so inorganic (mineralogenic) sedimentation dominates the low marsh while organic sedimentation dominates the high marsh, indicating that the drowning of halophytic vegetation in organic sediment dominated marshes will dramatically reduce accretion ability (Townend et al., 2011). Rapid SLR induced marsh deterioration has already been observed in some regions (Kirwan and Guntenspergen, 2012), including the Delaware Bay (Stammerman and Piasecki, 2012).

According to Kirwan and Megonigal, 2013, mean RSL has risen 1 mm/yr for most of the last 2000 years, but the present rate is roughly 2-3 mm/yr. Vegetation has responded to this increased rate of rise, and, in New England, the inundation tolerant *Spartina alterniflora* has proliferated, replacing the prior occupant: the less flood resistant *Spartina patens* (Kirwan and Megonigal, 2013). Other estimates of recent rates of global sea level rise indicate 3.5 mm/yr (Webb et al., 2013). With ice sheet melt included in predictions, near future rates of sea level rise could reach 50 mm/yr (Kirwan and Megonigal, 2013). Most current models of increased rates of sea level rise, be they conservative or aggressive, at minimum predict the upland migration of the vegetated zones within marshlands and the loss of vegetation diversity (Fagherazzi et al., 2012), without consideration of the potential effects of anthropogenic barriers.

Additionally, in the face of quickly rising seas, the process of sediment autocompaction is one that some researchers believe needs to be included in measurements of past rates of accretion and predictions of future marsh survival. Sediment autocompaction can exert a major secondary control on marsh deposition and behavior, and it can limit the accuracy of estimates of paleo sea-level by distorting sedimentary stratigraphy. Autocompaction even has the ability to generate

accommodation space in peat marshes at the same rate as SLR, dramatically distorting stratigraphic sequences and introducing significant error into SLR rate estimates (Allen, 2000). Autocompaction can cause measurements of deeper sediments to appear to indicate successively lower accretion rates, even under constant sediment input rates (Bartholdy et al., 2010). Alternatively, other studies have suggested that autocompaction does not generate artificial sea level trends, despite the relative contribution of compaction to reconstructed sea level change being 12 percent (Brain et al., 2014). Brain et al. (2014), using a model that allowed samples to be returned to their original depositional altitudes via depth specific estimates of autocompaction, were able to define statistically significant relationships between organic content, initial void space, and compression indices which allowed for estimation of sediment-specific compression properties; their model shows that the maximum absolute contribution of autocompaction to sea-level reconstruction is 0.07 mm/yr, suggesting that it is possible to reliably compensate for autocompaction in paleo RSL reconstruction studies in marshes.

Anthropogenic controls on marsh evolution, such as embankments utilized by urban and agricultural practices, constrain upland migration of marshes, which could cause SLR to destroy marshes left with nowhere to relocate (Webb et al., 2013). Dams and reservoirs prevent roughly twenty percent of global sediment load from reaching coasts, and this effect, combined with reforestation and sediment control practices, could cause currently stable marshes to collapse in the future, even if SLR rates remain steady (Kirwan and Megonigal, 2013). With the aforementioned marsh controls and dynamics in mind, although they are far from exhaustive, it becomes evident that the salt marsh at Jones Narrows, not only an appropriate study area for late Holocene RSL trends, also provides an opportunity to study the powerful effects of human activity on salt marsh sedimentation, hydrology, and vegetation.

## 1.2 Research Questions

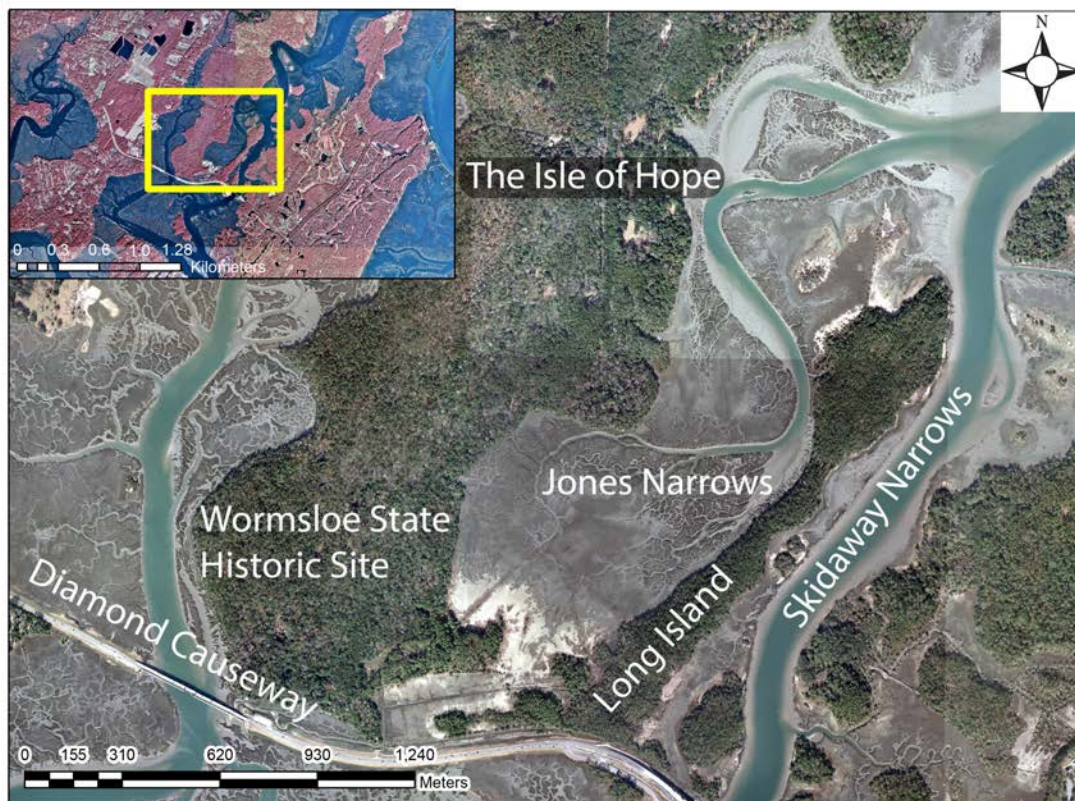
This study addresses the following questions: 1) What does the record of sedimentary deposition at Jones Narrows marsh reveal about late Holocene RSL?; 2) What is the nature of anthropogenic impacts upon the marsh, and can they be discerned and quantified through vibracore data analysis, radiocarbon analysis, and spatial analysis methods?; 3) Can XRF analysis reveal meaningful geochemical data that correspond with sedimentary facies and interpreted depositional environs?

The RSL reconstruction created by this research will be useful not only in helping to fill an important research gap, but, through comparison with previous Holocene RSL reconstructions, it can help confirm and inform RSL curves generated by other researchers. To be able to accurately and practically assess the nature of late Holocene RSL changes in the study area, anthropogenic impacts must also be investigated and quantified. This component of the research is not only important specifically to study area in question, but also in its potential application to the assessment of other similarly impacted modern marshes. Spatial analysis provides a crucial component of the characterization of the scale of anthropogenic impacts to the marsh in question, allowing for the area and volume of unnatural deposition to be measured in addition to generally documenting and the historic visible changes to the marsh topography, hydrology, and deposition. Building on the research methods of other geochemical investigations of Georgia barrier island system deposits (Meyer, 2013) the XRF investigations will allow for further analysis and quantification of the anthropogenic effects to marsh sediments, while also attempting to investigate the potential application of XRF data as a tool for the characterization and identification of salt marsh depositional subenvironments through statistical methods. In addition, the current study should provide a baseline in assessing the environmental history of

Jones Marsh. The Wormsloe State Historic Site is currently utilized for ecological research and an understanding of the lateral and vertical anthropogenic impacts resulting from the placement of dredged fill materials should assist in discerning natural and successional environments.

## 2 STUDY AREA

The study area of Jones Narrows is located on Wormsloe State Historic Site, which encompasses the southern half of Isle of Hope and its adjacent salt marshes (Fig. 2). Six vibracores were extracted from the marsh to the east of the southern tip of the Isle of Hope, and two were extracted from the more upland areas of the Isle.



*Figure 2: Study Area: Jones Narrows and surrounding area, 2012 TC satellite imagery; inset 1999 CIR imagery (imagery courtesy of UGA CGR)*

### 2.1 Geologic Setting

The Isle of Hope is situated 10 miles inland from the Atlantic Ocean and the modern barrier, Wassaw Island, and it is part of the barrier island complex that runs along the

southeastern coast of the United States. The study area lies within a section of the barrier island complex known as the Georgia Bight, a large regional embayment with the highest tides of the southern United States (Hubbard et al., 1979). This section of the coast is classified as mesotidal, with an average tidal range of 2.4 m and an average spring tide range of 3.4 m (Howard and Frey, 1985). The barrier islands of the Georgia coast are unique to the United States with their short curved compound beach ridges and relatively stable tidal inlets; all but two of Georgia's modern Holocene barriers are remnants of Pleistocene barriers upon which beach ridges have accreted during the Holocene epoch (Howard and Frey, 1980), forming "doublets" (Meyer, 2013) (Fig. 3b). The Pleistocene sequences of barriers, formed between ~110,000 and ~25,000 BP (years before present) (Howard and Frey, 1985), were produced by glacial melting induced submergences (Hoyt and Hails, 1967). Six major Pleistocene shorelines were created by this glacial melt pulsing, including the Wicomico (~29 to 30 m), Penholoway (~23 m), Talbot (~12 to 14 m), Princess Anne (~4.5 m), and the Silver Bluff (~1.5 m) (Hoyt and Hails, 1967) (Fig. 3a and 3c). The maximum sea level during the Quaternary in Georgia is considered to have formed the Wicomico Terrace coastal sedimentary deposits (Meyer, 2013). Radiocarbon dates suggest that the modern Holocene barriers formed prior to 4500 BP when sea level was 3.6 to 4.5 m below modern sea level (Hoyt, 1967). The Holocene components of the barrier islands represent the last 4000 to 5000 years of deposition, the amount of time elapsed since sea level reached its approximate current position following the Wisconsinian lowstand. While sea level appears to have reached ~1.5 to 2 m below MSL by 4500 BP, regression again lowered sea level to ~3 to 4 m around 3000 BP, with a subsequent transgression bringing sea level to its approximate modern elevation at ~2400 BP (Meyer, 2013).

## 2.2 Salt Marshes of the Georgia Bight

Another way in which the barrier island complex of Georgia differs from the rest of the US Atlantic Coast barriers is in that, due to the relatively higher mass flux of tidal water, the Georgia backbarrier area contains greater expanses of salt marshes and tidal streams (Hayden and Dolan, 1979). The backbarrier area of Georgia covers an area of  $\sim 1555 \text{ km}^2$ , most of which is intertidal, and much of which is dominated by marshes with small, dense, tidal drainages (Howard and Frey, 1985). Generally, the marshes of this expansive backbarrier area are veneers that overlie Pleistocene basement sediments (Basan and Frey, 1977; Frey and Basan, 1978).

The Isle of Hope was created as part of the Princess Anne Shoreline Complex, indicated by ichnofacies to have formed when sea level was  $\sim 4 \text{ m}$  above its current position, and these deposits reach a maximum elevation of approximately  $9 \text{ m}$  above modern sea level (Hoyt and Hails, 1967) (Fig. 3c). They are part of the Chatham Shoreline Sequence which includes the Pamlico, Princess Anne, and Silver Bluff Pleistocene deposits and the Holocene sea level sediments that lie to the east (Winker and Howard, 1977) (Fig. 3c). As indicated by this study, the modern salt marsh to the east of the Isle of Hope began accreting sediment during the late Holocene, initially covering the underlying Pleistocene sediments soon after sea level reached its approximate current level (2400 BP) and the modern transgression continued.

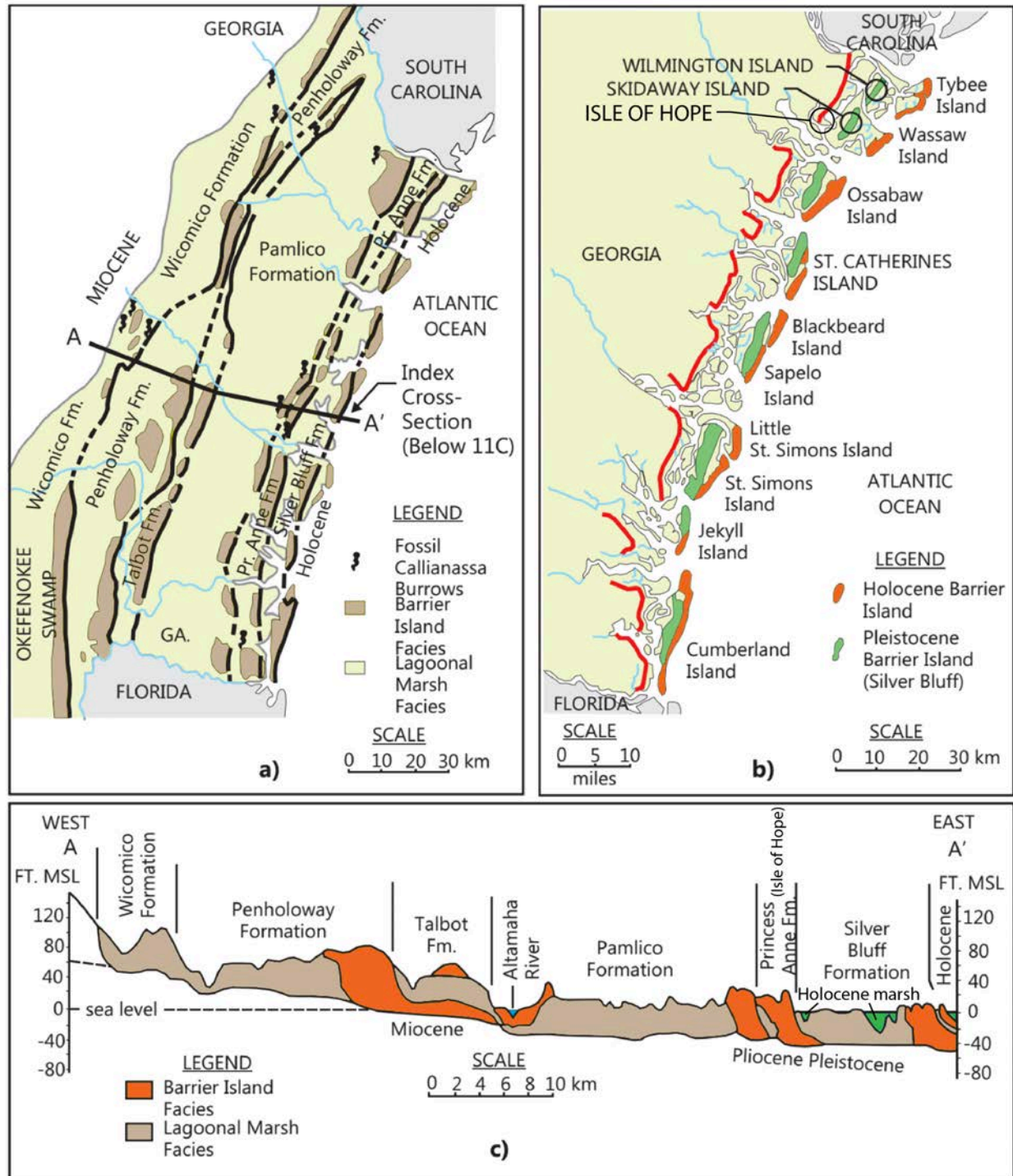


Figure 3: Successive shorelines of the Georgia Bight: a) Successive shorelines and marshes; b) Pleistocene and Holocene Shorelines; c) Cross-section of Pleistocene and Holocene formations on the Georgia Coastal Plain (modified from Meyer (2013); Hoyt (1969); Hoyt and Hails (1967))



### 2.2.1 Marsh Subenvironments and Sedimentation

Georgia's salt marshes occupy the upper extent of the intertidal zone, reaching as high as the mean high water spring tide, and they are the most common intertidal facies (Howard and Frey, 1985) (Fig. 4). This upper marsh boundary normally transitions into mainland environments or Pleistocene/Holocene barrier island remnants (Howard and Frey, 1980). The lower boundary of these marshes is usually an abrupt transition to a tidal stream bank (Howard and Frey, 1980). Within Georgia's salt marshes, low-marsh and high marsh areas are distinct sub-environments (Edwards and Frey, 1977), and the threshold between the two sub-environments lies around mean higher high water (Howard and Frey, 1980).

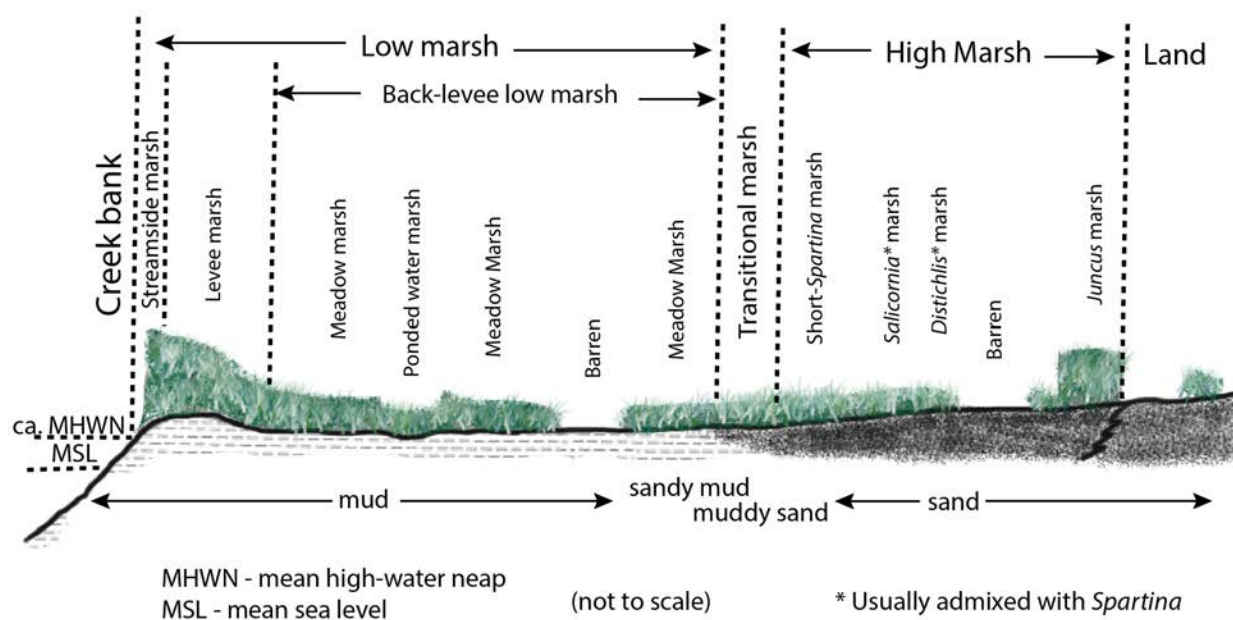


Figure 4: Salt marsh subenvironments (after Edwards and Frey, 1977)

While the transition from muddy low marsh to sandier high marsh is striking, several other smaller scale zones are discernible (Howard and Frey, 1985) (Fig. 4). The steeply sloping tidal stream banks that abut the low marsh, and they are capped by levees, behind which lies the

low marsh, analogous to fluvial floodplains (Frey and Howard, 1980). While sedimentary texture gradients show that there are nearly constant equal proportions of silt and clay throughout the marsh environment (Edwards and Frey, 1977), the sandy component of marsh sediment is more variable in concentration, becoming much more important in the transitional and high marsh (Howard and Frey, 1985). Quartz sand dominates the high marsh, with accessory mud, mica, and feldspar, all of which form discontinuous laminae in this setting (Edwards and Frey, 1980).



*Figure 5: Jones Narrows marsh and major subenvironments (facing east from The Isle of Hope, north of impacted marsh)*

Georgia's salt marshes are densely vegetated, especially by the salt marsh cordgrass *Spartina alterniflora*, the short form of which is characteristic of the high marsh, while the tall form of the grass dominates the low marsh (Howard and Frey, 1985) (Fig. 5). Higher elevation

portions of the high marsh are vegetated primarily by *Salicornia bigelovii* (glasswort), *Juncus roemarianus* (marsh rush), and the samphires (*Salicornia europaea*, *Salicornia virginica*) (Howard and Frey, 1980). The bivalve mollusk *Geukensia demissa* and the gastropod *Littorina littorea* (common periwinkle) are ubiquitous to both the high and low marsh, and the oyster *Crassostrea virginica* is commonly found in the tidal creek banks below the levee marsh (Howard and Frey, 1980). Marsh fiddler crabs, *Uca pugnax* are also present in high concentrations in Georgia's salt marshes.

The plant and animal populations of the Georgia salt marsh almost completely destroy any small scale sedimentary stratification (i.e., laminations) via bioturbation, and, although biogenic sedimentary structures are present throughout the marsh sub-environments, the high rate of bioturbation often obscures individual burrows (Edwards and Frey, 1980).

The rates of sedimentation on the marsh surface are highly variable seasonally, annually, and environmentally (Letzsch and Frey, 1980), with the mean rate of sedimentation increasing from the high marsh to the tidal stream-side levees (Howard and Frey, 1985). The fact that the high marsh environs are only inundated by the highest tides causes a low rate of accretion by suspended fine sediments (Frey and Basan, 1978). Most of the sands and some of the fines deposited on the marsh surfaces are derived from erosion of local Pleistocene and Holocene barrier island sediments, while a portion of the fines are derived from fluvial and offshore sources (Howard and Frey, 1980). Another substantial component of the mud content within the marsh also originates as fecal pellets and pseudofeces, rather than as flocculated clastic material, generated by suspension feeders like *G. demissa* (Howard and Frey, 1980), which also require vegetation and inundation.

### **2.3 History of Wormsloe and Jones Narrows Salt Marsh**

The first English colonist to settle on the Isle of Hope was Noble Jones, a Physician from Surrey, England, who was granted permission by the Trustees of Georgia to occupy the 822 acre plot and create Wormsloe Plantation in 1736. His ancestors have remained in constant ownership of some part of Wormsloe to this day, later under the surnames of DeRenne and Barrow. At the time of Jones' initial grant to the land, the tidal stream Jones Creek, which runs along the eastern margin of Wormsloe, functioned as the back door navigational avenue to Savannah for anyone who wished to approach the city more discreetly from the sea than was possible via Wassaw Sound or the mouth of the Savannah River itself. For this reason, Jones built a tabby fortification at the southern end of Wormsloe, which still stands today, along with garrison huts for the detachment of marines sent by the English to help repel Spanish soldiers and vessels approaching from the south (Swanson, 2012).

At the time of Noble Jones' arrival at the Isle of Hope, Wormsloe was covered by live oak hammocks, mixed pine forest, and some magnolia trees, with an understory featuring saw palmetto, scrub palmetto, and gallberry, with cabbage palm and bald cypress on the marsh margins. Wormsloe today still features much of the same vegetation, which has been modified to form its characteristic live oak-lined entrance road (Fig. 6). Until the time of slave emancipation, sea island cotton was grown at Wormsloe, along with corn. In addition to the biota noted above, the marsh also supports mullet, black drum, sheepshead, catfish, jackfish, marsh hens, osprey, and herons (Swanson, 2012).





*Figure 6: Wormsloe entrance road*

In the 1960s, the majority of Wormsloe was donated to the Nature Conservancy, which in turn gave the property to the State of Georgia one year later. The Georgia Department of Natural Resources (DNR) has managed the property since 1973, with the state owned portion of Wormsloe having been open to the public as a State Historic Site since 1979. More recently, the Wormsloe Institute for Environmental History (WIEH) was created, under the leadership of Ms. Sarah Ross. WIEH facilitates and promotes the preservation of Wormsloe through interdisciplinary academic study.

#### **2.4 Anthropogenic Impacts**

Aside from the impacts upon the marsh due to the operations of Wormsloe Plantation, ongoing anthropogenic activity has affected the marsh in ways that are still visible today. An

earthen causeway or dam was constructed during the US Civil War, connecting Wormsloe to Long Island (Rice et al., 2005), the lineation of which is discernible in satellite imagery and in person. An earthen battery was also built along the southern tip of the isle during the war, which still stands several meters higher than the surrounding forest floor. Construction of the battery likely had little impact on the marsh, but the causeway has affected hydrology in the area, and it forms the northern boundary of the impacted area examined by this study (Fig. 7 and 8).

The U.S. Army Corps of Engineers dredged the tidal stream known as Skidaway Narrows during the construction of the Intracoastal Waterway in 1910, which likely affected the tidal hydrology of the Jones Narrows marsh (Rice et al., 2005). By 1968, construction began on Diamond Causeway, a highway that runs past the southern tip of the Isle of Hope, connecting Skidaway Island to the mainland. Despite efforts to connect the tidal streams along the north side of the road, the causeway created a hydrologic barrier through its bisection of the marsh, isolating the Jones Narrows from flow coming from the south and east (Rice et al., 2005) (Fig. 7 and 8). The decreased drainage, stagnation, and evaporation of tidal flow that can still reach the upland areas created by the dredge sand has likely caused increased salinity of the sediment, limiting the ability of *S. alterniflora*, among other common biota, to survive on the flats (Pennings and Bertness, 2001).



*Figure 7: Impacted marsh area - 1951 aerial photograph; inset 1999 CIR imagery (imagery courtesy of UGA CGS)*





*Figure 8: Impacted marsh area - 2012 TC satellite imagery; inset 1999 CIR imagery (imagery courtesy of UGA CGR)*



### 3 RESEARCH METHODS

Stratigraphic methods were used to evaluate the dynamics of sedimentation and landscape evolution at the study site by investigating the vertical stratigraphy and depositional environmental successions in the vibracores. Spatial analyses assess the environmental progression during the Anthropocene in the GIS environment, and XRF analyses reveal the bulk geochemistry of the core sediments, which facilitates chemolog creation and the evaluation of the chemostratigraphy present in the marsh sediments

#### 3.1 Vibracoring Methods

Vibracoring is a technique that allows for continuous sediment core retrieval, preserving the stratigraphy and sedimentology of the sample in context (Howard and Frey, 1975). Limited in depth of penetration by the length of the aluminum core pipe and refusal by competent sediment or lithology, this method generates a sedimentary core with preserved sedimentary structures, fossils, and other biogenic material in their original context.

##### 3.1.1 Methodology

The aluminum core pipe is advanced into the substrate, with the vibration causing liquefaction of saturated sediment at the bottom edge of the pipe. The vibration of the pipe is achieved via the attachment of a concrete vibrator or head (Fig. 9b). The gasoline powered vibrator is clamped to the pipe at roughly eye level, and then the motor is initiated. While one individual controls the intensity of the vibration via controls on the engine, several others push the pipe into the ground by pulling down on the clamps that hold the vibrating rod head to the pipe. To fully advance the pipe into the subsurface, the point at which the vibrating rod is attached to the pipe must be raised several times and re-attached, as each interval of penetration is limited by the height at which the individuals advancing the pipe can reach. Once the core

encounters refusal or the pipe is fully advanced, the pipe is plugged to create a vacuum and is extracted from the subsurface with a chain hoist or come-along. Penetration depth is highly dependent upon the sediment pore water saturation and lithology. The core location is described, GPS coordinates and elevation are recorded, and vibration-induced compaction of the core is measured. This compaction value is determined by subtracting the depth to sediment within the core pipe from the depth to ground surface outside of the core pipe, prior to extraction. Once extracted, any loss of sediment from the bottom of the pipe is measured. The pipe is then trimmed of any excess empty length at the top of the core with a saw, and it is then cut into three sections of roughly equal length to ease transport. Each subsection of the core is labeled with respect to core location and directional relation to ground surface. The open ends of the core subsections are capped with plastic caps and/or duct tape to prevent loss of material.

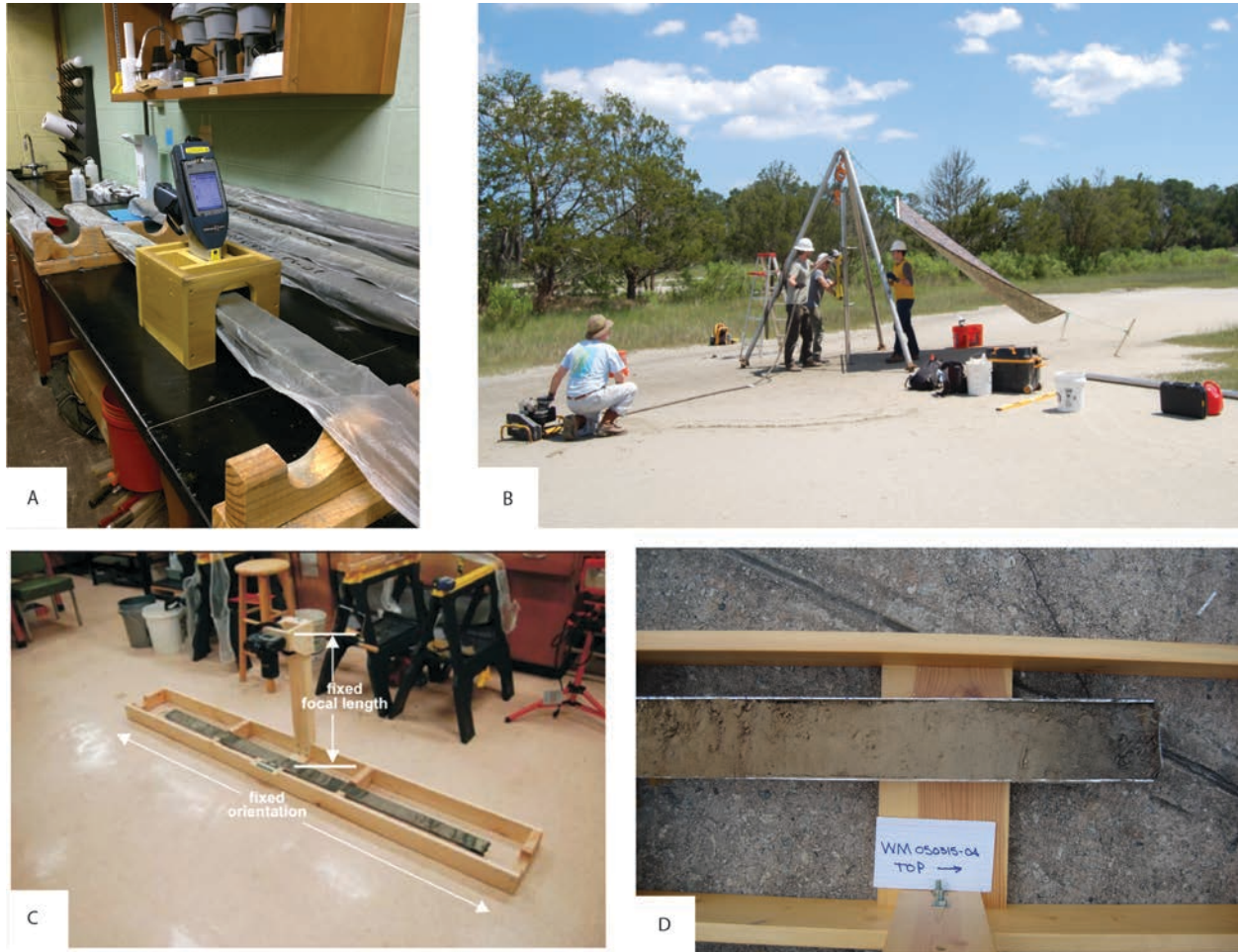


Figure 9: Vibracore extraction and analysis – a) Innov-X Systems  $\alpha$ -4000 XRF; b) Vibracore extraction on Jones Narrows; c) vibracore photo stand (Meyer, 2013); d) vibracore photo example

### 3.1.2 Data Processing

Once transported to the lab at Georgia State University, the core pipes were split in half lengthwise and prepared for description and photography (Fig. 9c and 9d). To cut each core section cleanly in half, each section is placed individually into a wooden core cutting box that allows for safer cutting. A hand-held circular saw is placed atop the cutting box, which only permits the blade of the saw through. This method prevents sediment and aluminum pipe cuttings from flying into the air. The saw blade is run along the length of the pipe, and then the core is rotated 180 degrees. The saw is run again along the length of the pipe to complete the cut

from the other side. With the two halves of the pipe still held together by hand, the core is removed from the cutting box and placed onto a core rack designed to hold lengths of core. The core section is then carefully pulled apart into halves, with careful attention to ensure that the sediment is cleanly split. Once separated into halves, the core sediment is cleaned for photography with a trowel or other bladed hand tool. One half of the core is wrapped in clear plastic wrap for archiving, and the other half is prepared for photography. The half chosen for photography is labeled at a 10 cm interval along one edge of the pipe. High-resolution photographs are taken of the core samples, which are set into a wooden photography stand for the process. The photo stand allows for constant camera height and angle. Each core requires several photographs in order to capture the entire core length. The core is advanced through the photo stand and photographed at an interval of roughly 0.5 meters. The series of photos that comprise the complete core are merged and aligned in Adobe Photoshop in order to create one complete image.

Sedimentary core logs are then created, describing sediment type, bedding and laminations, sedimentary structures, biogenic features, color, and more for each core. These logs are written out by hand, at first, as the core sediments are analyzed. Along with the written descriptions of the sediment, a hand drawn graphic log is created and inscribed alongside the descriptions, with different symbology used for the variety of lithologies and features present. Once the descriptive stage is completed, depositional environment interpretations are made based upon the facies descriptions. After the hand drawn logs are completed, a digital version is created which includes the high-resolution photographs of the cores in addition to the descriptions, environmental associations, and graphic lithologic logs (Fig. 10 and 11).

The depth of each core is corrected for field observed compaction in order to provide accurate elevations for radiocarbon samples and for cross-section representations. For the current study, total of 8 vibracores were extracted, with 6 extracted from the sand-flat covered section of Jones Narrows marsh and 2 extracted from the terrestrially vegetated southeastern edge of the Isle of Hope.


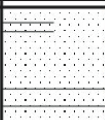

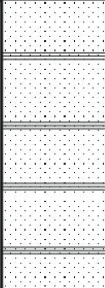

 <b>VIBRACORE BORING LOG</b> <i>Wormsloe</i>		<b>WM 050215-01</b> PAGE NO. 1 OF 2		
PROJECT NAME: <u>WORMSLOE STRATIGRAPHY RESEARCH</u>		TOTAL DEPTH: <u>5.51 METERS (COMPACTED)</u>		
W.O. NUMBER: <u>N/A</u>		NORTHING: <u>3,535,375</u>		
LOCATION: <u>JONES NARROWS MARSH, WORMSLOE S.H.S. ISLE OF HOPE, GA</u>		EASTING: <u>492,968</u>		
DRILLERS: <u>MEYER, VANCE, HUGHES, DOBSON, BANKHEAD</u>		GROUND SURFACE ELEVATION: <u>4.06 ft MSL</u>		
DRILL RIG TYPE: <u>UNIV. OF WEST GA VIBRACORE RIG</u>		DEPTH TO TOP OF CORE: <u>56 CM BTOP</u>		
DRILLING METHOD: <u>VIBRACORE</u>		HEIGHT ABOVE LAND SURFACE: <u>44 CM BTOP</u>		
SAMPLING METHOD: <u>3-INCH I.D. ALUMINUM PIPE</u>		COMPACTION (%): <u>2.1%</u>		
LOGGED BY: <u>JRH</u> WEATHER: <u>WARM/CLEAR</u>		BOREHOLE DIAMETER: <u>3-INCH BOREHOLE</u>		
DATE BEGUN: <u>05/02/15</u> DATE COMPLETED: <u>05/02/15</u>		LOGGER SIGNATURE: <u>JRH</u>		
DEPTH (m)	LITHOLOGIC DESCRIPTION	GRAPHIC LOG	PHOTOGRAPHIC LOG	COMMENTS
0	Sand, fine, w/ mudballs and some mud laminations, oxidation, shell fragments, color 10YR8/1 - 10YR4/6 - 10YR3/1			<del>land surface</del> Washover Fan Sequence
1.0	Sand, fine, w/ mud laminations and mud balls, liquid escape structures, color 10YR8/1 - 10YR3/1			Intertidal Sequence Low Marsh
2.0	Mud (clay/silt), with charcoal and plant material, color 2.5Y4/1 - 2.5Y2.5/1			
3.0				

Figure 10: Vibracore log form - WM050215-01 pg. 1


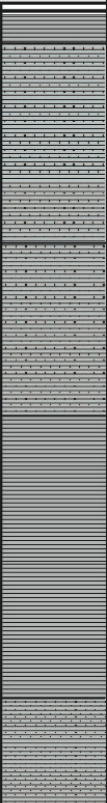

 <b>VIBRACORE BORING LOG</b> <i>Wormsloe</i>		<b>LOCATION NUMBER:</b> <b>WM 050215-01</b>		
		<b>PAGE NO. 2 OF 2</b>		
PROJECT NAME: <u>WORMSLOE STRATIGRAPHY RESEARCH</u>		TOTAL DEPTH: <u>5.51 METERS (COMPACTED)</u>		
W.O. NUMBER: <u>N/A</u>		NORTHING: <u>3,535,357</u>		
LOCATION: <u>JONES NARROWS MARSH, WORMSLOE S.H.S, ISLE OF HOPE, GA</u>		EASTING: <u>492,968</u>		
DRILLERS: <u>MEYER, VANCE, HUGHES, DOBSON, BANKHEAD</u>		GROUND SURFACE ELEVATION: <u>4.06 ftMSL</u>		
DRILL RIG TYPE: <u>UNIV. OF WEST GA VIBRACORE RIG</u>		DEPTH TO TOP OF CORE: <u>56 CM BTOP</u>		
DRILLING METHOD: <u>VIBRACORE</u>		HEIGHT ABOVE LAND SURFACE: <u>44 CM BTOP</u>		
SAMPLING METHOD: <u>3-INCH I.D. ALUMINUM PIPE</u>		COMPACTION (%): <u>2.1%</u>		
LOGGED BY: <u>JRH</u> WEATHER: <u>WARM/CLEAR</u>		BOREHOLE DIAMETER: <u>3- INCH BOREHOLE</u>		
DATE BEGUN: <u>05/02/15</u> DATE COMPLETED: <u>05/02/15</u>		LOGGER SIGNATURE: <u>JRH</u>		
DEPTH (m)	LITHOLOGIC DESCRIPTION	GRAPHIC LOG	PHOTOGRAPHIC LOG	COMMENTS
3.0	Mud (clay/silt) w/ some sand, fine, some plant fragments, color 10YR3/1 - 10YR7/2			Intertidal Sequence Low Marsh
4.0	Mud (clay/silt), w/ sand, fine, mottling, bioturbation, large shell(377-380cm), color 10YR3/1 - 10YR7/2			Intertidal Sequence Tidal Creek Levee
5.0	Mud(clay /silt), color 2.5Y3/1			Intertidal Sequence Low Marsh
	Mud (clay/silt) w/sand, fine, color 10YR3/1 - 10YR7/2			
6.0				

Figure 11: Vibracore log form - WM050215-01 pg. 2

## 3.2 XRF Methods

### 3.2.1 Methodology

X-Ray fluorescence (XRF) spectrometry is an analytical technique that is used to assess the elemental presence and abundance within a sample material. X-ray emissions are caused by the photoelectric effect, and a given x-ray source can cause the ejection of an electron from the inner shells of atoms within a sample. The source can be either a radioisotope source or an X-ray tube which emits radiation that impacts the sample material. After the interaction of radiation with the atoms in the sample, electrons will be ejected from the inner electron shells, while electrons from the outer shell will fill the empty inner shell void, emitting x-ray radiation characteristic of a given atom (Thomsen and Schatzlein, 2002). All of the elements in the given sample will generate a spectrum of x-rays, with each element generating several characteristic lines (Kalnicky and Singhvi, 2001). These lines are referred to as K-lines if caused by K-shell electrons or L-lines if emitted by L-shell electrons. These energies can be used to identify the elements and their concentrations within a given sample (Thomsen and Schatzlein, 2002).

Field-portable X-ray fluorescence (FPXRF) analyzers usually utilize energy dispersion for the separation of X-ray lines rather than the alternative wavelength dispersion. XRF units utilize X-ray detectors to convert the X-ray photon energies into quantifiable voltage pulses. There are several types of common detectors, and FPXRF units usually utilize solid state semiconductor detectors instead of gas flow proportional detectors or scintillation detectors, both of which offer reduced resolution, relative to the solid state detectors (Kalnicky and Singhvi, 2001).



### **3.2.2 Data Collection**

XRF data was collected from vibracores WM050215-03 and WM 050215-04 with an Innov-X Systems  $\alpha$ -4000 XRF unit, which is hand held, battery operated, and energy dispersive (Fig. 9a). The unit is capable of detecting elements with atomic numbers 15 (phosphorus) through 92 (uranium), with the ability to measure concentrations from ppm to 100 percent. The unit's excitation source is an X-ray tube with a W anode (10-40 kV, 5-50 uA), and the detector is a thermoelectrically cooled Si PiN diode with a resolution of <280 eV. The data storage and user interface computer is a detachable HP iPAQ which runs Windows CE. The Soil Analysis mode was used to analyze the core samples along with the additional Light Element Analysis Program (LEAP) mode. LEAP mode adds Ti, Ba, Cr, Cl, P, S, Ca and K to the suite of elements tested in the Standard Soil Analysis, which includes Pb, Cr, Hg, Cd, Sb, Ti, Mn, Fe, Ni, Cu, Zn, Sn, Ag, As, Se, Ba, Co, Zr, and Rb. Run in Sequential Testing mode, the FPXRF performs the Standard Test followed by the LEAP Test. The maximum testing time for each analysis was set at 60 seconds, which was the End Condition for each test. Prior to each session of analysis, a standardization plate was affixed to the analyzer and a standardization analysis was run. The Sequential Test was run on each core at a 10 cm interval, progressing down-core. The core sections were placed into a wooden mount that holds the halved cores horizontally for the analysis, with the open sediment side facing upward.

### **3.2.3 Data Processing and Analysis**

After the data collection, the results of the FPXRF testing were exported in a tabular .csv format from the HP iPAQ and imported onto a laptop computer. The exported table provides analysis date, reading numbers, testing mode, live time of test, standardization pass/fail info, elemental abundance values (ppm), and error values. Elements with insufficient abundance for

analysis read as <LOD, meaning the abundance of the given element was less than the Limit of Detection. Error for each reading are listed in the XRF Results tables in Appendix B. The bulk geochemistry values provided by the FPXRF analyses were then compared to the lithologic logs, photographic logs, and lithological descriptions in order to facilitate a chemostratigraphic study. Chemologs were created, displaying the lithologic and photographic data alongside the elemental data log plots, which show variation in abundance with depth.

It has been established that the environmental evolution of a landscape and information on the formation of a given sedimentary deposit can be gleaned from the geochemical signatures of the sediment, and, through chemostratigraphic study, the sedimentary sequence can be divided into geochemically distinct units (Montero-Serrano et al., 2010). The XRF data set was run through a matrix of intercorrelation program on Vassarstats.net to determine which elemental associations exist in all of the samples, with respect to all of those elements detected above LOD in every sample, plus sulfur. The data set was then broken down into descriptive lithological subsections, namely sands, muds, and shell lag deposits, and each lithologic subsection was then subjected to the same matrix of intercorrelation analysis.

Additionally, the selected analytes from the XRF data from Vibracores WM050215-03 and 050215-04 were subjected to multivariate cluster analysis using SAS (Statistical Analysis System) and Ward's method to determine if the data could be separated into geochemically and sedimentologically meaningful clusters. In Ward's method, which is a non-parametric test, the proximity between clusters is defined as the increase in the squared error when the clusters are merged, using the same objective function as the K-Means method, as utilized by Meyer, 2013.

### 3.3 Evaluation of Late Holocene Sedimentation Rate and Sea Level Rise

The relationship between salt marsh sub-environment sedimentation and mean sea level has been well established (Howard and Frey, 1980; Engelhart and Howard, 2012), and it is this established relationship that is used as a basis in the current study to reconstruct the Late Holocene sea level variation at Jones Creek Marsh. Together with the interpreted marsh subenvironmental deposits, gleaned from the vibracore lithostratigraphic data, radiocarbon data from organic material extracted from the cores were used to evaluate the relationship between the age of the deposited sediments and MSL elevation. All down-core depths and intervals utilized for radiocarbon analysis and RSL estimates have been corrected for compaction. Radiocarbon samples used in the evaluation of sea level conditions were comprised of biogenic materials associated with the given marsh environments known to be deposited, in-situ, in modern marshes, namely *Spartina* cordgrasses and native bivalves.

#### 3.3.1 Background

Georgia's salt marshes lie within the higher reaches of the intertidal zone, from mean neap high tide to mean spring high tide (Frey and Basan, 1978). The salt marsh sub-environments of the Georgia Bight are distinct and identifiable by evaluating the lithofacies, biofacies, and ichnofacies present (Edwards and Frey, 1977). Tidal stream channel banks demarcate the lower bound of the salt marsh, while the upper boundary generally lies in contact with the mainland or the remnants of Pleistocene or Holocene barrier islands (Frey and Howard, 1980). The upper bound of the low marsh, where it transitions to high marsh, lies at roughly higher high tide (mean annual higher of daily high tide) (Howard and Frey, 1980). Building on this, Engelhart and Horton, 2012, have established a method by which an indicative range (e.g., mean high water to mean tide level for low marsh deposits) is assigned to samples based upon

interpreted depositional environment with respect to a reference water level; in this case, mean tide level provides the sample with an indicative meaning.

With the relationships between MSL and salt marsh sub-environmental elevations in mind, a reconstruction and assessment of local sedimentation rate and Holocene sea level reconstruction is made possible via radiocarbon analysis of in-situ organic material, indicative range assessments, error calculations, and age data calibration.

### **3.3.2 Methodology**

Once selected and removed from the core sediments, the samples were rinsed with deionized water to remove attached sediment, and then oven dried in the lab at GSU at 100 °C degrees for up to 8 hours. The samples were then placed into small plastic bottles for shipment to the Center for Applied Isotope Studies (CAIS) at the University of Georgia for analysis. At the CAIS, the samples were chemically washed, dried, and subjected to accelerator mass spectrometry analysis to measure graphite  $^{14}\text{C}/^{13}\text{C}$  ratios using the CAIS 0.5MeV accelerator mass spectrometer. The ratios of  $^{13}\text{C}/^{12}\text{C}$  in the samples were measured with a stable isotope mass spectrometer and expressed as  $\delta^{13}\text{C}$  with respect to Pee Dee Belemnite. Uncalibrated dates for the samples were given in radiocarbon years before 1950, with error quoted as one standard deviation reflecting statistical and experimental errors, and the dates were corrected for isotope fractionation. The results returned from CAIS were calibrated for atmospheric  $^{14}\text{C}$  variability using the online CALIB 7.1 software (Stuiver and Reimer, 1993) and the IntCal13 and Marine13 databases (Reimer et al., 2013).

The data from radiocarbon analysis were used, together with lithostratigraphic data and facies interpretations, to evaluate the rate of late Holocene sedimentation on the paleomarch surface, and thus, the rate of local sea level rise for the same period of time. In addition, the

radiocarbon data were used in an attempt constrain the upper and lower bounds in years BP of natural marsh sedimentation at the site. Samples were selected from seemingly continuous low marsh deposits, from the underlying (assumed) Pleistocene deposits near the point of vibrocore refusal, and from the veneer of dredge sands that lie atop the marsh deposits. In the terminology established by Engelhart and Horton, 2012, it is important to establish the relationship of the sediment from which samples are extracted with respect to underlying, incompressible material, e.g., pre-Holocene sands. Samples pulled from the immediate contact zone between marsh sediments and the basal sands are considered base of basal, and thus likely free of compaction, while basal samples lie within the sedimentary unit directly overlying the incompressible unit and are potentially compacted, while intercalated samples are pulled from organic sediment positioned in between two clastic layers and are likely compacted (Engelhart and Horton, 2012). All samples used in the current study, aside from the dredge sand shell sample, can be considered basal or base of basal. Also after Engelhart and Horton, 2012, the methodology for estimating relative sea level for a given sample is performed using the following equation:

$$RSL_i = A_i - RWL_i$$

Where  $A_i$  is the altitude of the sample  $i$  and  $RWL_i$  is the reference water level of the sample, both expressed relative to the same tidal datum. For example, for low marsh samples in this study, the indicative range is the difference between mean high water and mean tidal level (~1.1m MHW - 0.0 MTL; Ft. Pulaski tide gauge), and the reference water level is estimated by dividing that difference by two ((MHW-MTL)/2). After Shennan and Horton, 2002, additional error is calculated using the equation:

$$E_i = (e_1^2 + e_2^2 + e_n^2)^{1/2}$$

in which each additional source of error is represented as  $e_1...e_n$ . These additional error sources account for altitudinal errors (survey errors), benchmark errors, sampling errors, borehole angle, and thickness of sample (Engelhart and Horton, 2012) (Table 1). The results of this error calculation for each sample are combined with the indicative range to arrive at the total RSL error.

*Table 1: Marsh sample errors (after Engelhart and Horton, 2012)*

Source of error	Example	Magnitude
Altitude	High precision surveying (e.g. total station)	$\pm 0.05$ m
	Position in tidal frame estimated salt marsh vegetation. Surface height is $(HAT-MTL)/2$	$\pm [(HAT-MTL)/2]$
	Offshore coring related to MTL	$\pm$ Tidal Range
Benchmark	NGS benchmark	$\pm 0.1$ m
Extrusion of sample	Angle of borehole	$\pm 1\%$ overburden
	Sampling error	$\pm 0.01$ m
	Compaction due to coring	$\pm 0.01$ m (for Russian hand corer) or author's correction for other devices (e.g., vibracorer)
Sample	Thickness of sample	$\pm$ Half of sample thickness

Once original depositional elevation and age range are established for the samples, rates of sedimentation and sea level rise can be calculated for Jones Creek marsh and compared to other Atlantic coast Holocene sea level reconstructions.

### 3.4 Spatial Analysis

Spatial analysis was performed to confirm the timing and magnitude of impacts from the construction of the Diamond Causeway and to evaluate the concurrent and subsequent transformation of subenvironments within the impacted area.

#### 3.4.1 Methodology

Historical maps, aerial imagery, and satellite imagery were used as sources for spatial analysis of the study area, with specific attention to the area and volume of the lens of dredge sand that covers portions of the marsh after the construction of Diamond Causeway. The

historical maps were used to assess the evolution of the landscape between the late 18th century and 2015. The database of imagery used for these analyses were provided by Dr. Tommy Jordan at the University of Georgia Center for Geospatial Research. The imagery were georectified using ground control points (GCPs) collected in the field with a Trimble GPS unit.

Shapefiles were generated to quantify the impacted areas and the transformation of subenvironments after the deposition of the Diamond Causeway dredge material. At the time of the deposition of the dredge sand atop the marsh, several salt marsh sub-environments occurred at the surface within the study area. Analysis of the shapefiles reveals the total area covered by the dredge sand between the original time of deposition and present day. Additionally, the present volume of the sand lens was estimated via a combined analysis of the satellite and aerial imagery, along with the sedimentary logs of the Vibracore data. The extent of the fill placement was estimated using the 2012 satellite imagery, and LiDAR digital elevation model (DEM) was used for the present surface elevation values. The Vibracore data provided the average elevation of the former, pre-dredge sand cover, marsh. In ArcMap 10.4, the 3D Analyst Volume Fill function was used to approximate the volume.

### **3.4.2 Data Sources**

#### *Historical Maps (year CE listed with title if applicable)*

- 1780 Map
- 1816 Map (McKinnon)
- 1867 T-Sheet
- 1890 Map (Blanford)
- 1908 Map
- 1912 USGS Topographic Map

- 1933 USCGS T-Sheet (Air Photo Compilation No. T-5214)
- 1935 USCGS T-Sheet (Savannah River and Wassaw Sound)
- 1944 USCGS T-Sheet (Savannah River and Wassaw Sound)
- 1945 USGS 7.5 Minute Topographic Map (Isle of Hope Quadrangle)
- 1957 USGS 7.5 Minute Topographic Map (Isle of Hope Quadrangle)
- 1960 Property Map (Hutton)
- 1988 USGS 7.5 Minute Topographic Map (Isle of Hope Quadrangle)

*Aerial and Satellite Imagery*

- 1951 USGS Black and White Aerial Photograph
- 1956 USGS Black and White Aerial Photograph
- 1961 USGS Black and White Aerial Photograph
- 1968 USGS Black and White Aerial Photograph
- 1971 Black and White Aerial Photograph
- 1972 True Color Aerial Photograph
- 1974 Black and White Aerial Photograph
- 1976 Black and White Aerial Photograph
- 1988 Black and White Aerial Photograph
- 1993 Black and White Aerial Photograph
- 1999 CIR Aerial Imagery
- 2003 True Color Satellite Imagery
- 2009 True Color Satellite Imagery
- 2009 LiDAR DEM
- 2012 True Color Satellite Imagery



## 4 RESULTS

The results of this study are provided in the subsequent sections, which include vibracore lithologic data, XRF analyses, stratigraphic cross-sections, Late Holocene relative sea level/sedimentation trends, and spatial analyses.

### 4.1 Vibracoring Results

A total of eight vibracores were extracted for the purposes of this study, six of which were collected from Jones Narrows Marsh, while the remaining two were extracted from the terrestrially vegetated upland Isle of Hope itself, to the southwest of the marsh cores (Table 2, Fig. 12). The cores were extracted on May 2nd and 3rd, 2015. The core locations were situated within the areas of Jones Marsh that were suspected to have been impacted by dredge fill operations associated with the construction of the Diamond Causeway based on aerial imagery. The vibracore log forms are attached in Appendix A.

*Table 2: Vibracore locations and depths*

Boring ID	Date	Latitude	Longitude	Easting	Northing	Surface EL (ft)	Total Depth (cm) Recovered	Total Depth (cm) Original	Compaction (%)
WM050215-01	5/2/2015	31.9543	-81.0744	492,968.00	3,535,375.00	4.06	554.0	566.0	2.1%
WM050215-02	5/2/2015	31.9540	-81.0736	493,045.00	3,535,343.00	4.49	519.0	545.0	4.8%
WM050215-03	5/2/2015	31.9536	81.0723	493,165.00	3,535,298.00	4.48	550.0	553.0	0.5%
WM050215-04	5/2/2015	31.9533	-81.0716	493,238.00	3,535,265.00	3.91	496.0	554.0	10.5%
WM050315-01	5/3/2015	31.9529	-81.0704	493,345.83	3,535,220.87	4.80	548.0	570.0	3.9%
WM050315-02	5/3/2015	31.9545	-81.0727	493,132.08	3,535,398.01	3.85	365.0	470.0	22.3%
WM050315-03	5/3/2015	31.9527	-81.0768	492,744.99	3,535,193.07	5.31	464.0	501.0	7.4%
WM050315-04	5/3/2015	31.9529	-81.0768	492,739.04	3,535,221.28	10.77	289.0	325.0	11.1%

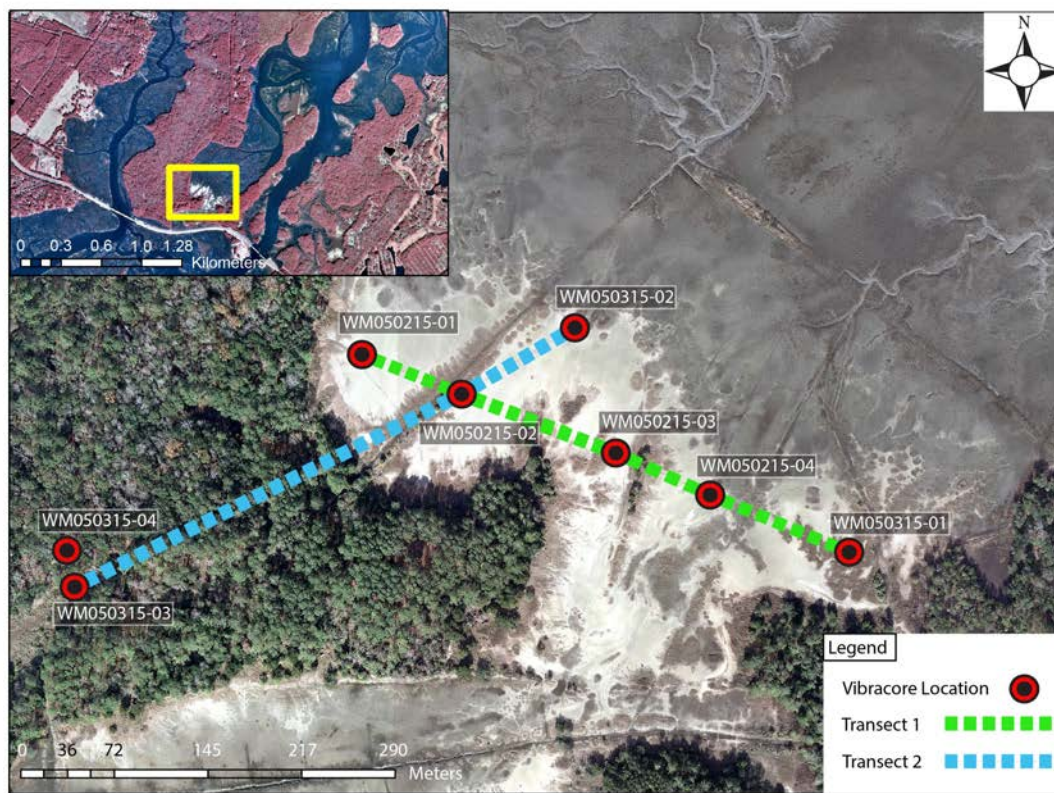


Figure 12: Jones Narrows transects and vibracore locations. 2012 TC satellite imagery; inset 1999 CIR imagery (imagery courtesy of UGA CGR)

#### 4.1.1 Jones Narrows Marsh Transect 1

Five vibracores (WM050215-01, WM050215-02, WM050215-03, WM050215-04, and WM050315-01) form Transect 1, which runs for ~409m at ~N60W from the Isle of Hope to Long Island (Fig. 12). WM050215-01 lies at the westernmost end of the transect, ~45m east of the Isle of Hope, and WM050315-01 lies at the easternmost end, roughly 20m northwest of Long Island. All five of the cores were extracted from marsh surface that is currently or has been covered by the veneer of dredge sand imparted by the Diamond Causeway construction. All

vibracore depth values in the following results sections are reported as compacted values, unless noted. Three of the cores in this transect reached maximum (compaction corrected) potential pipe penetration below land surface of 5.5m, and two of the five (WM050215-03 and WM050215-04) penetrated a densely compacted bioturbated gray/green muddy fine sand interval at ~5m BLS. This interval of sediment, in both cases, abruptly transitions into muddy fine sand above, with discontinuous mud lenses and multiple burrows present. The dense bioturbated muddy fine sand layer conforms with the “laminated” assumed Pleistocene facies described by Howard and Scott, 1983, which they interpret to be analogous to foreshore deposits. These deposits within the cores extracted for the current study are overprinted by intense mottling and terrestrial biofacies burrows. In WM050215-03, the foreshore deposit is capped by what may be a paleosol, indicating consistent terrestrial sub-aerial exposure prior to the subsequent deposition of the overlying Holocene marsh mud. In WM050215-04, the “laminated” facies is capped by a thin (5cm) bioturbated interval of charcoal material (460-465 cm BLS), again indicating sub-aerial exposure prior to the Holocene marsh mud deposition.

The three easternmost cores of Transect 1 penetrated a shell rich facies indicative of a tidal creek or creek bank depositional environments at ~3-4.5m BLS (Fig. 13). The shell rich intervals in all three cores are interpreted to be channel lag, with ubiquitous small bivalve shells, both whole and fragmented. This interval within WM050215-03 contains mostly whole and fragmented *Mulinia lateralis* (dwarf surf clam), with some fragments of *Dinocardium robustum* (Atlantic giant cockle), *Geukensia demissa* (Atlantic ribbed marsh mussel), and *Argopecten irradians* (Atlantic bay scallop). *M. Lateralis* is somewhat less dominant in WM050215-04, with many whole disarticulated *D. robustum* present. One very large (~9 cm) *Mercenaria mercenaria* is present in the shell lag interval of WM050215-03 at ~380 cm BLS. The matrix holding

together the shell lag material in all three cases consists mostly of fine sand with some mud. In all three instances of the shell lag facies, the interval is overlain and underlain by high or low marsh muddy deposits (Fig. 13). Aside from the shell lag intervals described above, the dense muddy fine sand facies at the base of WM050215-03 and WM050215-04, and the dredge sand that caps the cores, all of the deposits that are present within the rest of the cores within this transect are composed of either mud or muddy sand facies associated with the high marsh, low marsh, and tidal creek levee (or creek bank) depositional environments.

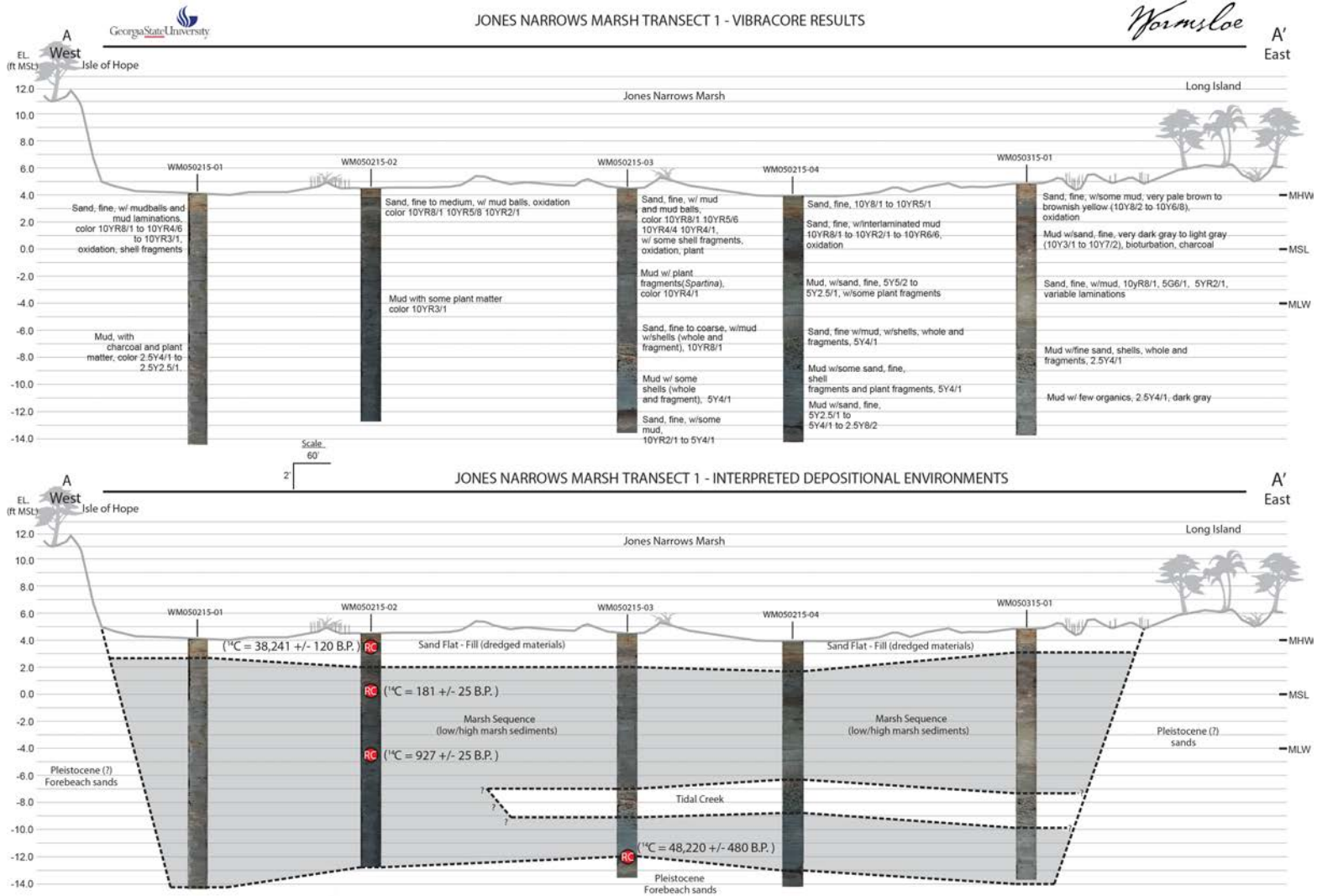


Figure 13: Jones Narrows Transect 1 cross-sections (corrected for compaction)

#### **4.1.2 Jones Narrows Marsh Transect 2**

Transect 2 is composed of three vibracores and intersects Transect 1 at vibracore WM050215-02, which it shares with Transect 1 (Fig. 14). Transect 2 runs for ~440 m at N55E, with WM050315-03 at its southwestern end and WM050315-02 at its northeastern end. Lying north of Transect 1, WM050315-02 is composed of a ~20 cm cap of dredge sand overlying an interval high/low marsh muddy sediment that is continuous down to its lower terminus at 365 cm BLS. This stratigraphy nearly mirrors that of the nearby WM050215-02, although WM050315-02 does not penetrate the same depth as WM050215-02. WM050315-03, however, differs substantially from the rest of the cores within Transect 2 and Transect 1 in its proximity to Diamond Causeway. This decreased distance from the source of the dredge sand that was deposited throughout the marsh during the construction of the causeway is likely the reason for the ~1m of sand that lies atop the marsh mud deposits within WM050315-03 (Fig. 14). The marsh surface that was covered by the sand within this core would have originally been at roughly the same elevation as that found in the rest of the cores in Transect 1. At the time of core extraction, unlike the previously described cores, the area surrounding WM050315-03 was vegetated by the terrestrial plants found throughout the rest of the Isle of Hope, and there are ~20 cm of O Horizon soil in the top of the core. Historical aerial imagery shows that, prior to the causeway construction, the marsh location of WM050315-03 lay only a few meters from the edge of the Isle of Hope.

#### **4.1.3 WM050315-04**

The final core collected, WM050315-04, was extracted from the Isle of Hope, roughly 30m northwest of WM050315-03 (Fig. 12). The location of the core was part of the isle prior to the construction of Diamond Causeway; its location is not part of the upland hammock

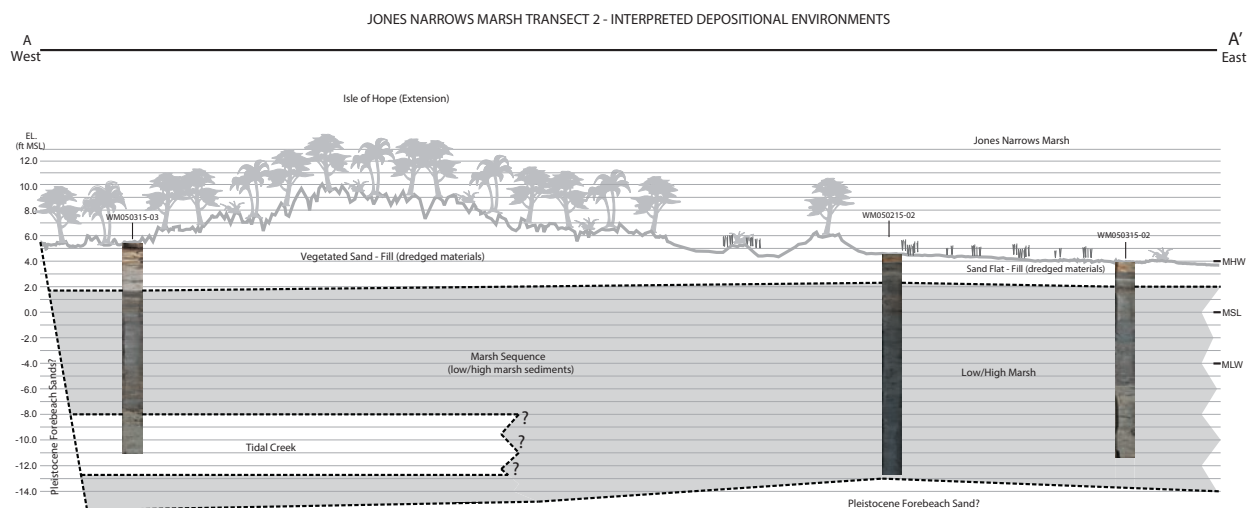
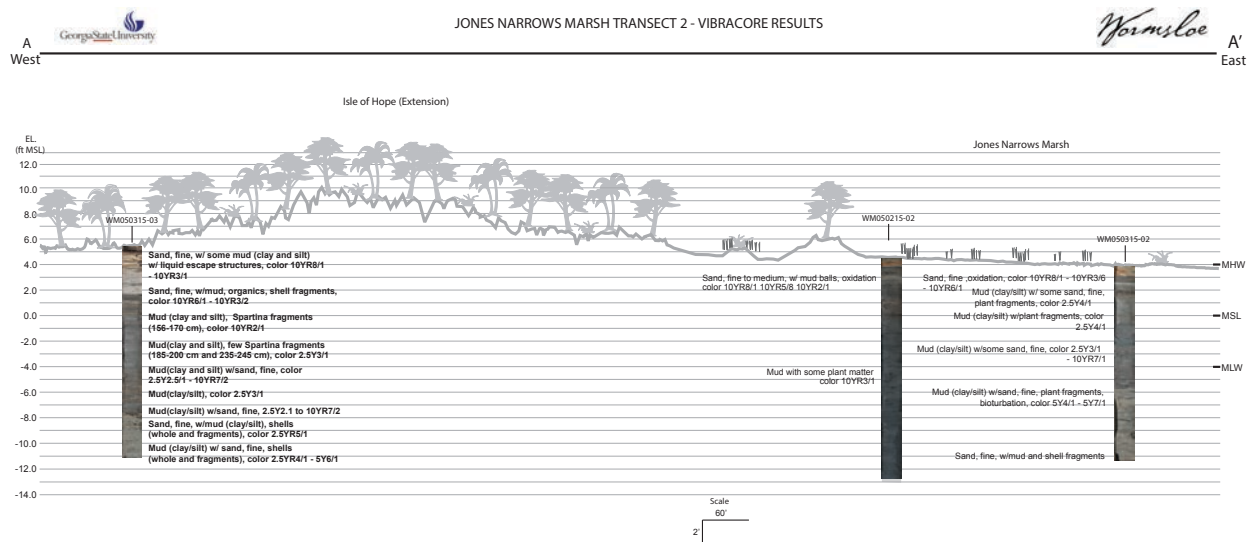


Figure 14: Jones Narrows Transect 2 cross-section (corrected for compaction)

added by the dredge sand fill material or overwash. As in WM050315-03, WM050315-04 is capped by a layer of humus, ~10 cm. Below the humus layer, however, the core is composed of fine sand, light brown/tan with some oxidation and mottling, down to its terminus of penetration at ~385 cm BLS. Bioturbation appears to have removed any clearly defined laminae throughout the core. Several discontinuous and faint laminae are visible in the lowest 20 cm, with one



oxidized lamination at ~350 cm BLS dipping at ~20 degrees, but no other well defined strata are present. The color of the sand does gradually lighten with depth, starting at 10YR6/2 at 20 cm BLS and lightening to 10YR8/3 at ~385 BLS. The deposits in this core fit the description of Pleistocene “mottled” facies described by Howard and Scott, 1983, which they interpret to be beach dune deposits.

## **4.2 XRF Results**

The initial results of the XRF analysis show that, out of 102 readings taken from cores WM050215-03 and WM050215-04, many elements were measured above the limit of detection (LOD) in every sample, including Cl, K, Ca, Ti, Mn, Fe, Rb, Sr, and Zr. Montero-Serrano et al., 2010, have shown that, because hydraulic sorting, weathering, and diagenesis can alter the geochemical composition of basin sediments, emphasis should be placed on variations in the relatively immobile elements such as Ti and Zr, the low mobility of which, during sedimentary processes, enables better characterization of source rock compositions and paleo-climatic conditions. In addition, attention has been given to those elements that have shown strong associations in the matrix of intercorrelations statistical analysis. Other elements measured at levels above detection in most of the samples include S, Cr, Ba and Cu.

### ***4.2.1 Chemostratigraphic Results***

Analysis of the chemologs represented in graphical form alongside their respective stratigraphic sections has produced the following results. Core WM050215-03 shows coincident Ca and Sr peaks just above and below 400 cm below ground surface. Core WM050215-04 shows similar Ca/Sr peaks around 300 cm below ground surface. These distinct peaks coincide in the stratigraphic sections with the sandy mud facies containing abundant shell material, interpreted to be tidal creek deposits. Below these Ca/Sr peaks in both cores is another visibly distinct trend,



manifested in the concentrations of K, Ti, and Fe. In WM050215-03, starting at ~400 cm below ground surface and terminating at 500 cm below ground surface, is an increase in K, Ti, and Fe content, with concentration values higher for all three elements than anywhere else in the chemolog. A similar distinct increase in concentration of the same three elements is present in the WM050215-04 chemolog, although at the interval from ~350 cm to ~450 cm. These increased concentrations coincide, in both cores, with muddy facies containing some sand, shell, and plant material, interpreted to be low marsh or tidal creek levee deposits. In both cases, these K/Ti/Fe deposits are overlain directly by tidal creek deposits and underlain by uniquely dense blue/green (Munsell Color 5Y4/1) muddy sand deposits, interpreted to be the Pleistocene island core deposit. The Pleistocene intervals are clearly visible in the chemologs, coincident with abrupt decreases in K, Ti, and Fe in both cores, while the Fe values do rebound with increased depth in WM050215-04. While the Pleistocene interval shows an abrupt increase in Zr in WM050215-03, it is coincident with an abrupt decrease of Zr in WM050215-04. The interpreted dredge sand intervals stand out from the marsh muds that they overlie in both cores with distinctly low K and Fe values and high Zr values.

#### **4.2.2 Correlation Analysis**

The XRF data set was processed through a matrix of intercorrelation program on vassarstats.net to determine which elemental associations exist in all of the samples, with respect to all of those elements detected above LOD in every sample, plus sulfur (see Table 1). The XRF data set was then broken down into descriptive lithological subsections, namely sands, muds, and shell rich deposits. The same matrix of intercorrelation analysis was then run on each of these descriptive lithological subsections. When analyzed as the raw matrix of intercorrelations output in tabular form, the following associations were detected in the samples. Within the complete

data set, strong correlations ( $<0.8$ ) are present between K/Ti, K/Fe, and Ca/Sr. Moderately strong correlations ( $<0.7$ ) are present in K/Rb, Ti/Fe, and Fe/Rb (Table 3a). Within the sandy facies subsections, very strong correlations ( $<0.9$ ) are present in K/Sr and Sr/Ba (Table 3c). Strong correlations are present within the sandy sections

Table 3: Matrices of intercorrelation. a) complete data set; b) muddy intervals; c) sandy intervals; d) shell rich intervals

A

Correlation Matrix - Complete Data Set  
Number of Variables = 11  
Observations per variable = 102

r	S	K	Ca	Ti	Mn	Fe	Rb	Sr	Zr	Ti/Zr	Fe/K
S	1										
K	0.152	1									
Ca	0.022	-0.187	1								
Ti	0.034	0.835	-0.322	1							
Mn	0.072	0.536	-0.095	0.427	1						
Fe	0.337	0.871	-0.26	0.705	0.556	1					
Rb	0.239	0.718	-0.312	0.492	0.438	0.761	1				
Sr	-0.062	-0.096	0.891	-0.215	-0.09	-0.274	-0.314	1			
Zr	-0.25	-0.174	-0.047	0.207	-0.257	-0.424	-0.454	0.045	1		
Ti/Zr	0.274	0.422	-0.229	0.195	0.377	0.634	0.806	-0.285	-0.701	1	
Fe/K	0.442	0.55	-0.229	0.394	0.406	0.866	0.635	-0.311	-0.547	0.671	1

B

Correlation Matrix - Muddy Intervals  
Number of Variables = 12  
Observations per variable = 51

r	S	K	Ca	Ti	Mn	Fe	Rb	Sr	Zr	Ba	Ti/Zr	Fe/K
S	1											
K	-0.092	1										
Ca	0.394	0.055	1									
Ti	-0.187	0.802	-0.081	1								
Mn	-0.058	0.467	0.085	0.331	1							
Fe	0.045	0.902	0.07	0.612	0.489	1						
Rb	0.108	0.494	0.051	0.124	0.247	0.623	1					
Sr	0.16	0.538	0.428	0.507	0.264	0.321	0.072	1				
Zr	-0.127	0.076	-0.09	0.586	-0.107	-0.129	-0.491	0.208	1			
Ba	-0.127	0.914	-0.024	0.75	0.553	0.871	0.493	0.412	0.062	1		
Ti/Zr	0.126	0.09	-0.036	-0.218	0.185	0.349	0.788	-0.283	-0.662	0.152	1	
Fe/K	0.281	0.158	0.082	-0.127	0.178	0.545	0.505	-0.224	-0.407	0.263	0.568	1

C

Correlation Matrix - Sandy Intervals  
Number of Variables = 12  
Observations per variable = 11

r	S	K	Ca	Ti	Mn	Fe	Rb	Sr	Zr	Ba	Ti/Zr	Fe/K
S	1											
K	0.047	1										
Ca	0.644	0.403	1									
Ti	0.022	0.498	0.38	1								
Mn	0.122	0.779	0.536	0.833	1							
Fe	0.321	0.815	0.637	0.712	0.792	1						
Rb	0.081	0.81	0.543	0.545	0.718	0.673	1					
Sr	0.129	0.948	0.523	0.391	0.663	0.79	0.863	1				
Zr	0.259	0.491	0.265	0.77	0.627	0.561	0.611	0.438	1			
Ba	0.1	0.887	0.383	0.358	0.547	0.697	0.792	0.909	0.484	1		
Ti/Zr	-0.336	0.05	0.195	0.317	0.293	0.254	-0.083	-0.021	-0.358	-0.135	1	
Fe/K	0.57	-0.032	0.582	0.481	0.267	0.527	0.058	0.028	0.25	-0.067	0.339	1

D

Correlation Matrix - Shelly Interval  
Number of Variables = 11  
Observations per variable = 21

r	S	K	Ca	Ti	Mn	Fe	Rb	Sr	Zr	Ti/Zr	Fe/K
S	1										
K	0.185	1									
Ca	0.286	-0.375	1								
Ti	0.156	0.935	-0.573	1							
Mn	0.162	0.776	-0.194	0.733	1						
Fe	0.203	0.87	-0.267	0.851	0.914	1					
Rb	0.011	0.921	-0.494	0.922	0.706	0.838	1				
Sr	0.397	-0.223	0.852	-0.447	-0.17	-0.258	-0.43	1			
Zr	-0.146	0.345	-0.462	0.452	0.014	0.026	0.463	-0.374	1		
Ti/Zr	0.226	0.594	-0.357	0.6	0.625	0.751	0.518	-0.3	-0.368	1	
Fe/K	0.256	0.569	-0.012	0.558	0.888	0.878	0.538	-0.088	-0.244	0.632	1

between K/Fe, K/Rb, K/Ba, Ti/Mn, and Rb/Sr. Moderately strong correlations are present in K/Mn, Ti/Fe, Ti/Zr, Mn/Fe, Mn/Rb, Fe/Sr, and Rb/Ba. Within the muddy subsections, very

strong correlations are present in K/Fe and K/Ba, with strong correlations present in K/Ti and Fe/Ba and Ti/barium only exhibit a moderately strong correlation. In the shell rich subsections, very strong correlations are present in K/Ti, K/Rb, Ti/Rb, and Mn/Fe, while strong correlations are present in K/Fe, Ca/Sr, Ti/Fe, and Fe/Rb (Table 3d). Moderately strong correlations occur within K/Mn, Ti/Mn, and Rb/Mn.

#### **4.2.3 Cluster Analysis**

Using Ward's method for multivariate cluster analysis, the geochemical data were run through SAS with the number of clusters set to 3, 4, 5, and 6. The data presented here reflect the 3 cluster setting for WM050215-03 and the 5 cluster setting for WM050215-04. These numbers of clusters were selected for the given cores because fewer clusters than the chosen numbers placed the vast majority of the data into one cluster, while a greater number of clusters placed less than 3 data points into multiple clusters.

Analysis of WM050215-03 produced 3 clusters, A<sub>3</sub>, B<sub>3</sub>, and C<sub>3</sub>. Cluster A<sub>3</sub> contains 40 of the 54 readings, while Cluster B<sub>3</sub> contains 12 readings, and Cluster C<sub>3</sub> contains 2 of the readings (Fig. 21). All of the lithologically shell rich intervals were placed into Clusters B<sub>3</sub> and C<sub>3</sub>. Similarly, all of the readings of material whose facies were interpreted to be analogous with tidal creek or tidal creek bank deposits were placed into Clusters B<sub>3</sub> and C<sub>3</sub>. Cluster A<sub>3</sub> contains all of the muddy sand facies readings except for 1 out of 14 total readings (93%) with the same facies description. Cluster A<sub>3</sub> also contains 36 out of 41 total readings, or 87%, with the muddy facies description, which, likewise, means that 36 out of 41 of the total low marsh subenvironmental interpreted deposit intervals are also included in Cluster A<sub>3</sub>. Cluster A<sub>3</sub> also contains 100% of both the high marsh interpreted deposits (2 of 2) and the Pleistocene "forebeach" sand deposits (5 of 5), as well as 86% (6 of 7) of the dredge sand deposits.

Core WM050215-04 best responded to the 5 cluster treatment, and its clusters are labeled A<sub>4</sub>, B<sub>4</sub>, C<sub>4</sub>, D<sub>4</sub>, and E<sub>4</sub> (Fig. 22). Despite the higher number of clusters, the 48 readings are spread more evenly between the clusters in WM050215-04, with 15 in Cluster E<sub>4</sub>, 14 in A<sub>4</sub>, 12 in B<sub>4</sub>, 4 in D<sub>4</sub>, and 3 in C<sub>4</sub>. Cluster E<sub>4</sub> is dominantly composed of mud rich intervals, with the only other lithology present in the cluster being the entirety of the muddy sand facies intervals (4 of 4) interpreted to be the Pleistocene “forebeach” deposits from the base of the core. Cluster A<sub>4</sub> is sandier, containing 4 of the 5 total dredge sand intervals from the core, in addition to the majority of the high marsh sandy mud deposits. Cluster B<sub>4</sub> features nearly an even split between low marsh muds and high marsh sandy muds (6 to 5), with one dredge fill deposit interval present. Clusters C<sub>4</sub> and D<sub>4</sub> contain 100% (7 of 7) of the tidal creek shell-rich deposit intervals within the core, which make up the entirety of both clusters.

### **4.3 Evaluation of Late Holocene Sedimentation Rate and Sea Level Rise**

#### **4.3.1 Radiocarbon Data**

One radiocarbon sample composed of charcoal was extracted and submitted from the dense muddy fine sand at the base (500cm BLS) of WM050215-03 (Sample WM08; AMS 14C = 48,220 +/- 480 B.P.), while three radiocarbon samples were extracted and submitted from WM050215-02 (WM03; AMS 14C = 33,710 +/- 120 B.P.; WM25; 1000 +/- 25 B.P.; WM26; 160 +/- 25 B.P.) (Table 4). The ages are reported as years before present (B.P.) with respect to 1950 CE. Sample WM03 was composed of small bivalve shell fragments extracted from the dredge sand material at the top of the core (36cm BLS), while samples WM25 and WM26 were *Spartina alterniflora* fragments or macrofossils extracted from continuous low marsh muds (280cm BLS and 135 BLS, respectively) within the core.

*Table 4: Radiocarbon samples*

Sample ID	UGA MS#	Material	14C Age	Years BP (+/-)	$\delta^{13}C$	Calibrated Deposition year (+/-) 2 $\sigma$
WM03	24035	marine shell	33710	120	0.6	35666 BCE 358
WM08	24036	charcoal	48220	480	-29.3	N/A N/A
WM25	24037	plant macrofossil	1000	25	-14.8	1017 CE 32
WM26	24038	plant macrofossil	160	25	-14.3	1753 CE 30

#### **4.3.2 Calibrated Radiocarbon Data**

The radiocarbon samples were calibrated with the CALIB 7.1 software, with the plant macrofossils and charcoal calibrated to the IntCal13 curve and the marine shell material calibrated to the MARINE13 curve. Once run through the CALIB 7.1 software, the ages of the samples from WM050215-02 were updated as follows, and are reported in years of the Common Era or Before Common Era (CE/BCE) with a 95.4% CI (2 $\sigma$ ): (WM03; AMS 14C = 35,362 +/- 635 (2 $\sigma$ ) BCE.; WM25; 1017 +/- 30 (2 $\sigma$ ) CE; WM26; 1753 +/- 32 (2 $\sigma$ ) CE) (Table 4). Sample WM08, extracted from WM050215-03, was not able to be calibrated via the software due to the age representing greater than 50,000 years Cal BP, “radiocarbon infinity,” and is only reported in its uncalibrated form.

#### **4.3.3 Late Holocene Sedimentation Rate and Sea Level Rise**

With the calibrated radiocarbon ages and relative sea level elevations calculated for the samples, interpreted sedimentation rate and, thus, RSL change can be calculated for the paleommarsh (Fig. 15). For core WM050215-02 the calculation yields a rate of sedimentation and RSL rise, from 1017 CE to 1753 CE (Interval A), of 2.1 mm/year. As indicated by data from the same core, the calculated rate of sedimentation and RSL rise from 1769 CE to ~1968 CE (Interval B) is 3.2 mm/year. If the assumption is made that the same rate of sedimentation applies to the marsh deposits that extend from radiocarbon sample WM25 to the base of the core, which terminates directly above the cross section estimate of the laterally extending Pleistocene

basement sand, then the time of initial marsh deposition and tidal inundation of the basement sands can be approximated at ~220 BCE, shortly after the onset of the modern transgression at 2400 BP (Meyer, 2013).

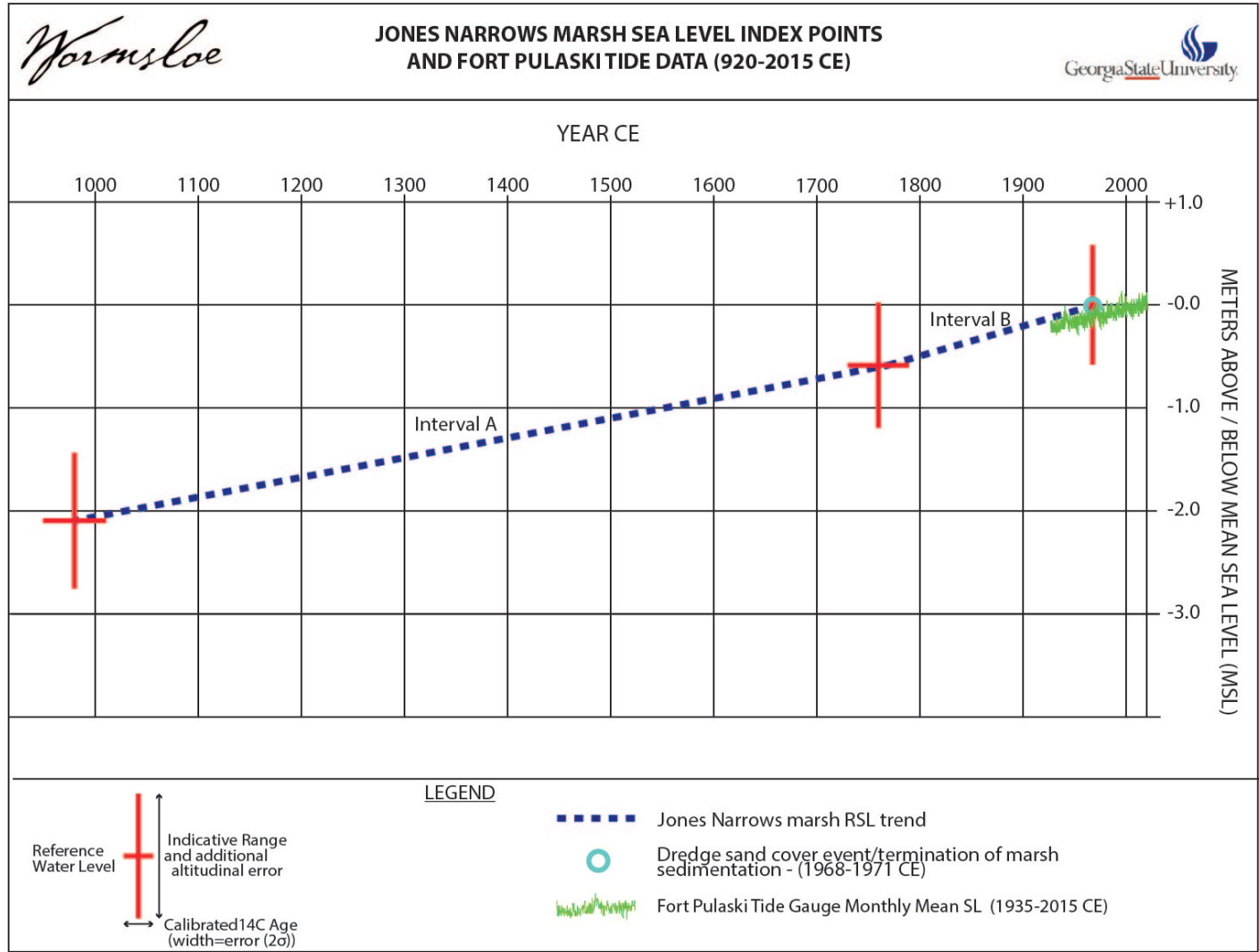


Figure 15: Jones Narrows RSL trends

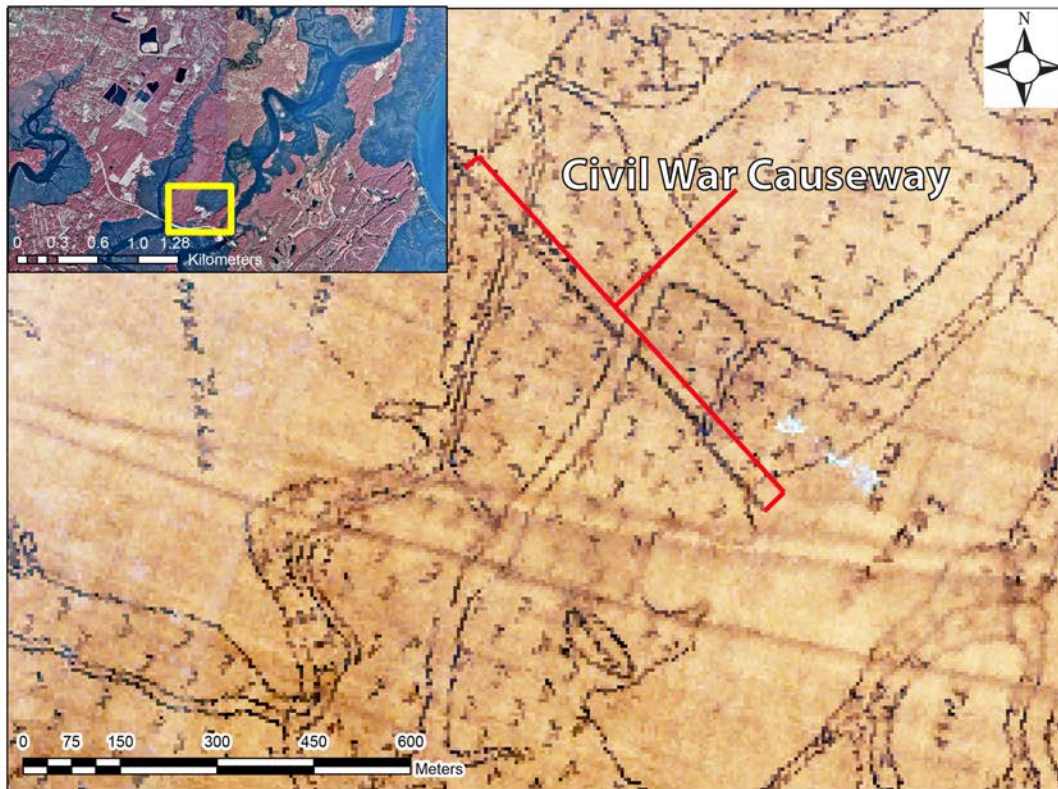


#### 4.4 Spatial Analysis

The historical maps, dating back to 1780 at the oldest, provide some sense of the recent conditions at the Isle of Hope. The 1780 and 1816 maps, while rather crude when compared to maps for the site from the later 19th century and early 20th century, do at least indicate that the boundaries of the upland Isle and the adjacent salt marsh were roughly in the same locations as they were at the time of the initial construction of Diamond Causeway. The locations of Bethesda orphanage and the residence/fortifications on Wormsloe plantation are also indicated, and appear to be reasonably accurate in their geographic representation. The most noticeable improvement in the maps, starting with the 1867 T-Sheet, is the greater detail in the representation of the marsh and tidal channels. Generally, the quality of the maps improves with time, and, due to their agreement with the earliest aerial images used by this study (1951), the maps from the early 20th century are assumed to portray tidal stream locations with moderate precision. The connective tidal channel that once ran through the study area is variably referred to in the historical maps as Jones Narrows (1867 T-Sheet, 1935 T-Sheet, 1938 T-Sheet, 1944 T-Sheet, 1957 Topo, 1988 Topo), Lones Narrows Creek (1912 Topo, 1945 Topo), and the Isle of Hope River (1933 T-Sheet). For consistency, Jones Narrows was chosen as the only title by which the stream is referenced within the current study.

The earthen causeway (aka dam) that runs across the marsh from the Isle of Hope to Long Island, initially shown on the 1908 map (Fig. 16), appears to be the earliest substantial 19th century anthropogenic impact to the marsh shown on the maps, having been built during the Civil War but not represented on any of the 19th century maps (Rice et al., 2005). The 1960 property map displays and refers to the feature as simply “old dam.” The residual effects of the dam as a hydrologic and sedimentologic barrier are visible from the 1951 aerial imagery onward,

through the time of this study. The dam seems to potentially represent a northern barrier for migration of the dredged sandy material deposited during the construction of Diamond Causeway, an effect first captured by the 1968 aerial imagery (Fig. 17). The 1968 aerial shows an accumulation of a material with a high albedo (sand) atop the marsh, in addition to the visible beginnings of the construction of Diamond Causeway to the west of the Isle of Hope and the clearing of the causeway path to the south and east of the Isle of Hope. The dates of construction indicated by the aerials do not agree with the statement in Rice et al., 2005, that Diamond Causeway was constructed in 1972, although this may be the year of the completion of the entire construction project. The construction of the section of Diamond Causeway that lies adjacent to the Isle of Hope appears to be complete by the time of the 1971 aerial imagery (28 December 1971) (Fig. 18).



*Figure 16: Study area - 1908 map; inset 1999 CIR imagery (courtesy UGA CGR)*

Prior to the construction of Diamond Causeway, Skidaway Narrows was initially dredged and modified for the purpose of the establishment of the Intracoastal Waterway in 1910, which likely altered the hydrology of Jones Marsh (Rice et al., 2005). These changes are not yet documented by the 1912 USGS Topo map, but Skidaway Narrows is noticeably more regular in width and less sinuous in the 1933 T-Sheet. Potentially related, the connectivity and width of channels running through Jones Marsh is shown to be dramatically reduced after the time of composition of the 1912 Topo and before the 1933 T-Sheet. Jones Narrows channel width at

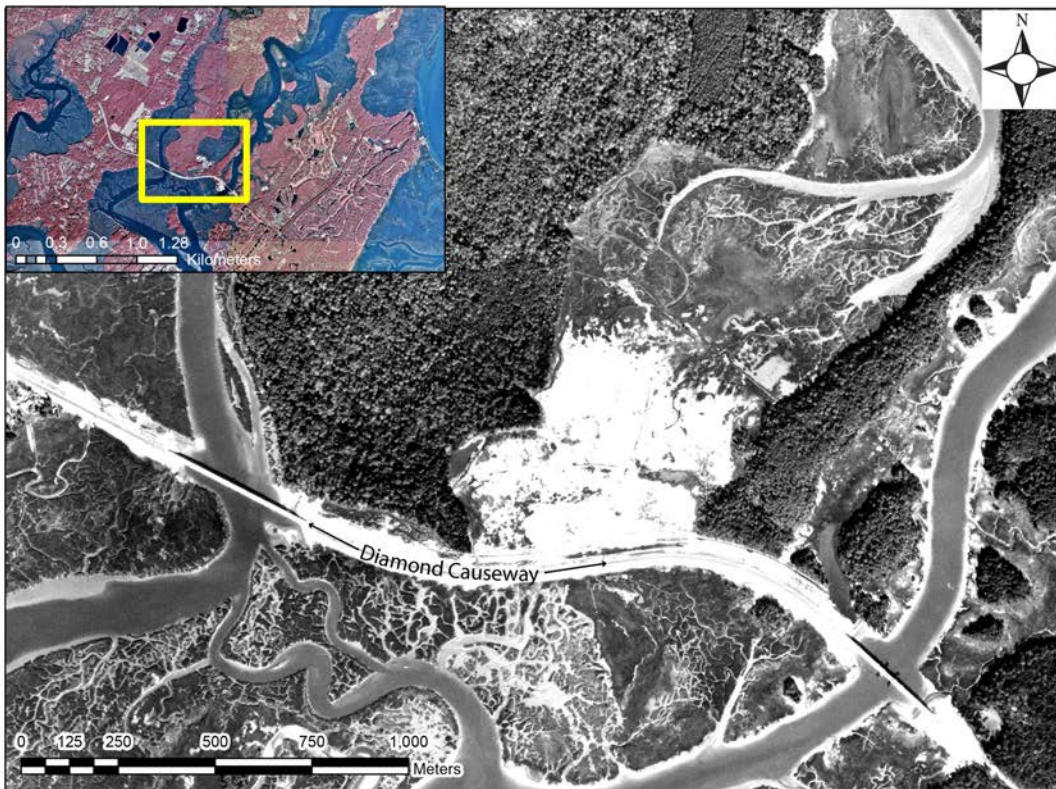
Transect A is shown to be ~7 m in the 1933 T-Sheet, while channel width in the same location shown on the 1912 Topo is greater than 25 m.



*Figure 17: Study area - 1968 aerial imagery; inset 1999 CIR imagery (courtesy UGA CGR)*

By the time of the 1951 aerial photograph, the width of the main Jones Narrows channel at Transect A is ~4 meters. The main channel reach is barely visible in the 1956 aerial, and the channel appears to terminate north of Transect A by the time of the 1961 aerial. In the 1968 aerial, the scars of the main channel are visible, but the tidal flow appears to terminate at the Civil War dam, 250 meters north of Transect A, at which point its width is ~6 m. This same

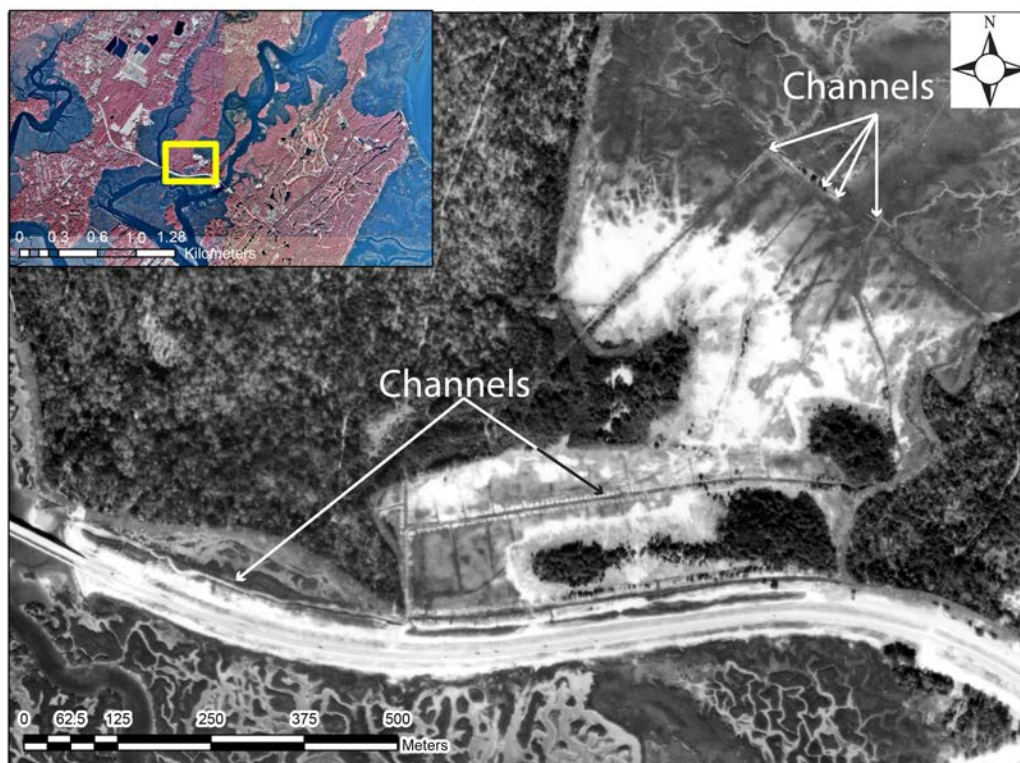




*Figure 18: Study area mid Diamond Causeway construction - 1971 aerial imagery; inset 1999 CIR imagery (courtesy UGA CGR)*

channel termination is visible in the 1971 aerial and all subsequent aerials, although, beginning with the 1988 aerial, there are linear drainages or channels connecting the tidal channels north of the dam to a series of channels that run adjacent to the southern tip of the Isle of Hope, eventually feeding into Moon River (Fig. 19). These channels are the products of an attempt to restore tidal connectivity through the marsh to Moon River (Rice et al., 2005). The channels are still present at the time of the current study, although their connectivity through the study area portion of the marsh is limited, with tidal flow from Jones Narrows extending only ~60 m south of the Civil War dam, still ~90 m north of Transect A. While the E-W running section of the

man-made channel, which runs to the south of the Isle of Hope and parallel to Diamond Causeway, still appears to be hydrologically active at the time of the 2012 satellite imagery, all of the NW-SE components of the channel network are dry. The scars of these channels, which cross Transect A at several points, are made visible in the aerial and satellite imagery by parallel vegetated upland hammocks. The channels are also characterized by the lack of once-present dredge sand in their vicinity. They appear to have acted to reduce the volume of dredge sand beginning sometime before 1988, although the reduction in dredge sand cover surrounding the channels appears to have ceased or slowed dramatically by 1999, as the area of dredge sand cover has remained constant from the 1999 imagery through the present.



*Figure 19: Reconnection channels- 1988 aerial imagery; inset 1999 CIR imagery. (imagery courtesy of UGA CGR)*

#### 4.4.1 *Dredge Sand Area and Volume*

Analysis of the aerial and satellite imagery from the 1951 aerial onward assessed the area and volume covered by the dredge sand in addition to quantifying the modifications to the marsh and Isle geomorphology. The total area covered initially by the dredge sand, per the 1971 aerial, is roughly 100 acres (over 400,000 m<sup>2</sup>). Some of the area initially covered by the sand (~32 acres) was eventually incorporated into the upland supratidal environments of the Isle of Hope and Long Island, becoming covered by the same terrestrial vegetation. The eventual addition to the Isle of Hope covers ~16 acres (~64,750 m<sup>2</sup>), and the sum area of the two extensions added to Long Island is ~10 acres (~40,000 m<sup>2</sup>) (**Fig. 20**). The remaining ~68 acres (~275,000 m<sup>2</sup>) of dredge covered area was raised enough in elevation to enter either the high marsh range of the tidal frame or the sandflat/saltpan range. Of the area covered by dredge sand and converted to a different environmental regime, the vast majority was low marsh prior to the Causeway construction, based upon the vibracore data from the current study.

Using the 3D Analyst Volume Fill tool in ArcMap, the volume of the present dredge sand lens was estimated. The LiDAR DEM provided the surface below which the average depth of the sand lenses as measured from the vibracore data provided the height of the volume. An average elevation (corrected for compaction) of 40.61 cm was used to represent the former marsh surface and used to estimate the volume of fill placement. The modern sand lens is estimated to be ~12.1 million ft<sup>3</sup> or ~450,000 yd<sup>3</sup>. This volume estimate is most likely a conservative estimate as the volume of material placed into the tidal creeks would be extremely variable in nature.



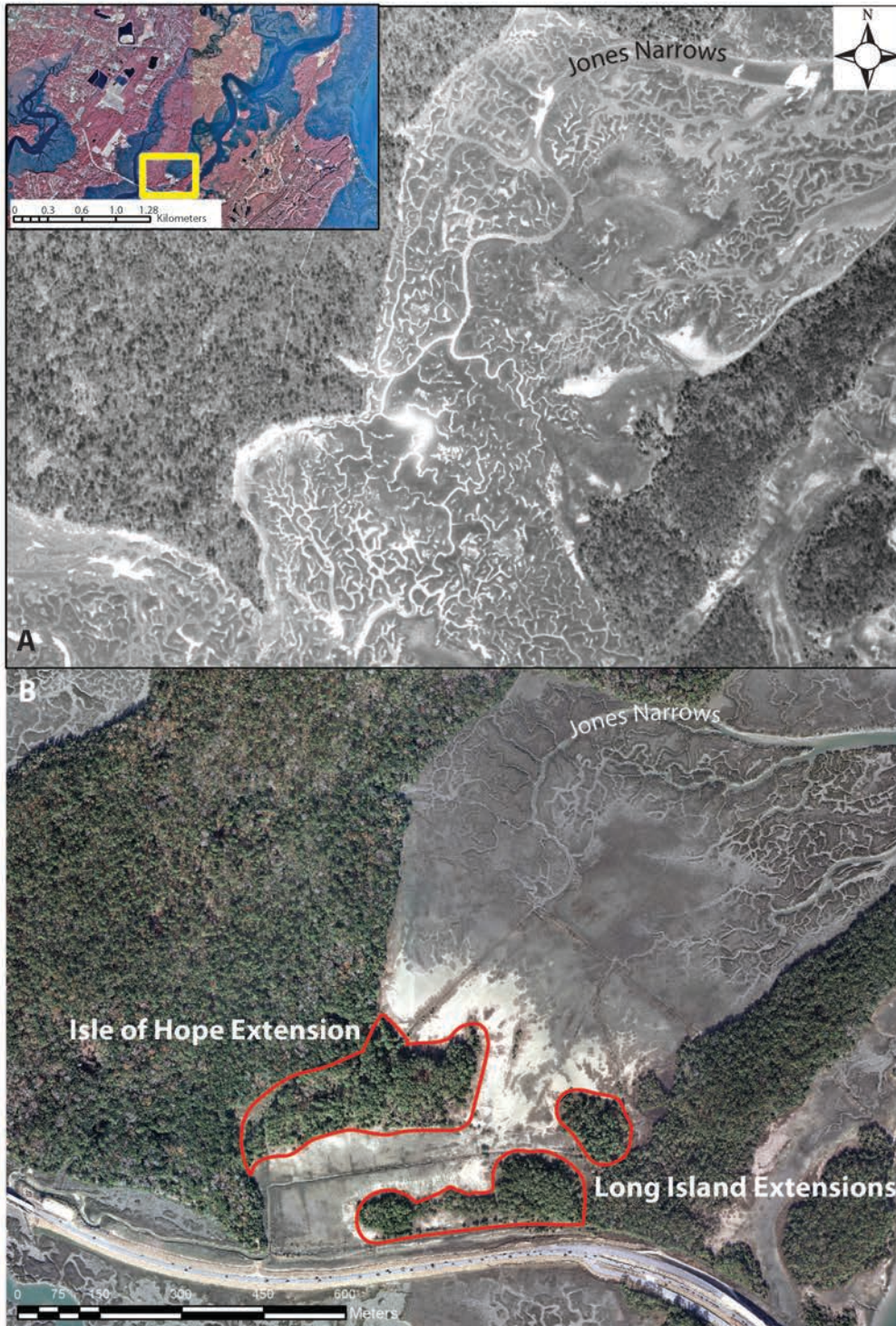


Figure 20: Extensions to The Isle of Hope and Long Island; a) 1951 aerial imagery; b) 2012 TC imagery; inset 1999 CIR imagery (imagery courtesy UGA CGR)



## 5 DISCUSSION

### 5.1 Jones Narrows Stratigraphy

Vibracoring proved to be an efficient method of obtaining the samples in the intertidal marsh setting. The sediment recovered in the two days of fieldwork required for the extraction of the cores has provided more than adequate data for examination in the current study. The cross-sections created from the lithologic data revealed by the vibracoring illustrate the vertical and lateral variation of deposits within the marsh and provide the basis for the RSL change estimates, chemostratigraphic investigations, and the evaluation of the anthropogenic impacts. Specifically, the vibracore data reveal the vertical extent of anthropogenic dredge sand impacts (mean depth 40 cm, corrected for compaction). The stratigraphy of the marsh shows, via the reconstructed tidal creek intervals, that for much of the late Holocene, tidal hydrology has been active enough through Jones Narrows to deposit shell lag. Additionally, the vibracore stratigraphy, along with the radiocarbon data, indicate that the depositional basin in which Jones Narrows marsh resides is framed and underlain by Pleistocene foreshore sands that comprise the cores of The Isle of Hope and Long Island. The similarity between the Pleistocene basal sands from the current study and the Pleistocene “foreshore” sand identified by Howard and Scott, 1983, reinforce this stratigraphic framework. Again, in concert with the radiocarbon samples age ranges, the vibracore data demonstrate that the Jones Narrows marsh sediments and intertidal system were created under continuous sedimentation during the ensuing late Holocene transgression.

### 5.2 Chemostratigraphy

The XRF chemostratigraphy provided insights in to the nature of sedimentation at Jones Narrows. The most striking patterns visible in the chemostratigraphy of the samples are the Ca and Sr peaks coincident with the marine shell lag that is characteristic of the interpreted tidal

creek deposits. Although marine tests are generally the main contributor to Ca concentration, it is important to note that Ca can also indicate the presence of hornblende, epidote, and tourmaline (Meyer, 2013), potentially indicating metamorphic or igneous provenance of the detrital sediment.

Additionally, the ratio of Sr/Ca in these shells can be applied as a proxy for high resolution daily light cycle reconstruction for the paleoenvironment, although the current study was not carried out at the appropriate scale or resolution for this application (Sano et al., 2012). The Sr/Na concentrations in molluscan shells can indicate levels of paleosalinity (Findlater et al., 2014), however, these analyses also exceed the scope and capabilities of the current study.

Sandy mud deposits with some marine shells and plant macrofossils are positioned above what is interpreted to be the Pleistocene island core at the base of each XRF vibracore section. These deposits are interpreted to be low marsh or tidal creek levee deposits, and they display distinct relatively high Fe, Ti, and K concentrations. Ti concentration is likely controlled by the presence of ilmenite, leucoxene, and rutile, while the Fe concentration is most likely associated with almandine, hornblende, epidote, tourmaline, and staurolite (Meyer, 2013). These concentrations potentially indicate a greater influence from HMS-rich washover fans on this sub-environment during this interval or variation in the nature of sediment load in the terrestrial fluvial source feeding into the marsh from the west. Changes in sediment supply source could imply large scale environmental change or fluvial dynamism, both of which could potentially be correlated with sediment deposition evidence in other coastal study areas. The increase in the concentration of this trio of elements (Fe, Ti, K), along with characteristic lithology, could potentially be used to identify the onset of sedimentation after the inundation of Pleistocene

island cores in surrounding barrier island Holocene marsh settings, if shown to be a common facies.

In the matrices of intercorrelation, the strong correlations seen between Fe, Mn, Ti and Zr in the sandy facies intervals are likely due to the influence of HMS transported from proximal beach deposits. Within the muddy facies interval, it was expected that there would be a very strong correlation between Fe and K, due to source clay mineralogy (Meyer, 2013), and there are very strong associations between these two elements within these samples. Meyer, 2013, also noted that the muddy chemofacies from St. Catherine's Island displayed strong correlations between Fe, Ca, and S, associated with the occurrence of calcareous shell material and secondary alteration to pyrite and/or marcasite due to subsurface marsh reducing conditions. These strong correlations do not appear within the Jones Narrows muddy facies XRF data, potentially because of the separation in this study of shell rich (tidal creek) facies from the general marsh muds during analysis; the absence of this correlation in the current study may also be due to the comparably small sample size or potential erroneous facies identification.

### ***5.2.1 Cluster Analysis***

Meyer, 2013, found that cluster analysis was successful at grouping barrier island system facies into meaningful groups, but stated that the separation of sediments into depositional subenvironments is dependent upon the recognition of primary physical and biogenic structures and could be difficult to achieve via cluster analysis, alone.

The current study attempted to assess the ability of cluster analysis of XRF data to separate the analyzed sediment into salt marsh depositional subenvironments. The analysis proved able to isolate intervals that correspond to tidal creek deposits more readily than any other subenvironmental intervals. These intervals, in both WM050215-03 and WM050215-04,

were grouped into clusters distinct from those clusters immediately above and below. Furthermore, unique clusters identified the aforementioned peaks in Ca and Sr, which also correspond with dips in the concentrations of Ti and Zr. While the peaks and dips in the concentrations would be evident in the analysis of the raw XRF data, the clusters also quickly divided these intervals into stratigraphically unique groups. Within WM050215-03, most of the cluster separation appears to correspond with the same Ca-Sr/Ti-Zr relationship, with Cluster A<sub>3</sub> indicating very low Ca-Sr/Ti-Zr values, cluster B<sub>3</sub> indicating moderate Ca-Sr/Ti-Zr ratios, and cluster C<sub>3</sub> indicating high Ca-Sr/Ti-Zr ratios. The increase in Ca and Sr relative to Ti and Zr in the tidal creek intervals is most likely caused by the tendency of these intervals to contain much more calcareous shell material, the source of both Ca and Sr, and correspondingly less heavy mineral sands from washover deposits, which would be expected to be limited to high marsh environments. Potentially significant within the same core (WM050215-03) is the low Fe concentration within Cluster C<sub>3</sub>, although Fe concentration does not appear to correspond as strongly with cluster division as does the Ca-Sr/Ti-Zr ratio.

The same Ca-Sr/Ti-Zr ratios present in the WM050215-03 clusters carry over to WM050215-04, as well. Alternatively, Clusters D<sub>4</sub> and C<sub>4</sub> from WM050215-04 correspond exclusively with the tidal creek interval within the core. Cluster E<sub>4</sub> is continuous from the base of the tidal creek deposits to the base of the core, identified as a low marsh deposit interval, and features a consistently low Ca-Sr/Ti-Zr-Fe ratio. The low marsh deposits above the tidal creek interval of Clusters D<sub>4</sub> and C<sub>4</sub> are consistently sandier than the cluster E<sub>4</sub> deposits and feature a slightly higher Ca-Sr/Ti-Zr-Fe ratio, possibly due to greater lateral proximity of the marsh surface to the tidal creek at the time of deposition. This trend could also potentially indicate the capability of XRF cluster analysis to identify older and muddier deposits within salt marsh basins

if this geochemical trend can be shown to be common, and while a similar interval in WM050215-03 was not separated into its own cluster, it was shorter and displayed relatively lower corresponding Zr values than the those in Cluster E<sub>4</sub>. Core WM050215-03 lies ~75 meters to the west of WM050215-04, which could be the source of a decreased influence from storm induced washover events from Long Island or Skidaway and, consequently, lower heavy metal content. Overall, the cluster analysis indicates that some salt marsh depositional subenvironments can be identified via the technique, especially tidal creek intervals due to their distinct geochemical signatures. With further refining and development of the method, cluster analysis shows promise as a useful tool for the confirmation, laboratory identification, and analysis of salt marsh subenvironments within sedimentary sequences.

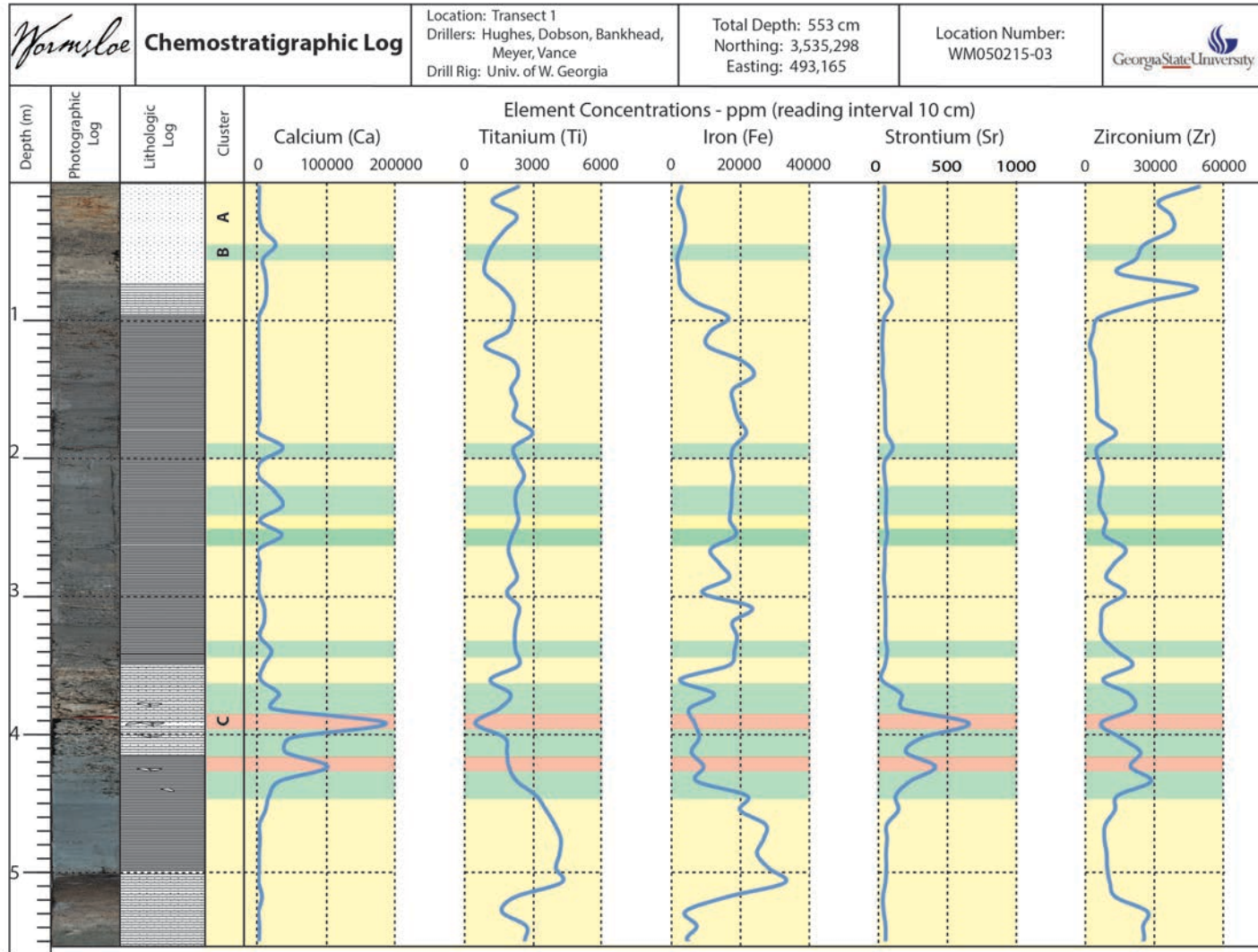


Figure 21: Chemostratigraphic Log - WM050215-03 (corrected for compaction)

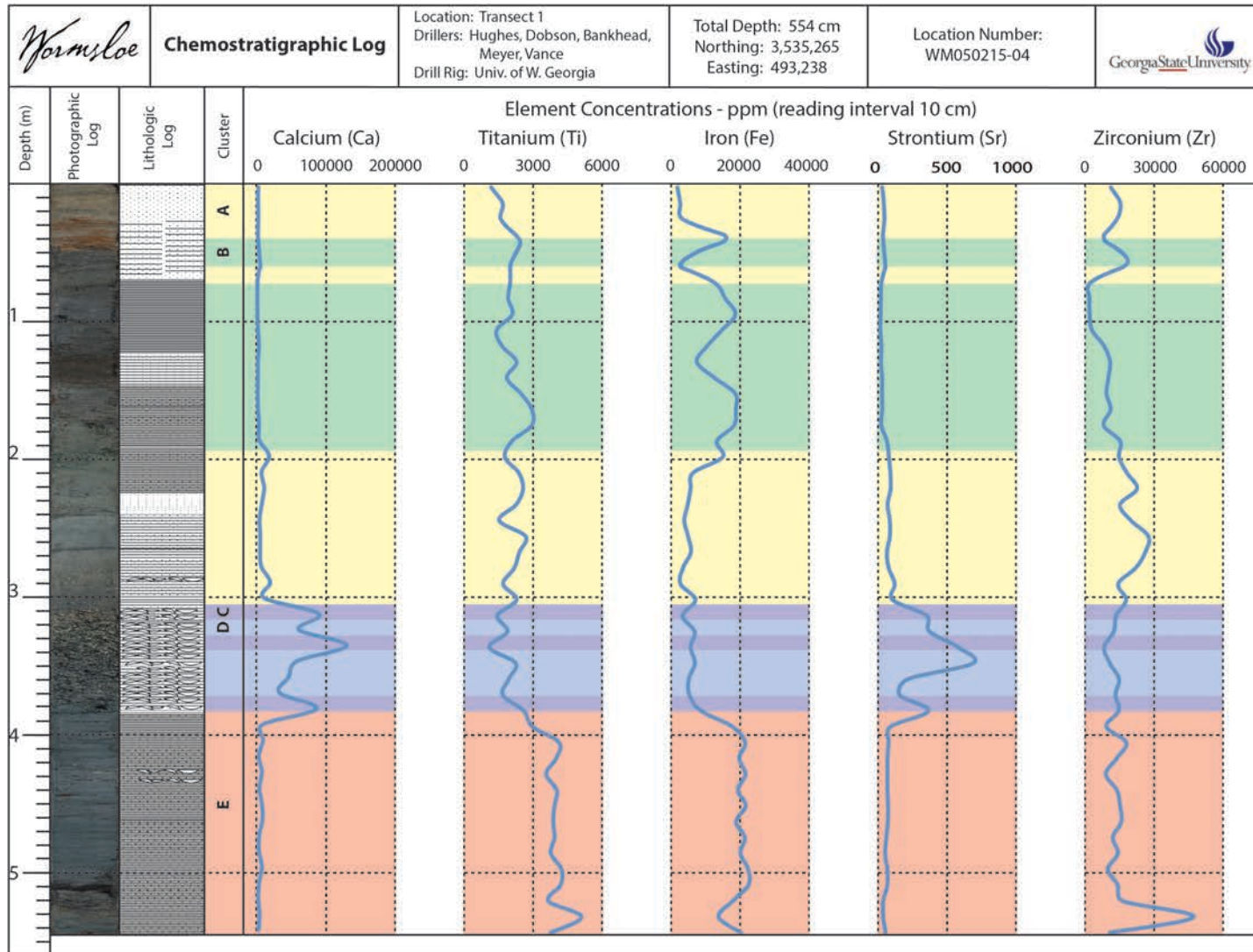


Figure 22: Chemostratigraphic Log - WM050215-04 (corrected for compaction)

### 5.3 Evaluation of Late Holocene Sea Level Rise

The reconstruction in this study helps to close a knowledge gap in Late Holocene sea level history for the Southeastern US Atlantic Coast. The sea level envelope proposed by Meyer, 2013, for St. Catherine's Island indicates that the reconstructed rate of 2.1 mm/year for Interval A (1017 CE  $\pm$  30 to 1753 CE  $\pm$  32) in the current study is somewhat representative of regional RSL rise for the Late Holocene (Fig. 23 and 24). The younger sample from Interval A, WM26, falls cleanly within the bound of the St. Catherine's sea level envelope, however, the older sample, WM25, even with its altitudinal error and indicative range taken into account, falls just outside of the lower limits of the envelope. This section of the envelope falls within a "data gap" in the St. Catherine's reconstruction which could potentially be one explanation for the lack of agreement, while local variability in tectonics and subsidence could also be the cause, as St. Catherine's Island is 25 miles SE of The Isle of Hope. Interval B (1753 CE  $\pm$  32 to 1968 CE), which indicates 3.2 mm/year of RSL rise, falls within the St. Catherine's RSL envelope.



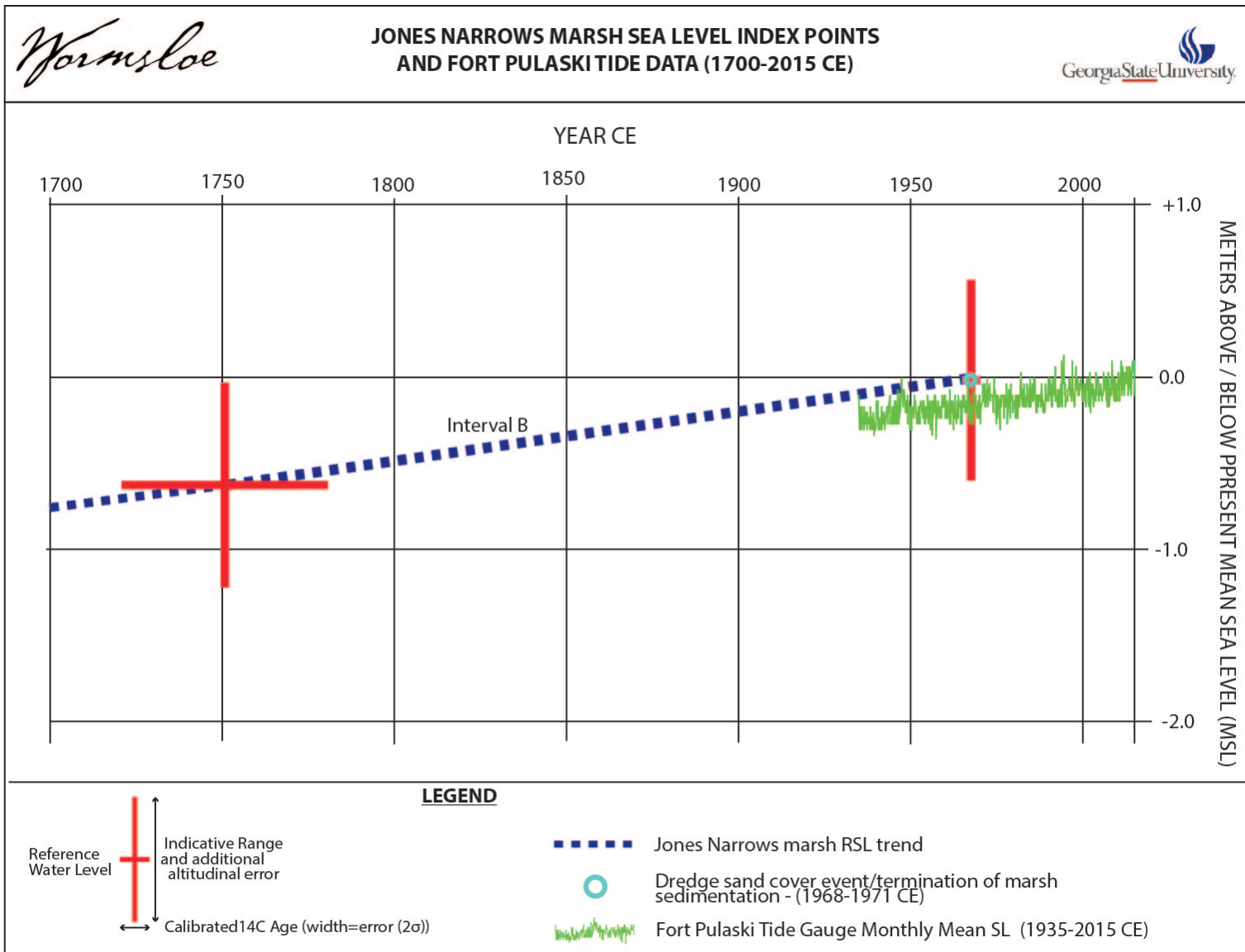


Figure 23: Jones Narrows RSL reconstruction and Ft. Pulaski Tide Data (NOAA)

The NOAA tide gauge record at Ft. Pulaski reports the history of local SLR for the Savannah, Ga, area since 1935 CE, and the gauge is located 10 miles NE Jones Narrows marsh. A mean sea level trend has been calculated from the monthly mean sea level for Ft. Pulaski, which indicates  $3.17 \pm 0.28$  mm/year of RSL rise from 1935 CE to 2015 (Fig. 23). This rate conforms well with and continues the trend of the rate of RSL rise indicated by the current study (Fig. 23) that terminates in 1968 with the onset of Diamond Causeway dredge material deposition. The rate at Jones Narrows is  $\sim 0.03$  higher than the rate at Ft. Pulaski, even though the time interval for Jones Narrows includes pre-19<sup>th</sup> and 20<sup>th</sup> century data which predates the 20<sup>th</sup> century acceleration in SLR. A potential cause for the higher rate of sedimentation at Jones Narrows marsh for the interval from  $\sim 1753$ -1968 CE could be the resuspension and subsequent deposition of sediment from the nearby Skidaway Narrows during its modification during the construction of the Intracoastal Waterway. This could introduce an artificially greater sediment input beginning in the early 20th century CE that would have no impact on the actual rate of RSL in the area. It should also be noted that the Interval B rate falls within the range of error (0.28 mm/yr) included in the Ft. Pulaski data.

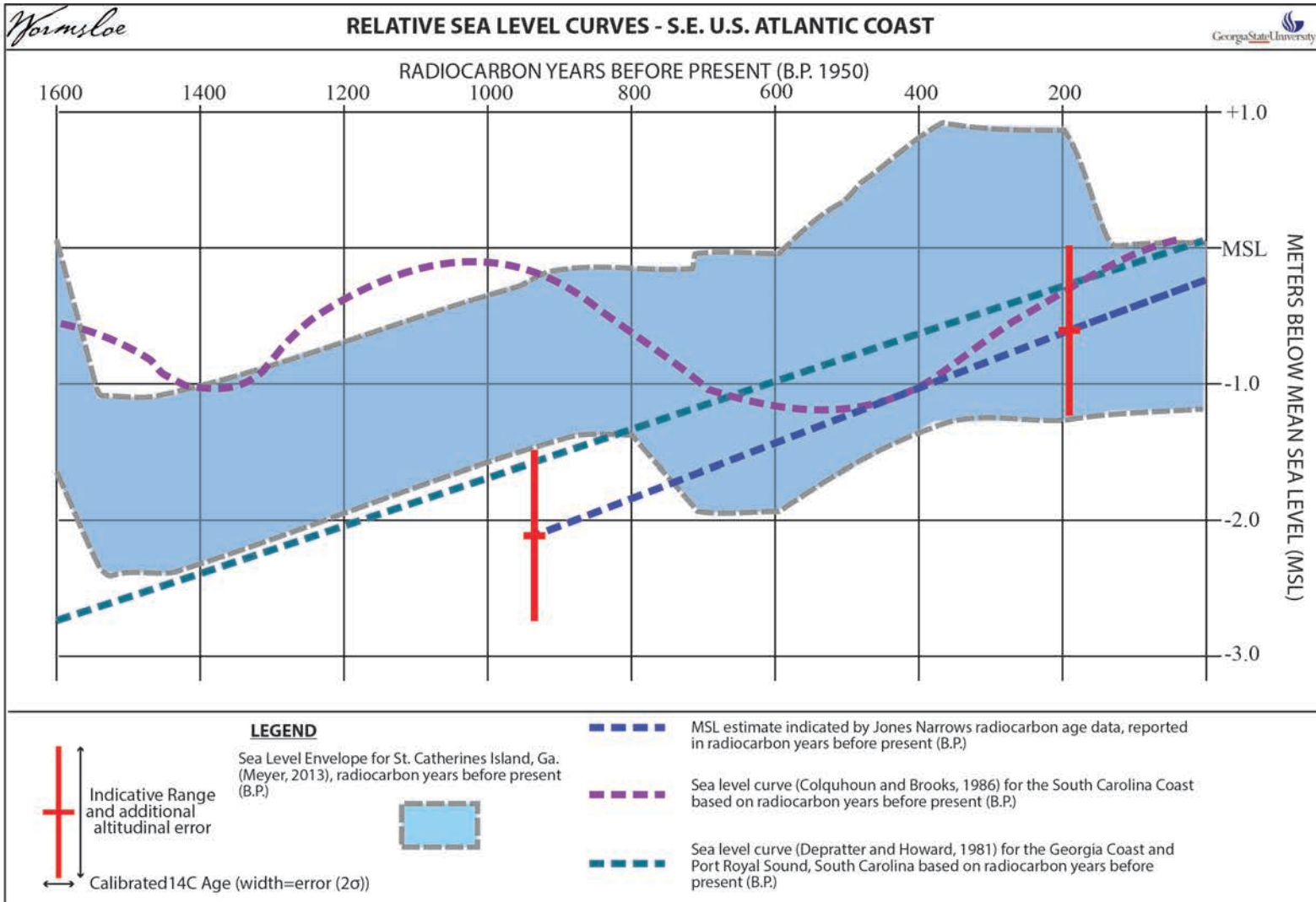


Figure 24: Southeastern US Atlantic Coast RSL curve

Also examined by Meyer, 2013, the study by Depratrer and Howard, 1981, reconstructed late Holocene RSL via archaeological investigations on the Georgia and South Carolina coasts. Intervals A and B of the current study conform well with the RSL curve proposed by Depratrer and Howard, 1981, with their reconstruction indicating roughly the same rates of SLR and depths that align with the higher reaches of the indicative range and altitudinal error in intervals A and B. The validity of their reconstruction, based on archaeological features, was called into question by Belknap and Hine, 1983, who stated that the indicative meaning derived from archaeological data is invalid due to its dependence upon the interpretation of human behavior. This point was reiterated by Hawkes et al., 2016, however, the assumptions made of human behavior that underpin the study in Depratrer and Howard, 1981, are the same that guide and validate many archaeological investigations and seem little different from the assumptions made of sedimentary processes involved in the most basic stratigraphic investigations.

Colquhoun and Brooks, 1986, reconstructed RSL on the South Carolina coast for a period partially concurrent with the reconstruction from the current study, indicating moderate conformity between the two reconstructions from ~600 CE forward. The Colquhoun and Brooks, 1986, RSL curve also falls within the bounds of Meyer's RSL envelope for the period covered by the current study (~1000 CE to ~1968 CE).

Engelhart and Horton, 2012, compiled a database of late Holocene RSL for the United States Atlantic coast based upon salt marsh index points, indicating that RSL rise from 8 to 4 ka BP ranges from 0.5 to 4.5 mm/yr, while the rate from 4 ka BP to 1900 CE ranges from 0.6 to 1.8 mm/yr, a decreased rate of RSL rise thought to be caused by a relaxation of GIA and northern hemisphere ice sheet minimums during the ~7-8 ka period. The furthest south that the database

extended at the time of publication was to southern South Carolina, where the authors state that the rate of RSL rise for the past 4 ka was found to be constant, although only one index point from the southern South Carolina data set was dated to less than  $\sim 1.8$  ka. The index points in the database for northern South Carolina indicate a rate of rise of  $\sim 0.8$  mm/yr from 4 ka BP to 1900 CE, although the youngest index point in this data set dates to 2 ka. The data from Engelhart and Horton, 2012, also show a decrease in rate of RSL rise during the Holocene in the southern North Atlantic that the authors ascribe to greater distance from the Laurentide Ice Sheet and its forebulge. The discrepancies in the RSL rates of rise calculated from the current study for the periods from 1017-1753 CE (2.1 mm/year) and 1753-1968 CE (3.2 mm/year) versus those indicated by the Atlantic RSL database for the southern North Atlantic could be due to the fact that periods of time covered by the two studies have only  $\sim 500$  years of overlap, which coincide with the earliest  $\sim 500$  years covered by the current study, prior to the Anthropocene acceleration of SLR. The index point at  $\sim 1753$  CE allows the interval B rate to avoid the assumption of constant RSL rise for the past 1 ka, and provides for the differentiation of the pre- and post-18<sup>th</sup> century rates of RSL rise.

Kemp et al., 2014, added a salt marsh RSL construction for NE Florida to the US Atlantic RSL database based upon salt marsh core radiocarbon dates and anthropogenic chemical chronohorizons, and the data from the cores was fused with tide gauge data from Fernandina Beach, Florida. This reconstruction of late Holocene RSL indicates a mean subsidence rate of  $\sim 0.41$  mm/year from 590 BCE to 2010 CE, with the Fernandina Beach tide gauge measuring  $1.9 \pm 0.3$  mm/year of RSL rise from 1900 CE to 2012 CE (Kemp et al., 2014). However, according to the authors, a GPS station 5.5 km from the Fernandina Beach tide gauge measured subsidence of  $3.58 \pm 0.30$  mm/year, a value deemed anomalous by the authors due to its disagreement with

the RSL rates from Miami Beach, Charleston, and Key West, locations that are up to ~420 miles from Fernandina. It should be noted that Fernandina Beach is ~90 miles to the SW of the Isle of Hope, and this discrepancy in subsidence rates could be due to local tectonic sags and/or subsidence in the areas showing increased rates of RSL rise. Also, Brain et al., 2014, found that, specifically within peat marshes like those utilized by Kemp et al., 2014, for their reconstruction, autocompaction can dramatically reduce the apparent rate of RSL rise.

The rate of RSL indicated by the current study for interval B (3.2 mm/year) is higher than the rates proposed by Kemp et al., 2014, the mean rate indicated by the Fernandina Beach tide gauge, and the South Carolina RSL values from the Atlantic Database (Engelhart and Horton, 2012). If corrected for the maximum potential effects of autocompaction (0.07 mm/yr) (Brain et al., 2014), the SLR rates at Jones Narrows are still markedly higher. However, the Anthropocene rate of SLR indicated by the more proximal Ft. Pulaski tide gauge is correspondingly higher (3.17 mm/year), again, potentially indicating the effect of local tectonics on the reconstructed late Holocene RSL rate at Jones Narrows marsh.

The Jones Narrows RSL reconstruction shows that, in agreement with the most recent updates to the North Atlantic US Late Holocene RSL database, an increase over the background Late Holocene rate of RSL rise occurs during the Anthropocene, and the contribution to RSL rise from global climate change can potentially be evaluated by incorporating the background rates of subsidence due to GIA from the total rate of rise in the Anthropocene.

#### **5.4 Anthropogenic Impacts**

While the temporal spacing of the aerial imagery at the time of the deposition of the lens of dredge sand atop Jones Narrows marsh is not high enough to know the exact dates of deposition, based on the coverage shown in the 1968 CE and 1972 CE aerials, it is likely safe to

assume that, at minimum, the depth of sand that currently exists atop the marsh was deposited within the span of 5 years. This would indicate a rate of deposition of at least 81.2 mm/year at Jones Narrows marsh due to the construction of Diamond Causeway, as opposed to the calculated natural rate of 3.2 mm/yr. The historical maps and aerial imagery also show that the causeway (aka “dam”) constructed during the Civil War (Rice et al., 2005) potentially prevented the Diamond Causeway dredge sand from being transported north beyond its position. If not for the presence of the Civil War causeway, however, the dredge sand introduced to the marsh from the south could have possibly been allowed to pass northward through Jones Narrows without being so dramatically deposited on the marsh surface. An alternative scenario would hold that the absence of the Civil War causeway could have caused a greater extent of the marsh system to be impacted by the dredge fill placement. Tidal flow through the marsh, of course, had also been reduced by the re-routing of flow to Skidaway narrows by ~1910 CE, so the potential for the great volume of sand introduced to the marsh (~340,000 m<sup>3</sup>) to have passed through without effectively blocking flow via sedimentation would have still been limited.

The attempt to restore the tidal hydrology of Jones Narrows in the late 1980’s CE (Rice et al., 2005) has, by and large, failed to do so, with only one section of one of the restoration channels extending southward from the Civil War causeway onto the affected portion of the marsh. While only 32 of the 101 acres of marsh covered by dredge sand were pushed out of the intertidal elevation range into the supratidal range, the prior impediments to tidal hydrology induced by the Civil War causeway and the Skidaway Narrows re-routing prevented the possibility of the affected area to survive the construction of Diamond Causeway.

It is important to note that the anthropogenic effects on Jones Narrows not only include changes to sedimentation and hydrology, but also the intrinsically connected impacts on marsh

vegetation. The measure of the marsh covered by dredge sand (101 acres) not only indicates the area of low/high marsh that was covered by a veneer of sand, but the number also roughly analogous to the area of marsh halophytic vegetation that was effectively removed, of which recovery has been limited. Rice et al., 2005, mention the possibility of future efforts to restore the natural marsh vegetation and hydrology, but any attempt to do so would have to include the removal of the entire depth of dredge sand, as well as the removal of the Civil War Causeway. This restoration effort would likely include collateral impacts to the surrounding non-impacted marsh systems in order to access the area, and a net environmental benefits analysis would be warranted to determine the overall benefit of the remedial effort. Even with these large scale efforts, the potential for effective restoration of the low/high marsh environments would still be impeded by the preferential tidal flow through Skidaway Narrows.

## 6 CONCLUSIONS

The purposes of this study were to evaluate the evaluate the sedimentary record of local Late Holocene SLR and to document and quantify the anthropogenic impacts to Jones Narrows salt marsh through the application of sedimentologic analyses, radiocarbon dating, XRF chemostratigraphy, and geospatial methods. The stratigraphic results reveal the continuous record, via vibracore Transects 1 and 2, of Holocene salt marsh deposition within the sedimentary basin that was created during the Late Pleistocene at Jones Narrows. The vibracore results also reveal more complete data concerning the vertical extent of the anthropogenically induced sedimentation on the marsh surface. These data, when examined in concert with the spatial analyses of the marsh based on historical maps and aerial imagery, effectively reveal new information concerning the scale and history of anthropogenic causes and effects on the



hydrology, sedimentation, and vegetation cover within the marsh. The chemostratigraphic study of the vibracore sediments bares information on the nature of the deposition of several intervals of the Holocene marsh mud, tidal creek lag, and the dredge sand veneer; this study also provides insight into the nature of the Pleistocene basement sediments that underlie the Holocene marsh. The subsequent cluster analyses of the XRF chemologs indicate that the methods described by this study, with modification and repeated iterations, could prove to be effective tools for identifying or confirming salt marsh depositional subenvironments within sedimentary sequences. Lastly, the Late Holocene relative sea level reconstruction of Jones Narrows marsh, based upon the radiocarbon analyses of the marsh deposits and the indicative meaning of the sediments, helps to add data to an important research gap that exists for the Southeastern US Atlantic Coast. The rates of RSL rise indicated by this study for the late Holocene (2.1 mm/year) and Anthropocene (3.2 mm/year) agree with some other local reconstructions (Meyer, 2013; Depratrer and Howard, 1981; Colquhoun and Brooks, 1983) and the Ft. Pulaski tide gauge data (NOAA), while revealing substantially higher SLR rates for the region during both periods than those rates indicated by several other North Atlantic salt marsh reconstructions (Engelhart and Horton, 2012; Kemp et al., 2014; Hawkes et al., 2016) and Earth-ice models (Argus et al., 2014). However, the results of the current study concur with most of these other studies by suggesting an increase in SLR rate for the Anthropocene as compared to the rest of the Late Holocene.

## **6.1 Recommendations for Further Study**

XRF analyses of other salt marshes and/or future studies at Jones Narrows would benefit from a higher resolution of XRF data collection within the upper 2 meters of sediment in order to be able to identify anthropogenic chemical chronohorizons (Kemp et al., 2014), which allows for more accurate age-depth models for the 19<sup>th</sup> and 20<sup>th</sup> centuries. Future vibracore investigations

and Late Holocene RSL reconstructions of other salt marshes on the northern Georgia coast are also recommended, in order to further confirm or question the SLR rates indicated by the current study while also investigating the variable effects of local tectonics on the record of Late Holocene RSL. Lastly, investigations of salt marsh remediation efforts could improve and inform methods for reviving and restoring salt marshes impacted by large volumes of exotic sediment, as in the case of Jones Narrows marsh.

## REFERENCES

- Allen, J.R.L., 2000, Morphodynamics of Holocene salt marshes: a review sketch from the Atlantic and Southern North Sea coasts of Europe: *Quaternary Science Reviews*, v. 19, p. 1155–1231.
- Argus, D.F., Peltier, W.R., Drummond, R., and Moore, A.W., 2014, The Antarctica component of postglacial rebound model ICE-6G\_C (VM5a) based on GPS positioning, exposure age dating of ice thicknesses, and relative sea level histories: *Geophysical Journal International*, v. 198, p. 537–563, doi: 10.1093/gji/ggu140.
- Bartholdy, A.T., Bartholdy, J., and Kroon, A., 2010, Salt marsh stability and patterns of sedimentation across a backbarrier platform: *Marine Geology*, v. 278, p. 31–42, doi: 10.1016/j.margeo.2010.09.001.
- Basan, P.B., and Frey, R.W., 1977, Actual-palaeontology and neoichnology of salt marshes near Sapelo Island, Georgia: *Trace fossils*, v. 2, p. 41–70.
- Belknap, D.F., and Hine, A.C., 1983, Evidence for a sea level lowstand between 4500 and 2400 years BP on the southeast coast of the United States: Discussion: *Journal of Sedimentary Research*, v. 53, <http://archives.datapages.com/data/doi/10.1306/212F829C-2B24-11D7-8648000102C1865D>.
- Brain, M.J., Kemp, A.C., Horton, B.P., Culver, S.J., Parnell, A.C., and Cahill, N., 2015, Quantifying the contribution of sediment compaction to late Holocene salt-marsh sea-level reconstructions, North Carolina, USA: *Quaternary Research*, v. 83, p. 41–51, doi: 10.1016/j.yqres.2014.08.003.
- Chen, Y., Thompson, C.E.L., and Collins, M.B., 2012, Saltmarsh creek bank stability: Biostabilisation and consolidation with depth: *Continental Shelf Research*, v. 35, p. 64–74, doi: 10.1016/j.csr.2011.12.009.

- Colquhoun, D.J., and Brooks, M.J., 1986, New evidence from the southeastern US for eustatic components in the late Holocene sea levels: *Geoarchaeology*, v. 1, p. 275–291.
- Crutzen, P.J., and Stoermer, E.F., 2000, *The Anthropocene* IGBP Newsletter, 41: Royal Swedish Academy of Sciences, Stockholm, Sweden.
- D’Alpaos, A., Lanzoni, S., Marani, M., and Rinaldo, A., 2007, Landscape evolution in tidal embayments: Modeling the interplay of erosion, sedimentation, and vegetation dynamics: *Journal of Geophysical Research-Earth Surface*, v. 112, p. F01008, doi: 10.1029/2006JF000537.
- DePratter, C.B., and Howard, J.D., 1981, Evidence for a Sea Level Lowstand Between 4500 and 2400 Years B.P. on the Southeast Coast of the United States: *Journal of Sedimentary Research*, v. 51, <http://archives.datapages.com/data/sepm/journals/v51-54/data/051/051004/1287.htm>.
- Edwards, J.M., and Frey, R.W., 1977, Substrate characteristics within a Holocene salt marsh, Sapelo Island, Georgia: *Senckenbergiana maritima*, v. 9, p. 215–259.
- Engelhart, S.E., and Horton, B.P., 2012, Holocene sea level database for the Atlantic coast of the United States: *Quaternary Science Reviews*, v. 54, p. 12–25, doi: 10.1016/j.quascirev.2011.09.013.
- Fagherazzi, S., Kirwan, M.L., Mudd, S.M., Guntenspergen, G.R., Temmerman, S., D’Alpaos, A., van de Koppel, J., Rybczyk, J.M., Reyes, E., Craft, C., and Clough, J., 2012, Numerical Models of Salt Marsh Evolution: Ecological, Geomorphic, and Climatic Factors: *Reviews of Geophysics*, v. 50, p. RG1002, doi: 10.1029/2011RG000359.
- Findlater, G., Shelton, A., Rolin, T., and Andrews, J., 2014, Sodium and strontium in mollusc shells: preservation, palaeosalinity and palaeotemperature of the Middle Pleistocene of eastern England: *Proceedings of the Geologists Association*, v. 125, p. 14–19, doi: 10.1016/j.pgeola.2013.10.005.

- Frey, R.W., and Basan, P.B., 1978, Coastal salt marshes, *in* Coastal sedimentary environments, Springer, p. 101–169, [http://link.springer.com/chapter/10.1007/978-1-4684-0056-4\\_4](http://link.springer.com/chapter/10.1007/978-1-4684-0056-4_4).
- de Groot, A.V., Veeneklaas, R.M., and Bakker, J.P., 2011, Sand in the salt marsh: Contribution of high-energy conditions to salt-marsh accretion: *Marine Geology*, v. 282, p. 240–254, doi: 10.1016/j.margeo.2011.03.002.
- Haslett, S.K., Cundy, A.B., Davies, C.F.C., Powell, E.S., and Croudace, I.W., 2003, Salt marsh, sedimentation over the past c. 120 years along the West Cotentin Coast of Normandy (France): Relationship to sea-level rise and sediment supply: *Journal of Coastal Research*, v. 19, p. 609–620.
- Hawkes, A.D., Kemp, A.C., Donnelly, J.P., Horton, B.P., Peltier, W.R., Cahill, N., Hill, D.F., Ashe, E., and Alexander, C.R., 2016, Relative sea-level change in northeastern Florida (USA) during the last ~8.0 ka: *Quaternary Science Reviews*, v. 142, p. 90–101, doi: 10.1016/j.quascirev.2016.04.016.
- Hayden, B.P., and Dolan, R., 1979, Barrier islands, lagoons, and marshes: *Journal of Sedimentary Research*, v. 49, <http://archives.datapages.com/data/doi/10.1306/212F78B0-2B24-11D7-8648000102C1865D> (accessed November 2014).
- Howard, J.D., and Frey, R.W., 1980, Holocene depositional environments of the Georgia coast and continental shelf: *Excursions in Southeastern Geology: The Archaeology-Geology of the Georgia Coast*, Georgia Geological Survey, Guidebook, v. 20, p. 66–134.
- Howard, J.D., and Frey, R.W., 1985, Physical and biogenic aspects of backbarrier sedimentary sequences, Georgia Coast, U.S.A.: *Marine Geology*, v. 63, p. 77–127, doi: 10.1016/0025-3227(85)90080-5.

- Howard, J.D., and Scott, R.M., 1983, Comparison of Pleistocene and Holocene barrier island beach-to-offshore sequences, Georgia and northeast Florida coasts, USA: *Sedimentary Geology*, v. 34, p. 167–183.
- Hoyt, J.H., 1967, Barrier Island Formation: *Geological Society of America Bulletin*, v. 78, p. 1125–1136, doi: 10.1130/0016-7606(1967)78[1125:BIF]2.0.CO;2.
- Hoyt, J.H., and Hails, J.R., 1967, Pleistocene shoreline sediments in coastal Georgia: deposition and modification: *Science*, v. 155, p. 1541–1543.
- Hubbard, D.K., Oertel, G., and Nummedal, D., 1979, The role of waves and tidal currents in the development of tidal-inlet sedimentary structures and sand body geometry: examples from North Carolina, South Carolina, and Georgia: *Journal of Sedimentary Research*, v. 49, <http://archives.datapages.com/data/doi/10.1306/212F78B5-2B24-11D7-8648000102C1865D>.
- Hughes, Z.J., FitzGerald, D.M., Wilson, C.A., Pennings, S.C., Wieski, K., and Mahadevan, A., 2009, Rapid headward erosion of marsh creeks in response to relative sea level rise: *Geophysical Research Letters*, v. 36, p. L03602, doi: 10.1029/2008GL036000.
- Kalnicky, D.J., and Singhvi, R., 2001, Field portable XRF analysis of environmental samples: *Journal of Hazardous Materials*, v. 83, p. 93–122, doi: 10.1016/S0304-3894(00)00330-7.
- Kemp, A.C., Bernhardt, C.E., Horton, B.P., Kopp, R.E., Vane, C.H., Peltier, W.R., Hawkes, A.D., Donnelly, J.P., Parnell, A.C., and Cahill, N., 2014, Late Holocene sea- and land-level change on the U.S. southeastern Atlantic coast: *Marine Geology*, v. 357, p. 90–100, doi: 10.1016/j.margeo.2014.07.010.
- Kirwan, M.L., and Guntenspergen, G.R., 2012, Feedbacks between inundation, root production, and shoot growth in a rapidly submerging brackish marsh: *Journal of Ecology*, v. 100, p. 764–770, doi: 10.1111/j.1365-2745.2012.01957.x.

- Kirwan, M.L., Guntenspergen, G.R., D'Alpaos, A., Morris, J.T., Mudd, S.M., and Temmerman, S., 2010, Limits on the adaptability of coastal marshes to rising sea level: *Geophysical Research Letters*, v. 37, p. L23401, doi: 10.1029/2010GL045489.
- Kirwan, M.L., and Megonigal, J.P., 2013, Tidal wetland stability in the face of human impacts and sea-level rise: *Nature*, v. 504, p. 53–60, doi: 10.1038/nature12856.
- Letzsch, W.S., and Frey, R.W., 1980, Deposition and erosion in a Holocene salt marsh, Sapelo Island, Georgia: *Journal of Sedimentary Research*, v. 50, <http://archives.datapages.com/data/sepm/journals/v47-50/data/050/050002/0529.htm>.
- Ma, Z., Ysebaert, T., van der Wal, D., de Jong, D.J., Li, X., and Herman, P.M.J., 2014, Long-term salt marsh vertical accretion in a tidal bay with reduced sediment supply: *Estuarine Coastal and Shelf Science*, v. 146, p. 14–23, doi: 10.1016/j.ecss.2014.05.001.
- Meyer, B.K., 2013, Shoreline dynamics and environmental change under the modern marine transgression: St. Catherines Island, Georgia: GEORGIA STATE UNIVERSITY, <http://gradworks.umi.com/35/91/3591094.html>.
- Montero-Serrano, J.C., Palarea-Albaladejo, J., Martín-Fernández, J.A., Martínez-Santana, M., and Gutiérrez-Martín, J.V., 2010, Sedimentary chemofacies characterization by means of multivariate analysis: *Sedimentary Geology*, v. 228, p. 218–228, doi: 10.1016/j.sedgeo.2010.04.013.
- Pennings, S.C., Wall, V.D., Moore, D.J., Pattanayek, M., Buck, T.L., and Alberts, J.J., 2002, Assessing salt marsh health: A test of the utility of five potential indicators: *Wetlands*, v. 22, p. 406–414, doi: 10.1672/0277-5212(2002)022[0406:ASMHAT]2.0.CO;2.
- Reimer, P.J., Bard, E., Bayliss, A., Beck, J.W., Blackwell, P.G., Bronk Ramsey, C., Buck, C.E., Cheng, H., Edwards, R.L., Friedrich, M., and others, 2013, IntCal13 and Marine13 radiocarbon

age calibration curves 0-50,000 years cal BP.:

<http://researchcommons.waikato.ac.nz/handle/10289/8955>.

Rice, D., Knudson, S., and Westberry, L., 2005, Restoration of the Wormsloe Plantation salt marsh in Savannah, Georgia: <https://smartech.gatech.edu/handle/1853/47317> (accessed December 2015).

Sano, Y., Kobayashi, S., Shirai, K., Takahata, N., Matsumoto, K., Watanabe, T., Sowa, K., and Iwai, K., 2012, Past daily light cycle recorded in the strontium/calcium ratios of giant clam shells: *Nature Communications*, v. 3, p. 761, doi: 10.1038/ncomms1763.

Shennan, I., and Horton, B., 2002, Holocene land-and sea-level changes in Great Britain: *Journal of Quaternary science*, v. 17, p. 511–526.

Stammermann, R., and Piasecki, M., 2012, Influence of Sediment Availability, Vegetation, and Sea Level Rise on the Development of Tidal Marshes in the Delaware Bay: A Review: *Journal of Coastal Research*, v. 28, p. 1536–1549, doi: 10.2112/JCOASTRES-D-11-00143.1.

Stuiver, M., and Reimer, P.J., 1993, Calib 7.1 Radiocarbon calibration program: *Radiocarbon*, v. 35, p. 2015–2030.

Swanson, D.A., 2012, *Remaking Wormsloe Plantation: The Environmental History of a Lowcountry Landscape*: University of Georgia Press, [https://books.google.com/books?hl=en&lr=&id=K2d3Yq\\_1QaEC&oi=fnd&pg=PP1&dq=drew+swanson+captain+jones+wormsloe&ots=Sa632pykTJ&sig=r6QrfwIZxroPrv97lGj3LkogKgQ](https://books.google.com/books?hl=en&lr=&id=K2d3Yq_1QaEC&oi=fnd&pg=PP1&dq=drew+swanson+captain+jones+wormsloe&ots=Sa632pykTJ&sig=r6QrfwIZxroPrv97lGj3LkogKgQ).




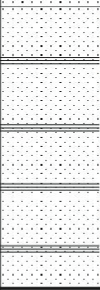

Temmerman, S., Govers, G., Wartel, S., and Meire, P., 2004, Modelling estuarine variations in tidal marsh sedimentation: response to changing sea level and suspended sediment concentrations: *Marine Geology*, v. 212, p. 1–19, doi: 10.1016/j.margeo.2004.10.021.


















- Thomsen, V., and Schatzlein, D., 2002, Advances in field-portable XRF: SPECTROSCOPY-  
SPRINGFIELD THEN EUGENE-, v. 17, p. 14–21.
- Townend, I., Fletcher, C., Knappen, M., and Rossington, K., 2011, A review of salt marsh dynamics:  
Water and Environment Journal, v. 25, p. 477–488, doi: 10.1111/j.1747-6593.2010.00243.x.
- Webb, E.L., Friess, D.A., Krauss, K.W., Cahoon, D.R., Guntenspergen, G.R., and Phelps, J., 2013, A  
global standard for monitoring coastal wetland vulnerability to accelerated sea-level rise: Nature  
Climate Change, v. 3, p. 458–465, doi: 10.1038/nclimate1756.
- Winker, C.D., and Howard, J.D., 1977, Correlation of tectonically deformed shorelines on the  
southern Atlantic coastal plain: Geology, v. 5, p. 123–127.
- Yong-Ming, S., Jing-Song, Y., Yan-Hong, W., Nian-Hua, F., Qin, Z., and Hua, Z., 2008, Impact of  
sediment supply on *Spartina* salt marshes: Pedosphere, v. 18, p. 593–598, doi: 10.1016/S1002-  
0160(08)60053-3.


APPENDICES

Appendix A – Vibracore Log Forms






 <b>VIBRACORE BORING LOG</b> <i>Wormsloe</i>		WM 050215-01 PAGE NO. 1 OF 2		
PROJECT NAME: <u>WORMSLOE STRATIGRAPHY RESEARCH</u>		TOTAL DEPTH: 5.51 METERS (COMPACTED)		
W.O. NUMBER: <u>N/A</u>		NORTHING: 3,535,375		
LOCATION: <u>JONES NARROWS MARSH, WORMSLOE S.H.S, ISLE OF HOPE, GA</u>		EASTING: 492,968		
DRILLERS: <u>MEYER, VANCE, HUGHES, DOBSON, BANKHEAD</u>		GROUND SURFACE ELEVATION: 4.06 ft MSL		
DRILL RIG TYPE: <u>UNIV. OF WEST GA VIBRACORE RIG</u>		DEPTH TO TOP OF CORE: 56 CM BTOP		
DRILLING METHOD: <u>VIBRACORE</u>		HEIGHT ABOVE LAND SURFACE: 44 CM BTOP		
SAMPLING METHOD: <u>3-INCH I.D. ALUMINUM PIPE</u>		COMPACTION (%): 2.1%		
LOGGED BY: <u>JRH</u> WEATHER: <u>WARM/CLEAR</u>		BOREHOLE DIAMETER: 3- INCH BOREHOLE		
DATE BEGUN: <u>05/02/15</u> DATE COMPLETED: <u>05/02/15</u>		LOGGER SIGNATURE: <u>JRH</u>		
DEPTH (m)	LITHOLOGIC DESCRIPTION	GRAPHIC LOG	PHOTOGRAPHIC LOG	COMMENTS
0				<i>land surface</i>
	Sand, fine, w/ mudballs and some mud laminations, oxidation, shell fragments, color 10YR8/1 - 10YR4/6 - 10YR3/1			Washover Fan Sequence
	Sand, fine, w/ mud laminations and mud balls, liquid escape structures, color 10YR8/1 - 10YR3/1			Intertidal Sequence Low Marsh
1.0	Mud (clay/silt), with charcoal and plant material, color 2.5Y4/1 - 2.5Y2.5/1			
2.0				
3.0				


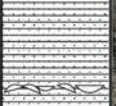

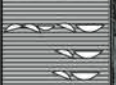
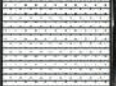
 <b>VIBRACORE BORING LOG</b> <i>Wormsloe</i>		<b>LOCATION NUMBER: WM 050215-01</b>		
		<b>PAGE NO. 2 OF 2</b>		
PROJECT NAME: <u>WORMSLOE STRATIGRAPHY RESEARCH</u>		TOTAL DEPTH: <u>5.51 METERS (COMPACTED)</u>		
W.O. NUMBER: <u>N/A</u>		NORTHING: <u>3,535,357</u>		
LOCATION: <u>JONES CREEK MARSH, WORMSLOE S.H.S. ISLE OF HOPE, GA</u>		EASTING: <u>492,968</u>		
DRILLERS: <u>MEYER, VANCE, HUGHES, DOBSON, BANKHEAD</u>		GROUND SURFACE ELEVATION: <u>4.06 RMSL</u>		
DRILL RIG TYPE: <u>UNIV. OF WEST GA VIBRACORE RIG</u>		DEPTH TO TOP OF CORE: <u>56 CM BTOP</u>		
DRILLING METHOD: <u>VIBRACORE</u>		HEIGHT ABOVE LAND SURFACE: <u>44 CM BTOP</u>		
SAMPLING METHOD: <u>3-INCH I.D. ALUMINUM PIPE</u>		COMPACTION (%): <u>2.1%</u>		
LOGGED BY: <u>JRH</u> WEATHER: <u>WARM/CLEAR</u>		BOREHOLE DIAMETER: <u>3- INCH BOREHOLE</u>		
DATE BEGUN: <u>05/02/15</u> DATE COMPLETED: <u>05/02/15</u>		LOGGER SIGNATURE: <u>JRH</u>		
DEPTH (m)	LITHOLOGIC DESCRIPTION	GRAPHIC LOG	PHOTOGRAPHIC LOG	COMMENTS
3.0	Mud (clay/silt) w/ some sand, fine, some plant fragments, color 10YR3/1 - 10YR7/2			Intertidal Sequence Low Marsh
4.0	Mud (clay/silt), w/ sand, fine, mottling, bioturbation, large shell(377-380cm), color 10YR3/1 - 10YR7/2			Intertidal Sequence Tidal Creek Levee
5.0	Mud(clay /silt), color 2.5Y3/1			Intertidal Sequence Low Marsh
6.0	Mud (clay/silt) w/sand, fine, color 10YR3/1 - 10YR7/2			




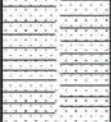






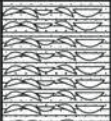
 <b>VIBRACORE BORING LOG</b>		<b>WM 050215-02</b> <b>PAGE NO. 1 OF 2</b>		
PROJECT NAME: <u>WORMSLOE STRATIGRAPHY RESEARCH</u>		TOTAL DEPTH: <u>5.19 METERS (COMPACTED)/24 cm LOSS</u>		
W.O. NUMBER: <u>N/A</u>		NORTHING: <u>3,535,343</u>		
LOCATION: <u>JONES CREEK MARSH, WORMSLOE S.H.S. ISLE OF HOPE, GA</u>		EASTING: <u>493,045</u>		
DRILLERS: <u>MEYER, VANCE, HUGHES, DOBSON, BANKHEAD</u>		GROUND SURFACE ELEVATION: <u>4.49R MSL</u>		
DRILL RIG TYPE: <u>UNIV. OF WEST GA VIBRACORE RIG</u>		DEPTH TO TOP OF CORE: <u>68 CM BTOP</u>		
DRILLING METHOD: <u>VIBRACORE</u>		HEIGHT ABOVE LAND SURFACE: <u>42 CM BTOP</u>		
SAMPLING METHOD: <u>3-INCH I.D. ALUMINUM PIPE</u>		COMPACTION (%): <u>4.8%</u>		
LOGGED BY: <u>JRH</u> WEATHER: <u>WARM/CLEAR</u>		BOREHOLE DIAMETER: <u>3- INCH BOREHOLE</u>		
DATE BEGUN: <u>05/02/15</u> DATE COMPLETED: <u>05/02/15</u>		LOGGER SIGNATURE: <u>JRH</u>		
DEPTH (m)	LITHOLOGIC DESCRIPTION	GRAPHIC LOG	PHOTOGRAPHIC LOG	COMMENTS
0	Sand, fine to medium, w/ mud balls, oxidation color 10YR8/1 - 10YR5/8 - 10YR2/1			<i>land surface</i> <b>Washover Fan Sequence</b>
	Mud (clay w/ silt), w/sand, fine, shells, liquid escape structure, color 10YR2/1 - 10YR8/1			WM 03 @ 36 cm ( <sup>14</sup> C = 36,290 +/- 120 B.P.)
	Sand, fine to medium, w/mud (clay and silt) liquid escape structures, plant matter, mud balls, color 10YR8/1 - 10YR2/1			<b>Intertidal Sequence</b> <b>Low Marsh</b>
1.0	Mud (clay w/silt) with some plant matter, color 10YR3/1			WM 26 @ 135 cm ( <sup>14</sup> C = 160 +/- 25 B.P.)
2.0				
3.0				WM 25 @ 280 cm ( <sup>14</sup> C = 1000 +/- 25 B.P.)

		<b>VIBRACORE BORING LOG</b>		<b>LOCATION NUMBER: WM 050215-02</b>	
		<b>PAGE NO. 2 OF 2</b>			
PROJECT NAME: <u>WORMSLOE STRATIGRAPHY RESEARCH</u>		TOTAL DEPTH: <u>4.18 METERS (COMPACTED) LOST 33i ON RETRIEVAL</u>			
W.O. NUMBER: <u>N/A</u>		NORTHING: <u>3,535,343</u>			
LOCATION: <u>JONES CREEK MARSH, WORMSLOE S.H.S, ISLE OF HOPE, GA</u>		EASTING: <u>493,045</u>			
DRILLERS: <u>MEYER, VANCE, HUGHES, DOBSON, BANKHEAD</u>		GROUND SURFACE ELEVATION: <u>4.49 ft MSL</u>			
DRILL RIG TYPE: <u>UNIV. OF WEST GA VIBRACORE RIG</u>		DEPTH TO TOP OF CORE: <u>68 CM BTOP</u>			
DRILLING METHOD: <u>VIBRACORE</u>		HEIGHT ABOVE LAND SURFACE: <u>42 CM BTOP</u>			
SAMPLING METHOD: <u>3-INCH I.D. ALUMINUM PIPE</u>		COMPACTION (%): <u>4.8%</u>			
LOGGED BY: <u>JRH</u> WEATHER: <u>WARM/CLEAR</u>		BOREHOLE DIAMETER: <u>3- INCH BOREHOLE</u>			
DATE BEGUN: <u>05/02/15</u> DATE COMPLETED: <u>05/02/15</u>		LOGGER SIGNATURE: <u>JRH</u>			
DEPTH (m)	LITHOLOGIC DESCRIPTION	GRAPHIC LOG	PHOTOGRAPHIC LOG	COMMENTS	
3.0		[Graphic Log Representation]	[Photographic Log Representation]	Intertidal Sequence Low Marsh	
4.0					
5.0					
6.0					


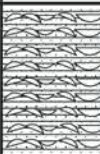
















 <b>VIBRACORE BORING LOG</b>		<b>WM 050215-03</b> <b>PAGE NO. 1 OF 2</b>		
PROJECT NAME: <u>WORMSLOE STRATIGRAPHY RESEARCH</u>		TOTAL DEPTH: <u>5.50 METERS (COMPACTED) LOST 0 CM ON RETRIEVAL</u>		
W.O. NUMBER: <u>N/A</u>		NORTHING: <u>3,535,298</u>		
LOCATION: <u>JONES CREEK MARSH, WORMSLOE S.H.S, ISLE OF HOPE, GA</u>		EASTING: <u>493,165</u>		
DRILLERS: <u>MEYER, VANCE, HUGHES, DOBSON, BANKHEAD</u>		GROUND SURFACE ELEVATION: <u>4.48 ft MSL</u>		
DRILL RIG TYPE: <u>UNIV. OF WEST GA VIBRACORE RIG</u>		DEPTH TO TOP OF CORE: <u>59 CM BTOP</u>		
DRILLING METHOD: <u>VIBRACORE</u>		HEIGHT ABOVE LAND SURFACE: <u>56 CM BTOP</u>		
SAMPLING METHOD: <u>3-INCH I.D. ALUMINUM PIPE</u>		COMPACTION (%): <u>0.5%</u>		
LOGGED BY: <u>JRH</u> WEATHER: <u>WARM/CLEAR</u>		BOREHOLE DIAMETER: <u>3- INCH BOREHOLE</u>		
DATE BEGUN: <u>05/02/15</u> DATE COMPLETED: <u>05/02/15</u>		LOGGER SIGNATURE: <u>JRH</u>		
DEPTH (m)	LITHOLOGIC DESCRIPTION	GRAPHIC LOG	PHOTOGRAPHIC LOG	COMMENTS
0	Sand, fine, w/ mud (clay and silt) and mud balls, w/ some shell fragments, oxidation, plant matter, color 10YR8/1-10YR5/6 -10YR4/4 -10YR4/1  Interlaminated sand w/mud (clay and silt), color 10YR7/1 to 10YR4/1  Mud (clay w/silt), w/plant fragments ( <i>Spartina</i> ), color 10YR4/1			<i>land surface</i>  Washover Fan Sequence
1.0				Intertidal Sequence High Marsh
2.0				Intertidal Sequence Low Marsh
3.0				




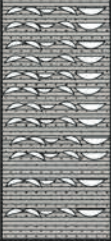



 <b>VIBRACORE BORING LOG</b>		LOCATION NUMBER: WM 050215-03		
		PAGE NO. 2 OF 2		
PROJECT NAME: <u>WORMSLOE STRATIGRAPHY RESEARCH</u>		TOTAL DEPTH: <u>5.50 METERS (COMPACTED) LOST 0 CM ON RETRIEVAL</u>		
W.O. NUMBER: <u>N/A</u>		NORTHING: <u>3,535,298</u>		
LOCATION: <u>JONES CREEK MARSH, WORMSLOE S.H.S, ISLE OF HOPE, GA</u>		EASTING: <u>493,165</u>		
DRILLERS: <u>MEYER, VANCE, HUGHES, DOBSON, BANKHEAD</u>		GROUND SURFACE ELEVATION: <u>4.48 ft MSL</u>		
DRILL RIG TYPE: <u>UNIV. OF WEST GA VIBRACORE RIG</u>		DEPTH TO TOP OF CORE: <u>59 CM BTOP</u>		
DRILLING METHOD: <u>VIBRACORE</u>		HEIGHT ABOVE LAND SURFACE: <u>56 CM BTOP</u>		
SAMPLING METHOD: <u>3-INCH I.D. ALUMINUM PIPE</u>		COMPACTION (%): <u>0.5%</u>		
LOGGED BY: <u>JRH</u> WEATHER: <u>WARM/CLEAR</u>		BOREHOLE DIAMETER: <u>3- INCH BOREHOLE</u>		
DATE BEGUN: <u>05/02/15</u> DATE COMPLETED: <u>05/02/15</u>		LOGGER SIGNATURE: <u>JRH</u>		
DEPTH (m)	LITHOLOGIC DESCRIPTION	GRAPHIC LOG	PHOTOGRAPHIC LOG	COMMENTS
3.0				
	Sand, fine to coarse, w/mud (clay and silt), w/shells (whole and fragment), color 10YR8/1 -10YR4/1			Intertidal Sequence Tidal Creek
4.0	Mud (clay and silt) w/ some shells (whole and fragment), color 5Y4/1			Intertidal Sequence Low Marsh or Tidal Creek Levee
5.0	Sand, fine, w/some mud(clay and silt), color 10YR2/1 - 5Y4/1			Intertidal Sequence High Marsh (Pleistocene Island Core?)
6.0				

 <b>VIBRACORE BORING LOG</b>		<b>WM 050215-04</b> <b>PAGE NO. 1 OF 2</b>		
PROJECT NAME: <u>WORMSLOE STRATIGRAPHY RESEARCH</u>		TOTAL DEPTH: <u>4.96 METERS (COMPACTED) LOST 1CM ON RETRIEVAL</u>		
W.O. NUMBER: <u>N/A</u>		NORTHING: <u>3,535,268</u>		
LOCATION: <u>JONES CREEK MARSH, WORMSLOE S.H.S, ISLE OF HOPE, GA</u>		EASTING: <u>493,238</u>		
DRILLERS: <u>MEYER, VANCE, HUGHES, DOBSON, BANKHEAD</u>		GROUND SURFACE ELEVATION: <u>3.91 ft MSL</u>		
DRILL RIG TYPE: <u>UNIV. OF WEST GA VIBRACORE RIG</u>		DEPTH TO TOP OF CORE: <u>111 CM BTOP</u>		
DRILLING METHOD: <u>VIBRACORE</u>		HEIGHT ABOVE LAND SURFACE: <u>53 CM BTOP</u>		
SAMPLING METHOD: <u>3-INCH I.D. ALUMINUM PIPE</u>		COMPACTION (%): <u>10.5%</u>		
LOGGED BY: <u>JRH</u> WEATHER: <u>WARM/CLEAR</u>		BOREHOLE DIAMETER: <u>3- INCH BOREHOLE</u>		
DATE BEGUN: <u>05/02/15</u> DATE COMPLETED: <u>05/02/15</u>		LOGGER SIGNATURE: <u>JRH</u>		
DEPTH (m)	LITHOLOGIC DESCRIPTION	GRAPHIC LOG	PHOTOGRAPHIC LOG	COMMENTS
0	Sand, fine, color 10Y8/1 -10YR5/1			<i>land surface</i> Washover Fan Sequence/ Dredge Fill
	Sand, fine, w/interlaminated mud(clay and silt) oxidation, liquid escape structures, color 10YR8/1 - 10YR2/1 - 10YR6/6			Intertidal Sequence Low Marsh
	Mud(clay and silt), w/some plant fragments, ( <i>Spartina</i> ), color 2.5Y4/1			Interdtidal Sequence High Marsh
	Sand, fine, w/mud (clay and silt), color 2.5Y3/1			levee? normal grading?
	Mud (clay and silt), w/sand, fine, w/some plant fragments, color 5Y5/2 - 5Y2.5/1			
	Mud(clay and silt), w/sand, fine, w/some plant fragments and charcoal, color 5Y5/2 - 5Y2.5/1			
	Sand, coarse to medium, color 5Y5/2 - 5Y2.5/1			
	Sand, fine, w/mud(clay and silt), mud laminations , shell fragments, color 5Y7/1 - 5Y8/1 - 5Y3/1			
3.0	Sand, fine w/mud, shells (whole and fragments), color 5Y4/1			















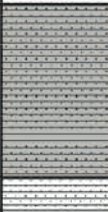

 <b>VIBRACORE BORING LOG</b>		<b>LOCATION NUMBER: WM 050215-04</b>		
		<b>PAGE NO. 2 OF 2</b>		
PROJECT NAME: <u>WORMSLOE STRATIGRAPHY RESEARCH</u>		TOTAL DEPTH: <u>4.96 METERS (COMPACTED) LOST 1 CM ON RETRIEVAL</u>		
W.O. NUMBER: <u>N/A</u>		NORTHING: <u>3,535,265</u>		
LOCATION: <u>JONES CREEK MARSH, WORMSLOE S.H.S, ISLE OF HOPE, GA</u>		EASTING: <u>493,238</u>		
DRILLERS: <u>MEYER, VANCE, HUGHES, DOBSON, BANKHEAD</u>		GROUND SURFACE ELEVATION: <u>3.91 ft MSL</u>		
DRILL RIG TYPE: <u>UNIV OF WEST GA VIBRACORE RIG</u>		DEPTH TO TOP OF CORE: <u>111 CM BTOP</u>		
DRILLING METHOD: <u>VIBRACORE</u>		HEIGHT ABOVE LAND SURFACE: <u>53 CM BTOP</u>		
SAMPLING METHOD: <u>3-INCH I.D. ALUMINUM PIPE</u>		COMPACTION (%): <u>10.5%</u>		
LOGGED BY: <u>JRH</u> WEATHER: <u>WARM/CLEAR</u>		BOREHOLE DIAMETER: <u>3- INCH BOREHOLE</u>		
DATE BEGUN: <u>05/02/15</u> DATE COMPLETED: <u>05/02/15</u>		LOGGER SIGNATURE: <u>JRH</u>		
DEPTH (m)	LITHOLOGIC DESCRIPTION	GRAPHIC LOG	PHOTOGRAPHIC LOG	COMMENTS
3.0				
	Mud (clay/silt) w/some sand, fine, shell fragments, plant fragments, color 5Y4/1			Intertidal Sequence Low Marsh
4.0				
	Mud (clay/silt) w/sand, fine, color 5Y2.5/1 - 5Y4/1 - 2.5Y8/2			Beach Sequence Forebeach?
5.0				
6.0				




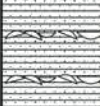







 <b>VIBRACORE BORING LOG</b>		<b>WM 050315-01</b> <b>PAGE NO. 1 OF 2</b>		
PROJECT NAME: STRATIGRAPHY RESEARCH		TOTAL DEPTH: 5.48 METERS (COMPACTED) LOST 0 CM ON RETRIEVAL		
W.O. NUMBER: N/A		NORTHING: 3,535,220		
LOCATION: JONES CREEK MARSH, WORMSLOE S.H.S, ISLE OF HOPE, GA		EASTING: 493,345		
DRILLERS: MEYER, VANCE, HUGHES, DOBSON, BANKHEAD		GROUND SURFACE ELEVATION: 4.80R MSL		
DRILL RIG TYPE: UNIV. OF WEST GA VIBRACORE RIG		DEPTH TO TOP OF CORE: 61 CM BTOP		
DRILLING METHOD: VIBRACORE		HEIGHT ABOVE LAND SURFACE: 39 CM BTOP		
SAMPLING METHOD: 3-INCH I.D. ALUMINUM PIPE		COMPACTION (%): 3.9%		
LOGGED BY: JRH WEATHER: WARM/CLEAR		BOREHOLE DIAMETER: 3- INCH BOREHOLE		
DATE BEGUN: 05/03/15 DATE COMPLETED: 05/03/15		LOGGER SIGNATURE: JRH		
DEPTH (m)	LITHOLOGIC DESCRIPTION	GRAPHIC LOG	PHOTOGRAPHIC LOG	COMMENTS
0	Sand, fine, w/some mud (clay/silt), oxidation, color 10Y8/2 -10Y6/8			<i>land surface</i> Washover Fan Sequence Dredge Fill
	Mud(clay/silt), color 10Y2/1			Intertidal Sequence Low Marsh
1.0	Mud (clay/silt) w/sand, fine, bioturbation, charcoal, color 10Y3/1 - 10Y7/2			Intertidal Sequence High Marsh
2.0	Sand, fine, w/mud, variable laminations, color 10YR8/1 - 5G6/1 - 5YR2/1			
3.0	Sand, fine to coarse, w/mud, 2.5Y4/1 -10YR6/1			Intertidal Sequence Tidal Creek Point Bar


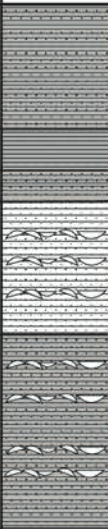

 <b>VIBRACORE BORING LOG</b>		<b>LOCATION NUMBER: WM 050315-01</b>		
		<b>PAGE NO. 2 OF 2</b>		
PROJECT NAME: STRATIGRAPHY RESEARCH		TOTAL DEPTH: 5.48 METERS (COMPACTED) LOST 0 CM ON RETRIEVAL		
W.O. NUMBER: N/A		NORTHING: 3,535,220		
LOCATION: JONES CREEK MARSH, WORMSLOE S.H.S, ISLE OF HOPE, GA.		EASTING: 493,345		
DRILLERS: MEYER, VANCE, HUGHES, DOBSON, BANKHEAD		GROUND SURFACE ELEVATION: 4.80 ft MSL		
DRILL RIG TYPE: UNIV. OF WEST GA VIBRACORE RIG		DEPTH TO TOP OF CORE: 61 CM BTOP		
DRILLING METHOD: VIBRACORE		HEIGHT ABOVE LAND SURFACE: 39 CM BTOP		
SAMPLING METHOD: 3-INCH I.D. ALUMINUM PIPE		COMPACTION (%): 3.9%		
LOGGED BY: JRH WEATHER: WARM/CLEAR		BOREHOLE DIAMETER: 3- INCH BOREHOLE		
DATE BEGUN: 05/03/15 DATE COMPLETED: 05/03/15		LOGGER SIGNATURE: JRH		
DEPTH (m)	LITHOLOGIC DESCRIPTION	GRAPHIC LOG	PHOTOGRAPHIC LOG	COMMENTS
3.0	Mud (clay/silt) w/sand, fine, color 2.5Y4/1 - 10YR6/1			Intertidal Sequence High Marsh
4.0	Mud (clay/silt) w/sand, fine, shells (whole and fragments), color 2.5Y4/1			Intertidal Sequence Tidal Creek
5.0	Mud (clay/silt) w/ few organics, color 2.5Y4/1			Intertidal Sequence Low Marsh
6.0				





 <b>VIBRACORE BORING LOG</b>		<b>WM-050315-02</b> <b>PAGE NO. 1 OF 2</b>		
PROJECT NAME: <u>WORMSLOE STRATIGRAPHY RESEARCH</u>		TOTAL DEPTH: 3.65 METERS (COMPACTED) LOST 58 CM ON RETRIEVAL		
W.O. NUMBER: <u>N/A</u>		NORTHING: <u>3,535,398</u>		
LOCATION: <u>JONES CREEK MARSH, WORMSLOE S.H.S, ISLE OF HOPE, GA</u>		EASTING: <u>493,132</u>		
DRILLERS: <u>MEYER, VANCE, HUGHES, DOBSON, BANKHEAD</u>		GROUND SURFACE ELEVATION: <u>3.85R MSL</u>		
DRILL RIG TYPE: <u>UNIV. OF WEST GA VIBRACORE RIG</u>		DEPTH TO TOP OF CORE: <u>147 CM BTOP</u>		
DRILLING METHOD: <u>VIBRACORE</u>		HEIGHT ABOVE LAND SURFACE: <u>42 CM BTOP</u>		
SAMPLING METHOD: <u>3-INCH I.D. ALUMINUM PIPE</u>		COMPACTION (%): <u>22.3%</u>		
LOGGED BY: <u>JRH</u> WEATHER: <u>WARM/CLEAR</u>		BOREHOLE DIAMETER: <u>3- INCH BOREHOLE</u>		
DATE BEGUN: <u>05/03/15</u> DATE COMPLETED: <u>05/03/15</u>		LOGGER SIGNATURE: <u>JRH</u>		
DEPTH (m)	LITHOLOGIC DESCRIPTION	GRAPHIC LOG	PHOTOGRAPHIC LOG	COMMENTS
0	Sand, fine ,oxidation, color 10YR8/1 - 10YR3/6 - 10YR6/1			<i>land surface</i> Washover Fan Sequence Dredge Fill
	Mud (clay/silt) w/ some sand, fine, plant fragments, color 2.5Y4/1			
	Mud (clay/silt) w/plant fragments, color 2.5Y4/1			Intertidal Sequence Low Marsh
1.0				
	Mud (clay/silt) w/some sand, fine, color 2.5Y3/1 - 10YR7/1			
2.0				
	Mud (clay/silt) w/sand, fine, plant fragments, bioturbation, color 5Y4/1 - 5Y7/1			Intertidal Sequence High Marsh
3.0				

 <b>VIBRACORE BORING LOG</b>		<b>LOCATION NUMBER: WM 050315-02</b>		
		<b>PAGE NO. 2 OF 2</b>		
PROJECT NAME: <u>WORMSLOE STRATIGRAPHY RESEARCH</u>		TOTAL DEPTH: <u>3.65 METERS (COMPACTED) LOST 58 CM ON RETRIEVAL</u>		
W.O. NUMBER: <u>N/A</u>		NORTHING: <u>3,535,398</u>		
LOCATION: <u>JONES CREEK MARSH, WORMSLOE S.H.S, ISLE OF HOPE, GA</u>		EASTING: <u>493,132</u>		
DRILLERS: <u>MEYER, VANCE, HUGHES, DOBSON, BANKHEAD</u>		GROUND SURFACE ELEVATION: <u>3.85 ft MSL</u>		
DRILL RIG TYPE: <u>UNIV. OF WEST GA VIBRACORE RIG</u>		DEPTH TO TOP OF CORE: <u>147 CM BTOP</u>		
DRILLING METHOD: <u>VIBRACORE</u>		HEIGHT ABOVE LAND SURFACE: <u>42 CM BTOP</u>		
SAMPLING METHOD: <u>3-INCH I.D. ALUMINUM PIPE</u>		COMPACTION (%): <u>22.3%</u>		
LOGGED BY: <u>JRH</u> WEATHER: <u>WARM/CLEAR</u>		BOREHOLE DIAMETER: <u>3- INCH BOREHOLE</u>		
DATE BEGUN: <u>05/03/15</u> DATE COMPLETED: <u>05/03/15</u>		LOGGER SIGNATURE: <u>JRH</u>		
DEPTH (m)	LITHOLOGIC DESCRIPTION	GRAPHIC LOG	PHOTOGRAPHIC LOG	COMMENTS
3.0				Intertidal Sequence High Marsh
	Sand, fine, w/mud and shell fragments			Tidal Creek Point Bar
4.0				
5.0				
6.0				

 <b>VIBRACORE BORING LOG</b>		<b>WM 050315-03</b> <b>PAGE NO. 1 OF 2</b>		
PROJECT NAME: <u>WORMSLOE STRATIGRAPHY RESEARCH</u>		TOTAL DEPTH: <u>4.64 METERS (COMPACTED) LOST 57 CM ON RETRIEVAL</u>		
W.O. NUMBER: <u>N/A</u>		NORTHING: <u>3,535,193</u>		
LOCATION: <u>JONES CREEK MARSH, WORMSLOE S.H.S. ISLE OF HOPE, GA</u>		EASTING: <u>492,744</u>		
DRILLERS: <u>MEYER, VANCE, HUGHES, DOBSON, BANKHEAD</u>		GROUND SURFACE ELEVATION: <u>5.31 ft MSL</u>		
DRILL RIG TYPE: <u>UNIV. OF WEST GA VIBRACORE RIG</u>		DEPTH TO TOP OF CORE: <u>79 CM BTOP</u>		
DRILLING METHOD: <u>VIBRACORE</u>		HEIGHT ABOVE LAND SURFACE: <u>42 CM BTOP</u>		
SAMPLING METHOD: <u>3-INCH I.D. ALUMINUM PIPE</u>		COMPACTION (%): <u>7.4%</u>		
LOGGED BY: <u>JRH</u> WEATHER: <u>WARM/CLEAR</u>		BOREHOLE DIAMETER: <u>3- INCH BOREHOLE</u>		
DATE BEGUN: <u>05/03/15</u> DATE COMPLETED: <u>05/03/15</u>		LOGGER SIGNATURE: <u>JRH</u>		
DEPTH (m)	LITHOLOGIC DESCRIPTION	GRAPHIC LOG	PHOTOGRAPHIC LOG	COMMENTS
0	Sand, fine, w/some mud (clay and silt), w/ liquid escape structures, color 10YR8/1 - 10YR3/1			<i>land surface</i> Washover Fan Sequence Dredge Fill
1.0	Sand, fine, w/mud, organics, shell fragments, color 10YR6/1 - 10YR3/2			
	Mud (clay and silt), <i>Spartina</i> fragments (156-170 cm), color 10YR2/1			Intertidal Sequence Low Marsh
2.0	Mud (clay and silt), few <i>Spartina</i> fragments (185-200 cm and 235-245 cm), color 2.5Y3/1			
3.0	Mud (clay and silt) w/sand, fine, color 2.5Y2.5/1 - 10YR7/2			Intertidal Sequence High Marsh

 <b>VIBRACORE BORING LOG</b>		<b>LOCATION NUMBER: WM 050315-03</b>		
		<b>PAGE NO. 2 OF 2</b>		
PROJECT NAME: <u>WORMSLOE STRATIGRAPHY RESEARCH</u>		TOTAL DEPTH: <u>4.64 METERS (COMPACTED) LOST 57 CM ON RETRIEVAL</u>		
W.O. NUMBER: <u>N/A</u>		NORTHING: <u>3,535,193</u>		
LOCATION: <u>JONES CREEK MARSH, WORMSLOE S.H.S, ISLE OF HOPE, GA</u>		EASTING: <u>492,744</u>		
DRILLERS: <u>MEYER, VANCE, HUGHES, DOBSON, BANKHEAD</u>		GROUND SURFACE ELEVATION: <u>5.31 ft MSL</u>		
DRILL RIG TYPE: <u>UNIV. OF WEST GA VIBRACORE RIG</u>		DEPTH TO TOP OF CORE: <u>79 CM BTOP</u>		
DRILLING METHOD: <u>VIBRACORE</u>		HEIGHT ABOVE LAND SURFACE: <u>42 CM BTOP</u>		
SAMPLING METHOD: <u>3-INCH I.D. ALUMINUM PIPE</u>		COMPACTION (%): <u>7.4%</u>		
LOGGED BY: <u>JRH</u> WEATHER: <u>WARM/CLEAR</u>		BOREHOLE DIAMETER: <u>3- INCH BOREHOLE</u>		
DATE BEGUN: <u>05/03/15</u> DATE COMPLETED: <u>05/03/15</u>		LOGGER SIGNATURE: <u>JRH</u>		
DEPTH (m)	LITHOLOGIC DESCRIPTION	GRAPHIC LOG	PHOTOGRAPHIC LOG	COMMENTS
3.0	Mud(clay/silt), w /sand, fine, color 2.5Y2.1/1 - 10YR7/2			
	Mud(clay/silt), color 2.5Y3/1			
	Mud(clay/silt) w/sand, fine, 2.5Y2.1 to 10YR7/2			
	Sand, fine, w/mud (clay/silt), shells (whole and fragments), color 2.5YR5/1			
4.0	Mud (clay/silt) w/ sand, fine, shells (whole and fragments), color 2.5YR4/1 - 5Y6/1			Intertidal Sequence Tidal Creek
5.0				
6.0				



 <b>VIBRACORE BORING LOG</b>		<b>WM 050315-04</b> <b>PAGE NO. 1 OF 1</b>		
PROJECT NAME: <u>WORMSLOE STRATIGRAPHY RESEARCH</u>		TOTAL DEPTH: <u>2.89 METERS (COMPACTED) LOST 2 CM ON RETRIEVAL</u>		
W.O. NUMBER: <u>N/A</u>		NORTHING: <u>3,535,221</u>		
LOCATION: <u>JONES CREEK MARSH, WORMSLOE S.H.S, ISLE OF HOPE</u>		EASTING: <u>492,739</u>		
DRILLERS: <u>MEYER, VANCE, HUGHES, DOBSON, BANKHEAD</u>		GROUND SURFACE ELEVATION: <u>10.77 ft MSL</u>		
DRILL RIG TYPE: <u>UNIV OF WEST GA VIBRACORE RIG</u>		DEPTH TO TOP OF CORE: <u>57 CM BTOP</u>		
DRILLING METHOD: <u>VIBRACORE</u>		HEIGHT ABOVE LAND SURFACE: <u>21 CM BTOP</u>		
SAMPLING METHOD: <u>3-INCH I.D. ALUMINUM PIPE</u>		COMPACTION (%): <u>11.1%</u>		
LOGGED BY: <u>JRH</u> WEATHER: <u>WARM/CLEAR</u>		BOREHOLE DIAMETER: <u>3- INCH BOREHOLE</u>		
DATE BEGUN: <u>05/03/15</u> DATE COMPLETED: <u>05/03/15</u>		LOGGER SIGNATURE: <u>JRH</u>		
DEPTH (m)	LITHOLOGIC DESCRIPTION	GRAPHIC LOG	PHOTOGRAPHIC LOG	COMMENTS
0	Humus, dark gray/black, 10YR2/1			<i>land surface</i>
	Sand, fine, w/organic content, plant fragments, color 10YR6/2			Intertidal Sequence Forebeach
	Sand, fine, w/some mottling, color 10YR7/3 - 10YR4/4			
1.0	Sand, fine, color 10YR8/3			
2.0				
3.0				



Appendix B – XRF Results

TEST_ID	Depth	BORING_ID	DESCRIPTION	Date	Reading	Mode	LiveTime	Match1	MN1	Pass/Fail	Pass Fail St LE	LE +/-	P	P +/-	S	S +/-	Cl	Cl +/-	K
26	10.0	WM050215-04	sand	17-Sep-15	26	Soil	46.22				<LOD	<LOD	0	13474	<LOD	2223	6663	383	3516
27	20.0	WM050215-04	sand	17-Sep-15	27	Soil	44.73				<LOD	0	<LOD	14026	2616	836	7292	385	3543
28	30.0	WM050215-04	sand	17-Sep-15	28	Soil	46.91				<LOD	0	<LOD	15660	<LOD	2569	8245	437	3380
29	40.0	WM050215-04	sand/mud	17-Sep-15	29	Soil	45.88				<LOD	0	<LOD	17128	5382	1209	27770	736	5542
32	50.0	WM050215-04	sand/mud	17-Sep-15	32	Soil	45.83				<LOD	0	<LOD	15191	3061	935	9969	453	3578
33	60.0	WM050215-04	sand/mud	17-Sep-15	33	Soil	43.98				<LOD	0	<LOD	15132	7182	1157	29677	686	5138
34	70.0	WM050215-04	mud	17-Sep-15	34	Soil	44.39				<LOD	0	17639	5827	10193	1348	33779	778	5472
35	80.0	WM050215-04	mud	17-Sep-15	35	Soil	44.21				<LOD	0	22936	6279	11743	1430	33017	786	6390
36	90.0	WM050215-04	mud	17-Sep-15	36	Soil	44.2				<LOD	0	<LOD	17945	14392	1458	35888	790	4757
37	100.0	WM050215-04	mud	17-Sep-15	37	Soil	43.57				<LOD	0	<LOD	17592	13091	1418	27374	700	4725
38	110.0	WM050215-04	mud	17-Sep-15	38	Soil	45.13				<LOD	0	<LOD	16465	7694	1273	26076	708	4437
39	120.0	WM050215-04	mud/sand	17-Sep-15	39	Soil	44.95				<LOD	0	<LOD	15942	11985	1398	27735	713	4699
40	130.0	WM050215-04	mud/sand	17-Sep-15	40	Soil	45.16				<LOD	0	<LOD	17401	9914	1344	31047	752	5761
41	140.0	WM050215-04	mud/sand	17-Sep-15	41	Soil	45.4				<LOD	0	23016	6175	7517	1279	28780	738	5969
42	150.0	WM050215-04	mud/sand	17-Sep-15	42	Soil	52.77				<LOD	0	<LOD	57692	21305	3809	22272	1538	6243
43	160.0	WM050215-04	sand/mud	17-Sep-15	43	Soil	47.06				<LOD	0	<LOD	19626	7696	1323	21716	674	6399
44	170.0	WM050215-04	mud/sand	17-Sep-15	44	Soil	46.28				<LOD	0	<LOD	27748	37195	2297	18175	611	6678
45	180.0	WM050215-04	mud/sand	17-Sep-15	45	Soil	46.55				<LOD	0	<LOD	19885	<LOD	3329	12427	574	6405
46	190.0	WM050215-04	mud/sand	17-Sep-15	46	Soil	45.59				<LOD	0	<LOD	18619	4467	1030	11606	462	5670
47	200.0	WM050215-04	mud/sand	17-Sep-15	47	Soil	44.35				<LOD	0	<LOD	17246	<LOD	2737	10960	454	5031
48	210.0	WM050215-04	coarse sand	17-Sep-15	48	Soil	47.56				<LOD	0	<LOD	20353	4310	1249	13614	619	6014
49	220.0	WM050215-04	sand	17-Sep-15	49	Soil	45.8				<LOD	0	<LOD	17363	<LOD	2871	11053	472	6280
50	230.0	WM050215-04	sand	17-Sep-15	50	Soil	46.14				<LOD	0	<LOD	16487	6849	1120	10523	453	5361
2	240.0	WM050215-04	sand	18-Sep-15	2	Soil	46.57				<LOD	0	<LOD	17040	<LOD	2773	10288	466	5365
3	250.0	WM050215-04	mud/sand	18-Sep-15	3	Soil	47.2				<LOD	0	<LOD	23131	<LOD	3053	8340	462	5494
4	260.0	WM050215-04	mud/sand	18-Sep-15	4	Soil	45.33				<LOD	0	<LOD	18914	5162	1122	15256	538	5795
5	270.0	WM050215-04	mud/sand/shell	18-Sep-15	5	Soil	48.61				<LOD	0	<LOD	40898	<LOD	5512	14100	711	3855
6	280.0	WM050215-04	mud/sand/shell	18-Sep-15	6	Soil	48.77				<LOD	0	<LOD	39050	8584	2035	20058	878	4624
7	290.0	WM050215-04	shell/mud/sand	18-Sep-15	7	Soil	50.74				<LOD	0	<LOD	62820	16925	3045	21328	1100	4104
8	300.0	WM050215-04	shell/mud/sand	18-Sep-15	8	Soil	46				<LOD	0	<LOD	30019	10569	1673	24107	742	7003
9	310.0	WM050215-04	shell/mud/sand	18-Sep-15	9	Soil	49.37				<LOD	0	<LOD	35815	6255	1781	18244	806	4920
10	320.0	WM050215-04	shell/mud/sand	18-Sep-15	10	Soil	48.86				<LOD	0	<LOD	31370	<LOD	4591	15592	726	4822
11	330.0	WM050215-04	shell/mud/sand	18-Sep-15	11	Soil	47.21				<LOD	0	<LOD	44927	21613	2517	24615	926	6139
12	340.0	WM050215-04	shell/mud/sand	18-Sep-15	12	Soil	45.31				<LOD	0	<LOD	20454	7168	1209	16743	536	8501
13	350.0	WM050215-04	mud	18-Sep-15	13	Soil	47.48				<LOD	0	28587	7853	13563	1517	17238	552	8512
14	360.0	WM050215-04	mud	18-Sep-15	14	Soil	44.54				<LOD	0	19466	5863	7469	1126	17441	507	9262
15	370.0	WM050215-04	mud	18-Sep-15	15	Soil	45.21				<LOD	0	24794	6247	7441	1097	16719	469	9090
16	380.0	WM050215-04	mud	18-Sep-15	16	Soil	44.27				<LOD	0	25858	6199	7058	1091	15616	470	8953
17	390.0	WM050215-04	mud	18-Sep-15	17	Soil	45.57				<LOD	0	28024	6554	7676	1121	15481	454	8997
18	400.0	WM050215-04	mud	18-Sep-15	18	Soil	47.18				<LOD	0	<LOD	20494	8423	1313	14074	508	8586
19	410.0	WM050215-04	mud	18-Sep-15	19	Soil	46.24				<LOD	0	<LOD	15977	6144	1069	14670	459	9163
20	420.0	WM050215-04	mud	18-Sep-15	20	Soil	45.69				<LOD	0	24307	7058	15186	1482	12939	439	8567
21	430.0	WM050215-04	mud	18-Sep-15	21	Soil	46.32				<LOD	0	31222	7052	7763	1176	14929	464	9325
22	440.0	WM050215-04	mud	18-Sep-15	22	Soil	45.94				<LOD	0	22858	6196	10365	1217	14840	437	9636
23	450.0	WM050215-04	mud	18-Sep-15	23	Soil	45.19				<LOD	0	28927	6268	10615	1171	12244	388	7822
24	460.0	WM050215-04	mud	18-Sep-15	24	Soil	44.82				<LOD	0	<LOD	19397	11767	1271	10219	390	6013
25	470.0	WM050215-04	mud	18-Sep-15	25	Soil	44.74				<LOD	0	19420	6465	15610	1431	13184	421	8064
26	480.0	WM050215-04	mud/sand	18-Sep-15	26	Soil	45.53				<LOD	0	33145	8017	21205	1744	13928	460	6798

K +/-	Ca	Ca +/-	Ti	Ti +/-	Cr	Cr +/-	Mn	Mn +/-	Fe	Fe +/-	Co	Co +/-	Ni	Ni +/-	Cu	Cu +/-	Zn	Zn +/-	As	As +/-	Se	Se +/-	Rb	Rb +/-	Sr	
149	1235	91	1166	67	<LOD	13	67	6	2009	35	<LOD	43	<LOD	31	<LOD	18	<LOD	8	<LOD	6	<LOD	3	16	1	50	
145	1480	94	1690	78	<LOD	13	73	7	2862	45	<LOD	50	<LOD	31	<LOD	20	<LOD	8	<LOD	6	<LOD	3	15	1	59	
152	1710	106	1612	82	<LOD	15	61	7	3614	59	62	21	<LOD	33	<LOD	20	<LOD	8	<LOD	7	<LOD	3	19	1	64	
164	1110	91	2269	104		38	7	505	15	16019	225	<LOD	105	<LOD	35	<LOD	19	16	3	9	2	<LOD	3	38	2	52
148	3486	132	2020	86	<LOD	13	54	6	2953	47	<LOD	52	<LOD	31	<LOD	19	<LOD	8	<LOD	6	<LOD	2	19	1	70	
140	588	69	2019	87	37	6	111	7	12978	162	130	30	<LOD	30	<LOD	18	29	3	<LOD	6	<LOD	2	57	2	42	
148	495	71	1933	92	47	6	128	8	16211	211	138	34	<LOD	33	<LOD	18	31	4	<LOD	7	<LOD	2	57	2	38	
168	623	78	2115	104	36	7	137	9	19197	258	232	39	<LOD	34	<LOD	19	34	4	<LOD	6	<LOD	3	58	2	36	
131	1265	83	1425	78	19	5	159	8	15175	192	124	33	<LOD	31	<LOD	17	15	3	<LOD	6	<LOD	3	42	2	34	
146	2797	114	1664	84	26	6	96	7	10819	144	<LOD	82	<LOD	31	<LOD	18	10	3	<LOD	6	<LOD	3	32	2	42	
150	1173	89	2303	94	21	5	81	7	7775	108	<LOD	71	<LOD	31	<LOD	19	<LOD	8	<LOD	6	<LOD	2	20	1	38	
144	1251	88	1872	90	31	6	100	8	13007	175	124	31	<LOD	32	<LOD	19	<LOD	8		6	<LOD	3	23	1	47	
155	935	84	2497	107	46	7	129	9	19196	258	170	40	<LOD	37	<LOD	19	17	3	<LOD	7	<LOD	3	27	2	46	
166	1307	95	2972	119	60	7	153	9	19333	268	118	37	<LOD	34	<LOD	20	15	3	<LOD	7	<LOD	3	23	1	48	
447	2891	278	2968	246	61	17	149	22	18804	580	<LOD	188	<LOD	61	<LOD	40	<LOD	18	<LOD	11	<LOD	5	16	2	41	
198	3092	137	2098	108	40	7	141	9	13699	204	<LOD	104	<LOD	36	<LOD	21	15	3	<LOD	7	<LOD	3	29	2	83	
206	17305	365	1789	103	25	7	159	10	15418	231	142	40	<LOD	38	<LOD	21	10	3	<LOD	7	<LOD	3	31	2	97	
231	6564	213	2397	116	29	7	126	9	6599	111	<LOD	78	<LOD	36	<LOD	22	<LOD	10	<LOD	7	<LOD	3	28	2	108	
181	10226	234	2582	99	17	5	118	8	5888	85	<LOD	70	<LOD	33	<LOD	20	9	3	<LOD	6	<LOD	3	27	2	110	
171	7001	187	2282	94	26	5	91	7	5059	74	<LOD	64	<LOD	34	<LOD	20	13	3	<LOD	6	<LOD	3	25	1	88	
227	3551	158	1541	96	<LOD	18	80	8	4041	71	<LOD	64	<LOD	36	<LOD	21	<LOD	10	<LOD	7	<LOD	3	28	2	104	
199	4581	156	2697	104	<LOD	15	109	8	5165	78	<LOD	64	<LOD	32	<LOD	21	<LOD	9	<LOD	6	<LOD	2	31	2	104	
180	4380	151	2421	99	<LOD	15	89	7	5973	89	<LOD	71	<LOD	33	<LOD	20	10	3	<LOD	6	<LOD	3	22	1	83	
185	6050	178	2201	94	<LOD	15	100	7	3619	57	66	19	<LOD	32	<LOD	20	<LOD	9	<LOD	6	<LOD	3	30	2	96	
203	18964	386	1712	88	22	5	82	7	2894	50	<LOD	53	<LOD	31	<LOD	20	<LOD	9	<LOD	6	<LOD	3	23	2	141	
185	10395	240	2300	98	16	5	103	8	7353	106	119	26	<LOD	32	<LOD	19	14	3		2	<LOD	3	33	2	125	
220	89521	1608	1456	104	<LOD	19	66	8	3504	67	<LOD	63	<LOD	39	<LOD	23	<LOD	10	<LOD	7	<LOD	3	18	2	376	
240	60258	1215	1900	127	25	8	97	10	7067	135	<LOD	91	<LOD	42	<LOD	26	15	4	<LOD	8	<LOD	3	23	2	398	
296	129589	2825	1110	129	<LOD	25	78	11	5905	133	<LOD	92	<LOD	49	<LOD	28	14	5	11	3	<LOD	4	14	2	611	
223	57280	908	2261	107	20	6	123	8	7155	107	<LOD	84	<LOD	36	<LOD	22	11	3	8	2	<LOD	3	24	2	721	
236	45531	918	1957	114	29	7	91	10	5384	102	<LOD	80	<LOD	37	<LOD	24	<LOD	10	<LOD	8	<LOD	3	32	2	240	
226	32397	680	1698	105	<LOD	19	81	9	5552	103	<LOD	80	<LOD	40	<LOD	25	<LOD	11	<LOD	7	<LOD	3	26	2	176	
261	86337	1592	2611	136	33	8	126	10	9000	161	<LOD	95	<LOD	40	<LOD	24	<LOD	11	<LOD	7	<LOD	4	23	2	392	
230	8185	221	2994	128	57	8	183	10	18265	266	147	39	<LOD	35	<LOD	20	22	4	<LOD	7	<LOD	3	50	2	110	
235	8515	236	4167	153	47	8	195	11	22114	334	<LOD	142	<LOD	40	<LOD	22	29	4	<LOD	8	<LOD	3	38	2	96	
227	2679	125	4037	140	65	8	209	10	20372	281	<LOD	118	<LOD	35	<LOD	20	34	4	<LOD	7	<LOD	3	51	2	87	
218	6931	189	3603	131	69	8	222	11	22188	300	176	40	<LOD	35	<LOD	19	31	4	11	2	<LOD	3	52	2	87	
224	3322	135	4065	140	44	7	181	10	19963	277	<LOD	117	<LOD	36	<LOD	21	28	4	<LOD	7	<LOD	3	50	2	87	
223	6696	190	3969	138	64	8	241	11	22275	309	<LOD	129	<LOD	37	<LOD	22	31	4	8	3	<LOD	3	54	2	92	
248	7868	232	3907	153	69	9	215	12	19414	303	<LOD	130	<LOD	40	<LOD	22	24	4	<LOD	8	<LOD	3	44	2	90	
237	3193	140	3965	147	64	8	181	11	22010	320	<LOD	125	<LOD	38	<LOD	21	35	4	8	2	<LOD	3	47	2	78	
233	2742	135	3809	142	50	8	169	10	20711	308	<LOD	132	<LOD	38	<LOD	22	28	4	7	2	<LOD	3	32	2	69	
240	6776	201	4276	151	58	8	209	11	23005	336	137	43	<LOD	39	<LOD	21	37	4	9	3	<LOD	3	50	2	86	
235	3215	137	4230	143	66	8	199	11	23063	323	142	42	<LOD	37	<LOD	20	34	4	<LOD	7	<LOD	3	44	2	85	
200	1653	103	3702	129	45	7	149	9	18430	251	<LOD	106	<LOD	33	<LOD	20	23	3	<LOD	7	<LOD	3	32	2	55	
180	3694	141	5151	152	41	7	128	9	14223	202	<LOD	109	<LOD	37	<LOD	22	55	5	<LOD	7	<LOD	3	26	2	55	
212	2185	120	3797	136	48	7	148	10	20824	297	<LOD	128	<LOD	37	<LOD	21	26	4	<LOD	7	<LOD	2	31	2	72	
198	4021	160	2478	123	60	8	122	10	23302	356	<LOD	151	<LOD	39	<LOD	21	17	4	<LOD	7	<LOD	3	24	2	52	



Sr +/-	Zr	Zr +/-	Mo	Mo +/-	Ag	Ag +/-	Cd	Cd +/-	Sn	Sn +/-	Sb	Sb +/-	I	I +/-	Ba	Ba +/-	Hg	Hg +/-	Pb	Pb +/-	Tl/Zr	Fe/K	
2	371	6	<LOD	8	<LOD	27	<LOD	31	<LOD	52	<LOD	54	<LOD	169	48	13	<LOD	7	<LOD	7	3.14	0.57	
2	512	7	<LOD	8	<LOD	26	<LOD	31	<LOD	51	<LOD	53	<LOD	178	66	15	<LOD	8	<LOD	7	3.30	0.81	
2	460	7	<LOD	8	<LOD	28	<LOD	33	<LOD	56	<LOD	58	<LOD	191	60	16	<LOD	8	<LOD	8	3.50	1.07	
2	268	5	<LOD	7	<LOD	26	<LOD	31	<LOD	51	<LOD	53	<LOD	220	185	21	<LOD	7	11	3	8.47	2.89	
2	541	7	<LOD	8	<LOD	27	<LOD	31	<LOD	52	<LOD	54	<LOD	210	71	16	<LOD	7	7	2	3.73	0.83	
2	74	3	<LOD	6	<LOD	24	<LOD	28	<LOD	46	<LOD	48	<LOD	177	177	18	<LOD	6	16	2	27.28	2.53	
2	57	3	<LOD	7	<LOD	25	<LOD	29	<LOD	47	<LOD	49	<LOD	188	193	19	<LOD	6	16	3	33.91	2.96	
2	61	3	<LOD	7	<LOD	26	<LOD	30	<LOD	49	<LOD	51	<LOD	210	281	22	<LOD	7	14	3	34.67	3.00	
2	97	3		9	2	<LOD	25	<LOD	28	<LOD	47	<LOD	49	<LOD	167	164	17	<LOD	7	<LOD	7	14.69	3.19
2	273	5	<LOD	7	<LOD	25	<LOD	29	<LOD	49	<LOD	51	<LOD	194	164	17	<LOD	7	<LOD	7	6.10	2.29	
2	360	5		8	2	<LOD	26	<LOD	30	<LOD	50	<LOD	52	<LOD	205	115	18	<LOD	7	<LOD	7	6.40	1.75
2	336	5	<LOD	7	<LOD	25		10	<LOD	49	<LOD	52	<LOD	189	159	18	<LOD	7	<LOD	7	5.57	2.77	
2	308	5	<LOD	7	<LOD	26	<LOD	31	<LOD	51	<LOD	53	<LOD	220	223	22	<LOD	8	10	2	8.11	3.33	
2	369	6	<LOD	7	<LOD	26	<LOD	31	<LOD	51	<LOD	53	<LOD	240	246	24	<LOD	7	19	3	8.05	3.24	
3	268	9	<LOD	13	<LOD	49	<LOD	56	<LOD	93	<LOD	98	<LOD	528	234	49	<LOD	14	<LOD	13	11.07	3.01	
2	509	7	<LOD	8	<LOD	28	<LOD	33	<LOD	55	<LOD	57	<LOD	241	223	22	<LOD	8	13	3	4.12	2.14	
3	492	7	<LOD	8	<LOD	28	<LOD	33	<LOD	55	<LOD	58	<LOD	346	192	21	<LOD	8	11	3	3.64	2.31	
3	607	9	<LOD	9	<LOD	30	<LOD	35	<LOD	58	<LOD	61	<LOD	299	164	22	<LOD	8	15	3	3.95	1.03	
3	755	9	<LOD	8	<LOD	27	<LOD	31	<LOD	52	<LOD	54	<LOD	276	112	18	<LOD	8	<LOD	7	3.42	1.04	
2	508	7	<LOD	8	<LOD	27	<LOD	32	<LOD	53	<LOD	55	<LOD	246	107	17	<LOD	8	<LOD	7	4.49	1.01	
3	666	9	<LOD	9	<LOD	30	<LOD	35	<LOD	58	<LOD	60	<LOD	245	149	20	<LOD	8	<LOD	8	2.31	0.67	
3	922	11	<LOD	8	<LOD	27	<LOD	31	<LOD	52	<LOD	54	<LOD	251	107	19	<LOD	7	11	3	2.93	0.82	
2	876	10	<LOD	8	<LOD	27	<LOD	32	<LOD	53	<LOD	55	<LOD	239	111	18	<LOD	8	<LOD	7	2.76	1.11	
3	734	9	<LOD	8	<LOD	27	<LOD	32	<LOD	53	<LOD	55	<LOD	246	113	18	<LOD	8	11	3	3.00	0.67	
3	479	7	<LOD	8	<LOD	28	<LOD	32	<LOD	54	<LOD	57	<LOD	345	75	17	<LOD	8	<LOD	7	3.57	0.53	
3	595	8	<LOD	8	<LOD	27	<LOD	31	<LOD	52	<LOD	54	<LOD	272	140	19	<LOD	7	8	2	3.87	1.27	
6	450	8	<LOD	9	<LOD	32	<LOD	37	<LOD	62	<LOD	65	<LOD	740	96	19	<LOD	9	<LOD	9	3.24	0.91	
7	414	8	<LOD	10	<LOD	34	<LOD	40	<LOD	66	<LOD	69	<LOD	689	154	25	<LOD	9	<LOD	9	4.59	1.53	
11	274	8	<LOD	11	<LOD	38	<LOD	44	<LOD	74	<LOD	78		1436	366	98	24	<LOD	12	<LOD	10	4.05	1.44
9	357	7	<LOD	8	<LOD	29	<LOD	34	<LOD	56	<LOD	59	<LOD	534	170	20	<LOD	8	9	3	6.33	1.02	
5	491	8	<LOD	9	<LOD	32	<LOD	37	<LOD	62	<LOD	65	<LOD	578	74	21	<LOD	9	12	3	3.99	1.09	
4	441	8	<LOD	9	<LOD	32	<LOD	37	<LOD	63	<LOD	66	<LOD	480	93	20	<LOD	10	<LOD	8	3.85	1.15	
7	487	8	<LOD	9	<LOD	32	<LOD	37	<LOD	63	<LOD	66	<LOD	770	114	24	<LOD	9	<LOD	8	5.36	1.47	
3	308	5	<LOD	8	<LOD	28	<LOD	32	<LOD	53	<LOD	56	<LOD	308	308	26	<LOD	8	12	3	9.72	2.15	
3	597	8	<LOD	9	<LOD	29	<LOD	34	<LOD	57	<LOD	59	<LOD	352	296	29	<LOD	8	12	3	6.98	2.60	
2	458	7	<LOD	8	<LOD	27	<LOD	31	<LOD	52	<LOD	54	<LOD	284	346	27	<LOD	8	16	3	8.81	2.20	
2	299	5	<LOD	7	<LOD	26	<LOD	29	<LOD	49	<LOD	51	<LOD	298	334	26	<LOD	7	9	2	12.05	2.44	
2	459	7	<LOD	8	<LOD	27	<LOD	31	<LOD	52	<LOD	53	<LOD	284	330	27	<LOD	7	16	3	8.86	2.23	
2	507	7	<LOD	8	<LOD	27	<LOD	32	<LOD	52	<LOD	54	<LOD	308	285	26	<LOD	8	16	3	7.83	2.48	
3	525	8	<LOD	9	<LOD	30	<LOD	35	<LOD	58	<LOD	60	<LOD	348	319	29	<LOD	9	14	3	7.44	2.26	
2	401	6	<LOD	8	<LOD	27	<LOD	32	<LOD	53	<LOD	55	<LOD	297	357	29	<LOD	8	10	3	9.89	2.40	
2	475	7	<LOD	8	<LOD	29	<LOD	33	<LOD	56	<LOD	58	<LOD	292	246	27	<LOD	8	<LOD	8	8.02	2.42	
2	329	6	<LOD	8	<LOD	28	<LOD	32	<LOD	54	<LOD	56	<LOD	330	315	28	<LOD	8	14	3	13.00	2.47	
2	475	7	<LOD	8	<LOD	27	<LOD	31	<LOD	52	<LOD	54	<LOD	301	272	26	<LOD	8	15	3	8.91	2.39	
2	547	7	<LOD	8	<LOD	26	<LOD	30	<LOD	50	<LOD	52	<LOD	257	267	24	<LOD	7	11	2	6.77	2.36	
2	1584	17	<LOD	9	<LOD	28	<LOD	32	<LOD	53	<LOD	55	<LOD	301	216	26	<LOD	9	12	3	3.25	2.37	
2	357	6	<LOD	8	<LOD	27	<LOD	32	<LOD	53	<LOD	55	<LOD	288	217	25	<LOD	8	14	3	10.64	2.58	
2	355	6	<LOD	8	<LOD	29	<LOD	35	<LOD	57	<LOD	60	<LOD	280	231	25	<LOD	8	11	3	6.98	3.43	

TEST_ID	Depth	BORING_ID	DESCRIPTION	Date	Reading	Mode	LiveTime	Match1	MNI	Pass/Fail	Pass Fail St:LE	LE +/-	P	P +/-	S	S +/-	Cl	Cl +/-	K
4	10.0	WM050215-03	sand	16-Sep-15	4	Soil	44.76				<LOD	0	<LOD	16438	<LOD	3014	18503	614	2963
5	20.0	WM050215-03	sand	16-Sep-15	5	Soil	45.76				<LOD	0	<LOD	13020	<LOD	2654	11222	473	2242
6	30.0	WM050215-03	sand	16-Sep-15	6	Soil	44.97				<LOD	0	<LOD	14673	<LOD	2804	15296	545	3218
7	40.0	WM050215-03	sand	16-Sep-15	7	Soil	45.16				<LOD	0	<LOD	18181	9961	1295	15945	558	2950
8	50.0	WM050215-03	muddy sand	16-Sep-15	8	Soil	46.24				<LOD	0	<LOD	28611	27214	1978	13025	557	2165
9	60.0	WM050215-03	sand/mud	16-Sep-15	9	Soil	45.62				<LOD	0	<LOD	17128	9069	1178	6481	389	2607
10	70.0	WM050215-03	sand/mud	16-Sep-15	10	Soil	45.76				<LOD	0	<LOD	18691	6347	1091	8889	431	2349
11	80.0	WM050215-03	sand/mud	16-Sep-15	11	Soil	43.81				<LOD	0	<LOD	20259	17528	1506	11994	485	2273
12	90.0	WM050215-03	sand/mud	16-Sep-15	12	Soil	45.56				<LOD	0	<LOD	20015	10622	1406	22794	671	5521
13	100.0	WM050215-03	mud	16-Sep-15	13	Soil	43.13				<LOD	0	<LOD	17711	10211	1398	40555	868	5789
14	110.0	WM050215-03	mud	16-Sep-15	14	Soil	43.75				<LOD	0	<LOD	15806	10420	1334	33659	766	4431
15	120.0	WM050215-03	mud	16-Sep-15	15	Soil	44.74				<LOD	0	<LOD	16019	11693	1322	33886	742	3409
16	130.0	WM050215-03	mud	16-Sep-15	16	Soil	45.34				<LOD	0	<LOD	19293	19265	1618	31649	748	6395
17	140.0	WM050215-03	mud	16-Sep-15	17	Soil	50.23				<LOD	0	<LOD	31670	17926	2410	28256	1088	6723
18	150.0	WM050215-03	mud	16-Sep-15	18	Soil	45.73				<LOD	0	<LOD	19841	16372	1594	29493	754	6486
19	160.0	WM050215-03	mud	16-Sep-15	19	Soil	42.93				<LOD	0	17272	5502	12516	1258	23361	573	6516
20	170.0	WM050215-03	mud	16-Sep-15	20	Soil	44.19				<LOD	0	22194	6174	14316	1381	23843	606	6560
21	180.0	WM050215-03	mud	16-Sep-15	21	Soil	45.31				<LOD	0	28553	6702	17495	1527	25158	640	7771
22	190.0	WM050215-03	mud	16-Sep-15	22	Soil	45.73				<LOD	0	<LOD	35805	61446	2994	28940	820	6514
23	200.0	WM050215-03	mud	16-Sep-15	23	Soil	42.66				<LOD	0	<LOD	14128	8368	1040	17550	461	6611
24	210.0	WM050215-03	mud	16-Sep-15	24	Soil	42.78				<LOD	0	<LOD	12712	8163	1010	17894	458	7264
25	220.0	WM050215-03	mud	16-Sep-15	25	Soil	43.98				<LOD	0	34648	7443	7729	1101	15827	439	6517
26	230.0	WM050215-03	mud	16-Sep-15	26	Soil	44.05				<LOD	0	<LOD	23490	8723	1207	15175	446	6528
27	240.0	WM050215-03	mud	16-Sep-15	27	Soil	43.77				<LOD	0	16350	5148	7112	985	14997	424	6687
28	250.0	WM050215-03	mud	16-Sep-15	28	Soil	44.02				<LOD	0	<LOD	23286	8491	1173	15281	433	6835
29	260.0	WM050215-03	mud	16-Sep-15	29	Soil	45.42				<LOD	0	<LOD	17703	15937	1376	11614	420	5488
30	270.0	WM050215-03	mud	16-Sep-15	30	Soil	44.68				<LOD	0	<LOD	18240	18678	1430	12528	410	5979
31	280.0	WM050215-03	mud	16-Sep-15	31	Soil	45.09				<LOD	0	22057	5789	10500	1148	12127	390	6386
32	290.0	WM050215-03	mud	16-Sep-15	32	Soil	45.35				<LOD	0	<LOD	17618	8476	1135	6888	354	4841
33	300.0	WM050215-03	mud	16-Sep-15	33	Soil	45.03				<LOD	0	23316	6625	17674	1411	15599	421	7565
2	310.0	WM050215-03	mud	17-Sep-15	2	Soil	44.3				<LOD	0	<LOD	18096	11773	1178	12418	374	6244
3	320.0	WM050215-03	mud	17-Sep-15	3	Soil	44.03				<LOD	0	<LOD	15142	9409	1034	13038	366	6568
4	330.0	WM050215-03	mud	17-Sep-15	4	Soil	45.41				<LOD	0	<LOD	22296	16287	1405	12846	396	6465
5	340.0	WM050215-03	mud	17-Sep-15	5	Soil	44.76				<LOD	0	<LOD	19067	11021	1249	14228	452	6149
6	350.0	WM050215-03	sand/mud	17-Sep-15	6	Soil	47.82				<LOD	0	<LOD	18956	6627	1150	2771	345	2588
7	360.0	WM050215-03	sand/mud	17-Sep-15	7	Soil	48.17				<LOD	0	<LOD	31607	8687	1620	10403	552	5056
8	370.0	WM050215-03	sand/mud/shell	17-Sep-15	8	Soil	51.85				<LOD	0	<LOD	45426	<LOD	6532	7163	988	3285
9	380.0	WM050215-03	sand/mud/shell (Merc.)	17-Sep-15	9	Soil	51.43				<LOD	0	<LOD	84575	<LOD	9971	18191	1289	3670
10	390.0	WM050215-03	sand/mud/shell	17-Sep-15	10	Soil	50.33				<LOD	0	<LOD	36054	10645	1912	12900	681	4645
11	400.0	WM050215-03	sand/mud/shell	17-Sep-15	11	Soil	51.41				<LOD	0	<LOD	37873	<LOD	5171	5751	643	4531
12	410.0	WM050215-03	sand/mud/shell	17-Sep-15	12	Soil	47.51				<LOD	0	<LOD	42441	9065	1762	9332	504	5553
13	420.0	WM050215-03	mud/shell	17-Sep-15	13	Soil	47.54				<LOD	0	<LOD	28704	4651	1348	6426	461	5304
14	430.0	WM050215-03	mud	17-Sep-15	14	Soil	46.67				<LOD	0	<LOD	21799	14845	1488	13912	447	8477
15	440.0	WM050215-03	mud	17-Sep-15	15	Soil	45.57				<LOD	0	31725	7426	11407	1284	12487	405	8083
16	450.0	WM050215-03	mud	17-Sep-15	16	Soil	45.29				<LOD	0	37571	6494	10269	1159	14285	383	9814
17	460.0	WM050215-03	mud	17-Sep-15	17	Soil	45.72				<LOD	0	47257	6922	9277	1114	14033	379	9940
18	470.0	WM050215-03	mud	17-Sep-15	18	Soil	45.46				<LOD	0	22400	5352	7620	996	13171	358	9450
19	480.0	WM050215-03	mud	17-Sep-15	19	Soil	44.11				<LOD	0	29423	5850	8752	1089	15498	407	10112
20	490.0	WM050215-03	mud	17-Sep-15	20	Soil	45.59				<LOD	0	37783	6338	11603	1224	17339	430	10988
21	500.0	WM050215-03	mud	17-Sep-15	21	Soil	54.16				<LOD	0	<LOD	57434	20736	3451	8766	1026	4193
22	510.0	WM050215-03	mud	17-Sep-15	22	Soil	44.15				<LOD	0	<LOD	15231	7836	1039	9771	405	2371
23	520.0	WM050215-03	mud	17-Sep-15	23	Soil	46.55				<LOD	0	<LOD	16913	9883	1204	5700	342	4471
24	530.0	WM050215-03	mud	17-Sep-15	24	Soil	47.78				<LOD	0	<LOD	17588	6079	1079	3335	329	4185
25	540.0	WM050215-03	sand/mud	17-Sep-15	25	Soil	46.05				<LOD	0	<LOD	18278	8287	1115	7856	342	5349



K +/-	Ca	Ca +/-	Ti	Ti +/-	Cr	Cr +/-	Mn	Mn +/-	Fe	Fe +/-	Co	Co +/-	Ni	Ni +/-	Cu	Cu +/-	Zn	Zn +/-	As	As +/-	Se	Se +/-	Rb	Rb +/-	Sr
134	1740	100	2310	91	24	5	72	7	2591	42 <LOD	48 <LOD	48 <LOD	31 <LOD	20	12	3 <LOD	6 <LOD	3	20	1	48				
119	1469	92	1194	66 <LOD		11	49	6	1528	27 <LOD	41 <LOD	30 <LOD	19 <LOD	19 <LOD	7 <LOD	5 <LOD	3	19	1	49					
136	1654	97	2259	88 <LOD		14	86	7	3082	48 <LOD	50 <LOD	31 <LOD	18 <LOD	18 <LOD	8 <LOD	5 <LOD	3	20	1	44					
131	7749	195	1738	79 <LOD		13	77	7	3537	54 <LOD	54 <LOD	31 <LOD	20 <LOD	20 <LOD	9 <LOD	6 <LOD	3	21	1	60					
133	25958	474	1224	74 <LOD		13	42	6	2543	43 <LOD	51 <LOD	32 <LOD	19 <LOD	19 <LOD	9 <LOD	5 <LOD	3	20	1	81					
133	7262	191	932	60	14	4	28	5	1269	25 <LOD	38 <LOD	31 <LOD	19 <LOD	19 <LOD	8 <LOD	5 <LOD	3	13	1	53					
124	10658	237	887	58 <LOD		12	30	5	1806	31 <LOD	42 <LOD	29 <LOD	19 <LOD	19 <LOD	8 <LOD	5 <LOD	2	15	1	63					
119	12603	261	1622	76 <LOD		13	52	6	2513	40 <LOD	45 <LOD	32 <LOD	20 <LOD	20 <LOD	8 <LOD	6 <LOD	3	18	1	51					
177	10347	236	2098	92	21	5	105	8	7046	100 <LOD	71 <LOD	31 <LOD	20 <LOD	20 <LOD	9 <LOD	6 <LOD	3	38	2	104					
152	1232	85	2079	90	35	6	142	8	16143	206	207	34 <LOD	32 <LOD	18	26	3	9	2 <LOD	2	50	2	48			
132	542	70	1854	82	34	5	89	7	10982	140 <LOD	82 <LOD	29 <LOD	18	18	3 <LOD	6 <LOD	2	54	2	36					
107	707	67	880	61	14	5	88	6	10106	125	104	27 <LOD	29 <LOD	17	13	3 <LOD	6 <LOD	3	42	2	32				
164	868	83	2096	99	42	7	136	9	19960	263	176	39 <LOD	34 <LOD	19	25	3	10	2 <LOD	2	59	2	37			
275	1067	140	2325	156	52	11	175	15	23662	486	288	68 <LOD	50 <LOD	27	38	6	13	3 <LOD	4	53	3	34			
179	1464	98	2022	100	41	7	167	9	17514	242	193	37 <LOD	32 <LOD	18	21	3 <LOD	6 <LOD	2	46	2	49				
160	1286	86	2249	97	52	6	176	9	17814	222	196	35 <LOD	32 <LOD	18	27	3	7	2 <LOD	2	51	2	50			
167	2482	111	2155	99	48	7	218	10	19042	248	235	39 <LOD	33 <LOD	18	42	4	7	2 <LOD	3	49	2	53			
192	1217	93	2963	116	59	7	224	10	21413	287	190	40 <LOD	35 <LOD	19	16	3	8	2 <LOD	3	49	2	60			
202	36688	649	2133	112	48	7	151	10	17674	262	244	41 <LOD	37 <LOD	21	18	4 <LOD	7 <LOD	3	59	2	109				
160	3751	124	2313	95	48	6	190	9	17058	210	176	33 <LOD	31 <LOD	17	24	3 <LOD	6 <LOD	2	47	2	49				
168	1218	83	2588	98	42	6	195	9	17729	215	228	34 <LOD	31 <LOD	17	29	3 <LOD	6 <LOD	2	49	2	49				
165	24289	393	2244	96	57	6	223	9	17188	214	206	34 <LOD	31 <LOD	17	23	3 <LOD	6 <LOD	2	47	2	61				
173	35983	553	2222	96	42	6	217	10	17094	220	206	35 <LOD	32 <LOD	17	28	3	8	2 <LOD	2	46	2	60			
167	2890	114	2341	96	47	6	210	9	16631	210	225	35 <LOD	31 <LOD	18	33	4	7	2 <LOD	2	46	2	58			
174	34988	533	2084	96	42	6	242	10	18347	232	163	35 <LOD	31 <LOD	18	28	3	9	2 <LOD	2	43	2	68			
165	929	85	1903	91	47	6	105	8	11038	151 <LOD	83 <LOD	32 <LOD	19	15	3 <LOD	6 <LOD	3	26	1	51					
165	2398	110	2083	95	41	6	114	8	13666	180 <LOD	89 <LOD	31 <LOD	18	17	3 <LOD	6 <LOD	2	32	2	50					
173	829	83	2271	102	49	7	122	8	16354	220	116	33 <LOD	32 <LOD	18	19	3 <LOD	6 <LOD	2	44	2	45				
170	1181	96	1839	91	28	6	85	8	8672	129	110	28 <LOD	34 <LOD	21	13	3 <LOD	6 <LOD	3	28	2	53				
182	9060	211	2369	106	51	7	236	10	23003	300	242	41 <LOD	34 <LOD	18	31	4	11	2 <LOD	2	39	2	55			
162	9128	208	2240	98	48	6	285	11	17467	225	103	34 <LOD	33 <LOD	17	26	3 <LOD	6 <LOD	2	38	2	56				
161	3022	115	2174	96	46	6	235	10	18700	235	204	36 <LOD	30 <LOD	17	31	3	7	2 <LOD	2	41	2	55			
172	19769	356	2218	100	37	6	310	11	17933	235	115	35 <LOD	33 <LOD	18	28	3 <LOD	6 <LOD	2	35	2	68				
173	8424	209	2347	103	45	7	313	12	16386	224 <LOD	100 <LOD	34 <LOD	19	13	3 <LOD	6 <LOD	2	26	1	52					
152	4011	159	1106	73 <LOD		15	37	7	2106	41 <LOD	45 <LOD	32 <LOD	19	15	3 <LOD	6 <LOD	3	7	1	28					
218	31371	666	1997	120	30	8	194	12	12047	212 <LOD	111 <LOD	43 <LOD	24	18	4 <LOD	8 <LOD	3	21	2	174					
345	21507	774	1489	159 <LOD		33	115	17	4815	144 <LOD	114 <LOD	64 <LOD	40 <LOD	17 <LOD	11 <LOD	5	15	2	184						
378	188713	4887	444	444 <LOD		31	127	16	6360	172 <LOD	128 <LOD	59 <LOD	39 <LOD	15 <LOD	12 <LOD	5	9	2	665						
230	49869	1005	1728	111	26	7	146	11	7698	143 <LOD	95 <LOD	40 <LOD	25 <LOD	12 <LOD	8 <LOD	4	18	2	324						
281	40550	993	1838	130 <LOD		24	94	12	5445	123 <LOD	94 <LOD	48 <LOD	28 <LOD	13 <LOD	9 <LOD	4	15	2	206						
222	102809	1660	1918	111	33	7	142	10	8975	142 <LOD	97 <LOD	36 <LOD	22	21	4 <LOD	7 <LOD	3	26	2	420					
225	31905	650	2272	120	23	7	129	10	6962	122 <LOD	86 <LOD	38 <LOD	23 <LOD	10 <LOD	7 <LOD	3	20	2	237						
226	16511	346	3113	130	44	8	467	15	21562	312	181	44 <LOD	37 <LOD	20	20	4	11	2 <LOD	3	39	2	131			
212	10967	255	3553	131	60	8	368	13	19625	275 <LOD	118 <LOD	37 <LOD	20	35	4 <LOD	7 <LOD	2	41	2	149					
230	1963	113	3939	145	88	9	1424	29	27076	374	165	46 <LOD	38 <LOD	20	44	4 <LOD	7 <LOD	3	56	2	65				
232	2920	129	4200	145	80	9	412	14	26473	364	165	44 <LOD	35 <LOD	19	40	4 <LOD	7 <LOD	2	57	2	67				
219	1530	101	4150	139	59	8	301	12	24574	330	202	42 <LOD	36 <LOD	18	44	4 <LOD	7 <LOD	2	55	2	60				
234	1522	104	3987	143	63	8	264	12	27926	385	266	47 <LOD	38 <LOD	20	28	4	8	3 <LOD	2	58	2	62			
248	1155	99	4229	150	84	9	259	12	32681	457	295	51 <LOD	39 <LOD	20	28	4	11	2 <LOD	3	51	2	55			
368	5881	363	2189	212 <LOD		45	162	21	15664	471 <LOD	180 <LOD	66 <LOD	42	20	7 <LOD	11 <LOD	5	20	3	37					
109	863	75	1614	74 <LOD		13	99	7	3635	52 <LOD	53 <LOD	30 <LOD	19 <LOD	8 <LOD	5 <LOD	2	14	1	42						
167	2081	114	2680	106	27	6	78	7	6960	106 <LOD	75 <LOD	32 <LOD	19 <LOD	9 <LOD	6 <LOD	3	21	1	56						
179	1439	107	2616	112	25	6	61	7	4280	72 <LOD	62 <LOD	33 <LOD	21 <LOD	9 <LOD	6 <LOD	3	13	1	56						
174	1367	101	2552	112	34	7	115	9	13235	194 <LOD	101 <LOD	35 <LOD	21	14	3	7	2 <LOD	2	19	1	52				

Sr +/-	Zr	Zr +/-	Mo	Mo +/-	Ag	Ag +/-	Cd	Cd +/-	Sn	Sn +/-	Sb	Sb +/-	I	I +/-	Ba	Ba +/-	Hg	Hg +/-	Pb	Pb +/-	Ti/Zr	Fe/K	
2	822	10 <LOD			8 <LOD		26 <LOD		31 <LOD		51 <LOD		54 <LOD		201	70	16 <LOD		8 <LOD		7	2.81	0.87
2	535	7 <LOD			8 <LOD		26 <LOD		30 <LOD		50 <LOD		52 <LOD		167	60	13 <LOD		7 <LOD		6	2.23	0.68
2	626	8 <LOD			8 <LOD		26 <LOD		30 <LOD		50 <LOD		52 <LOD		200	54	16 <LOD		7 <LOD		6	3.61	0.96
2	632	8 <LOD			8 <LOD		26 <LOD		30 <LOD		51 <LOD		53 <LOD		239	55	15 <LOD		7	11	2	2.75	1.20
2	427	6 <LOD			8 <LOD		27 <LOD		31 <LOD		53 <LOD		55 <LOD		364	48	14 <LOD		7 <LOD		6	2.87	1.17
2	366	6 <LOD			7 <LOD		26 <LOD		30 <LOD		50 <LOD		53 <LOD		212 <LOD		36 <LOD		7 <LOD		7	2.55	0.49
2	242	4 <LOD			7 <LOD		26 <LOD		30 <LOD		50 <LOD		52 <LOD		231 <LOD		34 <LOD		6 <LOD		6	3.67	0.77
2	811	9 <LOD			8 <LOD		26 <LOD		30 <LOD		51 <LOD		53 <LOD		261	61	14 <LOD		7 <LOD		7	2.00	1.11
2	429	6 <LOD			7 <LOD		26 <LOD		30 <LOD		50 <LOD		52 <LOD		270	117	18 <LOD		7	9	2	4.89	1.28
2	103	3 <LOD			7 <LOD		25 <LOD		29 <LOD		47 <LOD		49 <LOD		190	150	18 <LOD		6	9	2	20.18	2.79
2	56	3 <LOD			7 <LOD		24 <LOD		28 <LOD		46 <LOD		48 <LOD		179	130	16 <LOD		6	19	3	33.11	2.48
1	32	2	11		2 <LOD		23 <LOD		27 <LOD		44 <LOD		45 <LOD		135	114	13 <LOD		6	9	2	27.50	2.96
2	65	3	7		2 <LOD		25 <LOD		29 <LOD		48 <LOD		49 <LOD		210	216	21 <LOD		7	11	2	32.25	3.12
2	71	4 <LOD			10 <LOD		38 <LOD		44 <LOD		73 <LOD		76 <LOD		344	193	32 <LOD		11 <LOD		10	32.75	3.52
2	79	3 <LOD			7 <LOD		26 <LOD		30 <LOD		49 <LOD		51 <LOD		214	196	21 <LOD		7 <LOD		7	25.59	2.70
2	83	3 <LOD			7 <LOD		24 <LOD		28 <LOD		46 <LOD		48 <LOD		208	248	20 <LOD		6 <LOD		6	27.10	2.73
2	96	3 <LOD			7 <LOD		25 <LOD		29 <LOD		48 <LOD		50 <LOD		220	233	21 <LOD		7	8	2	22.45	2.90
2	222	4 <LOD			7 <LOD		26 <LOD		30 <LOD		49 <LOD		51 <LOD		237	230	23 <LOD		7	11	2	13.35	2.76
3	85	3 <LOD			8 <LOD		28 <LOD		33 <LOD		54 <LOD		56 <LOD		466	188	22 <LOD		8	8	3	25.09	2.71
2	96	3 <LOD			6 <LOD		24 <LOD		27 <LOD		45 <LOD		47 <LOD		216	219	19 <LOD		6	13	2	24.09	2.58
2	125	3	7		2 <LOD		24 <LOD		28 <LOD		46 <LOD		47 <LOD		205	232	20 <LOD		6	8	2	20.70	2.44
2	107	3 <LOD			6 <LOD		24 <LOD		27 <LOD		45 <LOD		47 <LOD		333	216	19 <LOD		7	8	2	20.97	2.64
2	101	3 <LOD			7 <LOD		25 <LOD		29 <LOD		47 <LOD		48 <LOD		379	180	19 <LOD		7	11	2	22.00	2.62
2	149	3 <LOD			7 <LOD		24 <LOD		28 <LOD		46 <LOD		48 <LOD		217	198	19 <LOD		7	8	2	15.71	2.49
2	136	3 <LOD			7 <LOD		24 <LOD		28 <LOD		46 <LOD		48 <LOD		378	230	20 <LOD		6	10	2	15.32	2.68
2	292	5 <LOD			7 <LOD		26 <LOD		30 <LOD		50 <LOD		52 <LOD		199	172	19 <LOD		6 <LOD		7	6.52	2.01
2	207	4 <LOD			7 <LOD		25 <LOD		29 <LOD		48 <LOD		50 <LOD		216	205	19 <LOD		6	11	2	10.06	2.29
2	152	4 <LOD			7 <LOD		25 <LOD		29 <LOD		47 <LOD		49 <LOD		213	215	21 <LOD		7	9	2	14.94	2.56
2	287	5 <LOD			8 <LOD		27 <LOD		31 <LOD		52 <LOD		54 <LOD		203	96	18 <LOD		8 <LOD		7	6.41	1.79
2	132	3 <LOD			7 <LOD		25 <LOD		29 <LOD		48 <LOD		49 <LOD		270	256	22 <LOD		7	12	2	17.95	3.04
2	113	3 <LOD			7 <LOD		24 <LOD		28 <LOD		46 <LOD		48 <LOD		263	208	20 <LOD		7	13	2	19.82	2.80
2	121	3 <LOD			6 <LOD		23 <LOD		27 <LOD		44 <LOD		46 <LOD		212	230	20 <LOD		6	11	2	17.97	2.85
2	225	4	8		2 <LOD		25 <LOD		29 <LOD		48 <LOD		49 <LOD		331	209	20 <LOD		7	14	2	9.86	2.77
2	341	5 <LOD			8 <LOD		26 <LOD		31 <LOD		51 <LOD		53 <LOD		271	189	21 <LOD		8 <LOD		7	6.88	2.66
2	127	4 <LOD			7 <LOD		28 <LOD		32 <LOD		54 <LOD		56 <LOD		217 <LOD		42 <LOD		7 <LOD		7	8.71	0.81
4	320	7 <LOD			9 <LOD		33 <LOD		38 <LOD		64 <LOD		67 <LOD		506	133	23 <LOD		9 <LOD		9	6.24	2.38
6	348	10 <LOD			14 <LOD		50 <LOD		57 <LOD		96 <LOD		99 <LOD		647	129	33 <LOD		13 <LOD		14	4.28	1.47
15	111	8 <LOD			13 <LOD		49 <LOD		57 <LOD		97 <LOD		102	3369	530 <LOD		83 <LOD		16 <LOD		13	4.00	1.73
6	255	6 <LOD			10 <LOD		34 <LOD		40 <LOD		66 <LOD		69 <LOD		597	77	21 <LOD		10 <LOD		9	6.78	1.66
5	400	9 <LOD			11 <LOD		40 <LOD		46 <LOD		76 <LOD		79 <LOD		646 <LOD		72 <LOD		13	13	4	4.60	1.20
6	328	6 <LOD			8 <LOD		29 <LOD		34 <LOD		57 <LOD		59	861	246	129	21 <LOD		8 <LOD		8	5.85	1.62
5	478	8 <LOD			9 <LOD		31 <LOD		36 <LOD		60 <LOD		63 <LOD		487	143	23 <LOD		9 <LOD		8	4.75	1.31
3	233	5	9		3 <LOD		27 <LOD		32 <LOD		52 <LOD		54 <LOD		364	271	26 <LOD		8	8	3	13.36	2.54
3	213	4 <LOD			7 <LOD		26 <LOD		31 <LOD		51 <LOD		54 <LOD		326	255	25 <LOD		8	14	3	16.68	2.43
2	144	4 <LOD			7 <LOD		27 <LOD		31 <LOD		52 <LOD		54 <LOD		290	424	29 <LOD		7	18	3	27.35	2.76
2	137	4 <LOD			7 <LOD		26 <LOD		30 <LOD		50 <LOD		51 <LOD		292	365	28 <LOD		7	19	3	30.66	2.66
2	153	4 <LOD			7 <LOD		26 <LOD		30 <LOD		49 <LOD		51 <LOD		269	341	27 <LOD		8	19	3	27.12	2.60
2	157	4 <LOD			7 <LOD		26 <LOD		31 <LOD		51 <LOD		53 <LOD		280	389	28 <LOD		7	19	3	25.39	2.76
2	177	4	9		2 <LOD		27 <LOD		31 <LOD		52 <LOD		53 <LOD		285	375	29 <LOD		8	10	3	23.89	2.97
3	219	8 <LOD			14 <LOD		51 <LOD		58 <LOD		97 <LOD		101 <LOD		533	229	45 <LOD		15 <LOD		13	10.00	3.74
2	449	6 <LOD			7 <LOD		25 <LOD		29 <LOD		49 <LOD		51 <LOD		164	84	14 <LOD		7 <LOD		7	3.59	1.53
2	419	6 <LOD			8 <LOD		27 <LOD		32 <LOD		53 <LOD		55 <LOD		230	86	19 <LOD		8	8	3	6.40	1.56
2	423	7 <LOD			8 <LOD		28 <LOD		33 <LOD		55 <LOD		57 <LOD		233	125	21 <LOD		8 <LOD		8	6.18	1.02
2	341	6 <LOD			8 <LOD		28 <LOD		33 <LOD		54 <LOD		57 <LOD		235	193	22 <LOD		7 <LOD		7	7.48	2.47